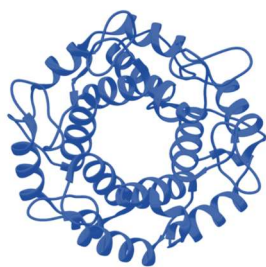


12TH INTERNATIONAL CONFERENCE

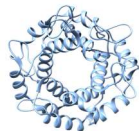
**STRUCTURE AND STABILITY OF
BIOMACROMOLECULES**



SSB2023

***BOOK OF
CONTRIBUTIONS***

5 - 7 SEPTEMBER 2023, KOŠICE, SLOVAKIA



12TH INTERNATIONAL CONFERENCE STRUCTURE AND STABILITY OF BIOMACROMOLECULES

"SSB 2023"



DEPARTMENT OF BIOPHYSICS,
INSTITUTE OF EXPERIMENTAL PHYSICS,
SAS, KOSICE



SLOVAK PHYSICAL SOCIETY



SLOVAK BIOPHYSICAL SOCIETY

SCIENTIFIC COMMITTEE

DIANA FEDUNOVA
ZUZANA GAZOVA
DANIEL JANCURA

ORGANIZING COMMITTEE

ANDREA ANTOSOVA
ZUZANA BEDNARIKOVA
VIKTORIA FEDOROVA
MIROSLAV GANCAR
JANA KUBACKOVA
MARIAN REIFFERS
KATARINA SIPOSOVA
DANA SVARCBERGEROVA

BOOK OF CONTRIBUTIONS, 12TH INTERNATIONAL CONFERENCE STRUCTURE AND STABILITY OF BIOMACROMOLECULES SSB2023, SEPTEMBER 5 – 7, 2023, KOŠICE, SLOVAKIA

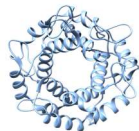
EDITORS: RNDr. Zuzana Bednarikova, PhD., Mgr. Viktoria Fedorova, RNDr. Diana Fedunova, PhD., RNDr., Ing. Katarina Siposova, PhD.

REVIEWERS: doc. MUDr. Marek Dudáš, PhD., doc. RNDr. Rastislav Varhač, PhD.

© INSTITUTE OF EXPERIMENTAL PHYSICS, SLOVAK ACADEMY OF SCIENCES

ISBN: 978-80-89656-26-4

EAN: 9788089656264



GENERAL INFORMATION

TOPICS

Biomacromolecules:

- structural aspects
- aggregation
- activity
- factors influencing stability
- ligand binding and inhibition
- modifications and engineering
- bioinformatics, molecular and nanodesign
- applications in medicine, bio- and nanotechnologies
- experimental and computational strategies for structural and conformational studies

VENUE

Auditorium of the Institutes
Institute of Experimental Physics, Slovak Academy of Sciences

Watsonova 47
040 01 Košice

REGISTRATION

Registration is possible at the registration desk, which is located in the foyer of the ground level of Institute.

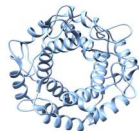
Opening hours:	Tuesday, September 5, 2023	14:00 - 17:00
	Wednesday, September 6, 2023	8:30 - 9:00

INFORMATION

Please pay kind attention to the boards located in the foyer of the Institute and at the entrance to the lecture hall (Auditorium of the Institutes) for further conference information and updates.

CERTIFICATE OF ATTENDANCE

If a Certificate of Attendance is required, please refer to the registration desk.



CATERING

Coffee Break: Coffee and tea with small snacks will be offered.

Lunch Break: A lunch will be provided in the Institute canteen starting at 13:00. Vegetarian/ vegan options will be available.

INTERNET ACCESS

Password for WiFi SAV_internet access: 14WifiSAV17

PUBLIC TRANSPORT

The closest bus station is "Botanická Záhřada" or "Havlíčková". Tickets can be purchased at the ticket machines at the bus stop or using UBIAN app. The price of 30 minutes' ticket is € 1.00.

EMERGENCY SERVICES

Dial 112 for police, fire and ambulance.

PRESENTATION GUIDELINES

CONFERENCE LANGUAGE: English

ORAL PRESENTATION

Speakers are required to have their presentation ready on a USB key. Your slides should be either in .pdf, .ppt or .pptx format.

Speakers using their own laptop are kindly asked to approach technical staff to clarify the technical prerequisites and to coordinate the processes involved.

PRESENTATION TIME:

Invited talks - speaking time 30 min plus 5 min discussion

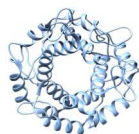
Short talks - speaking time 15 min plus 5 min discussion

Flash poster presentation - 5 min

POSTER GUIDELINES

Posters should have up to 90 cm (width) x 120 cm (height). Poster numbers will be communicated to authors at the Registration Desk.

Poster session will be held in the Promatech building at 6th floor (grey building next to the main building of the IEP SAS).



ACKNOWLEDGEMENT

The Organizing Committee of SSB 2023 would like to express appreciations and thanks to the following companies for their generous support.

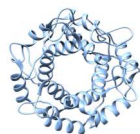


Váš špecialista pre laboratórium



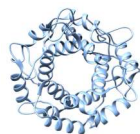
ABL&E-JASCO
Laboratory Equipment





CONTENT

SCIENTIFIC PROGRAM	7
LIST OF PLENARY LECTURES	11
LIST OF SHORT COMMUNICATIONS	12
LIST OF POSTERS	13
PLENARY LECTURES	16
SHORT COMMUNICATIONS	37
POSTERS	57
LIST OF PARTICIPANTS	109
INDEX OF AUTHORS	113

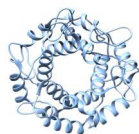


SCIENTIFIC PROGRAM


TUESDAY, SEPTEMBER 5, 2023

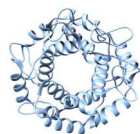
14:00 - 17:00	REGISTRATION	Foyer IEP
15:00 - 15:10	WELCOME ADDRESS Diana Fedunová & Zuzana Gažová, IEP SAS Košice	
		Chairman: Žoldák, Gabriel
15:10 - 15:45	MAI SUAN LI Protein folding and dimerization on ribosomes	PL1
15:45 - 16:20	GRZEGORZ WIECZOREK The importance of deep insight into discreet structural features of a target for successful drug design	PL2
16:20 - 16:55	DOROTA NIEDZIALEK The importance of proper treatment of electrostatics in biomolecular modelling and drug design	PL3
16:55 - 17:25	COFFEE BREAK	
		Chairman: Niedzialek Dorota
17:25 - 18:00	GABRIEL ŽOLDÁK Interrogating chaperones by force	PL4
18:00 - 18:20	MICHAL GALA Computational evolutionary analysis of insertion and deletion events in bacterial Hsp70	 SC1
18:30 - 19:30	WELCOME PARTY Foyer of the Institute of Experimental Physics, Watsonova 47	

 YOUNG SCIENTIST AWARD COMPETITOR



WEDNESDAY, SEPTEMBER 6, 2023



8:30 - 9:00	REGISTRATION	Foyer IEP
		Chairman: Škrabana, Rostislav
9:00 - 9:35	ONDREJ CEHLÁR	PL5
	Insights into the Alzheimer's disease specific pre-aggregation fold of tau proteins using conformational antibodies	
9:35 - 10:10	MICHAL NEMERGUT	PL6
	Identifying a new aggregation hotspot in Alzheimer's disease: Opportunities for drug discovery	
10:10 - 10:30	VERONIKA DŽUPPOVÁ	 SC2
	Supramolecular assembly of the pathological light chain under reducing conditions	
10:30 - 11:00	COFFEE BREAK	
		Chairman: Bauerová Vladena
11:00 - 11:35	VIKTOR VÍGLASKÝ	PL7
	Occurrence and use of non-canonical nucleic acid structural motifs in nanotechnology	
11:35 - 11:55	ADAM POLÁK	SC3
	Production of viral proteins and their characterisation	
11:55 - 12:15	ANDREJ HOVAN	 SC4
	Quenching of singlet oxygen in intracellular environment	
12:15 - 12:35	IGNAZIO GARAGUSO - BECKMAN COULTER	SC5
	Why Analytical Ultracentrifugation to investigate biomolecules	
12:35 - 12:55	KATEŘINA KOLKOVÁ - SPECION	SC6
	Modern methods for the analysis and characterization of biomolecules	
13:00 - 13:30	LUNCH	
		Chairman: Záhradníková Alexandra
14:00 - 14:35	PAVEL KADEŘÁVEK	PL8
	Study of the dynamics of flexible subunits of RNA polymerase from <i>Bacillus subtilis</i>	
14:35 - 15:10	ROSTISLAV ŠKRABANA	PL9
	Short-range folding of Intrinsically disordered proteins	

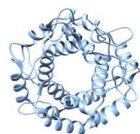


15:10 - 15:30	LAUTARO RIVERA SC7 Allosteric regulation of 14-3-3 protein family by Norharmane. Effects on adipogenic differentiation of 3T3L1 cells
15:30 - 16:00	COFFEE BREAK Chairman: Li, Mai-Suan
16:00 - 16:35	KATARÍNA ŠTROFFEKOVÁ PL10 Effects of photobiomodulation on oxidative stress and alpha-synuclein in 2D model of Parkinson's disease
16:35 - 16:55	MIROSLAV GANČÁR SC8 Herbal extracts' effect on protein amyloid aggregation - individual vs pooled constituents
16:55 - 17:15	VIKTÓRIA FEDOROVÁ  SC9 Self-assembly of spider protein-DNA hybrids
19:00 - 22:00	CONFERENCE DINNER (hotel Gloria Palace , Bottova 1, Košice)

THURSDAY, SEPTEMBER 7, 2023

Chairman: **Kadeřávek Pavel**

9:30 - 9:50	SU-CHUN HOW SC10 Fibril-based carrier systems for bioactive molecules
9:50 - 10:10	YOU-YEN LAI  SC11 Development of multi-dimensional whey protein amyloid fibril-based composite materials for various engineering applications
10:10 - 10:30	CHIA-YU CHANG  SC12 Synthesis of poly(acrylic acid)-whey protein isolate amyloid fibril-based hydrogel membranes for drug delivery
10:30 - 11:00	COFFEE BREAK Chairman: Bednáriková Zuzana
11:00 - 11:35	MAZDAK KHAJEHPOUR PL11 Ion-specific effects in biological systems



11:35 - 12:45

FLASH POSTER PRESENTATIONS

13:00 - 13:30

LUNCH

14:00 - 15:30

POSTER SESSION

6th Floor, Promatech

15:30 - 16:00

COFFEE BREAK

Chairman: **Khajepour Mazdak**

16:00 - 16:35

ALEXANDRA ZAHRADNÍKOVÁ

PL12

Ryanodine receptor inactivation by divalent ions

16:35 - 17:10

VLADENA BAUEROVÁ

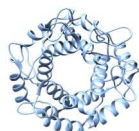
PL13

The effect of the central-helix mutations on the stability and dynamic motion of the N-terminal domain of the human ryanodine receptor 2

17:10 - 18:00

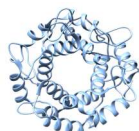
YOUNG AWARD CEREMONY

CONCLUDING REMARKS AND FAREWELL PARTY



PLENARY LECTURES

- PL 1 Protein Folding and Dimerization on Ribosomes.....17**
M. S. LI
- PL 2 The importance of deep insight into discrete structural features of a target for successful drug design.....18**
G. WIECZOREK, D. NIEDZIALEK
- PL 3 The importance of proper treatment of electrostatics in biomolecular modelling and drug design.....19**
D. NIEDZIALEK, G. WIECZOREK
- PL 4 Interrogating chaperones by force.....20**
G. ŽOLDÁK
- PL 5 Insights into the Alzheimer s disease specific pre-aggregation fold of tau proteins using conformational antibodies.....22**
O. CEHLAR, S. NJEMOGA, J. PIESTANSKY, Z. BEDNARIKOVA, R. SKRABANA, R. CRHA, J. HRITZ, P. KADERAVEK, L. FIALOVA, B. KOVACECH
- PL 6 Identifying a new aggregation hotspot in Alzheimer's disease: Opportunities for drug discovery24**
M. NEMERGUT
- PL7 Occurrence and use of non-canonical nucleic acid structural motifs in nanotechnology.....25**
V. VÍGLASKÝ, L. TRIZNA
- PL 8 Study of the Dynamics of Flexible Subunits of RNA Polymerase from *Bacillus subtilis*26**
D. TUŽINČIN, N. SALVI, V. ZAPLETAL, Z. JASEŇÁKOVÁ, M. ZACHRDLA, P. PADRTA, S. NARASIMHAN, T MARQUARDSEN, J.-M. TYBURN, H. ŠANDEROVÁ, A. RABATINOVÁ, K. BENDO VÁ, L. KRÁSNÝ, L. ŽÍDEK, M. BLACKLEDGE, F. FERRAGE, P. KADERÁVEK
- PL9 Short-range folding of intrinsically disordered proteins.....28**
R. SKRABANA, K. MARTONOVA, O. CEHLAR, M. HRICOVINI, M. HRICOVINI, K. MESKOVA, P. KADERAVEK, S. NJEMOGA, K. TOMKOVA
- PL 10 Effects of photobiomodulation on oxidative stress and α -synuclein in 2D model of Parkinson´s disease.....30**
K. STROFFEKOVA, E. WETTER, S. TOMKOVA
- PL 11 Ion-Specific Effects in Biological Systems.....32**
M. KHAJEHPUR, I. ASAKEREH, B. T. SHARAKI, H. REZASOLTANI



PL 12 Ryanodine receptor inactivation by divalent ions.....33

A. ZAHRADNÍKOVÁ, J. PAVELKOVÁ, I. ZAHRADNÍK

PL 13 The effect of the central-helix mutations on the stability and dynamic motion of the N-terminal domain of the human ryanodine receptor 2.....35

V. BAUEROVA-HLINKOVÁ, T. HROMÁDKOVÁ, E. KUTEJOVÁ, J. A. BAUER

SHORT COMMUNICATIONS

SC 1 Computational evolutionary analysis of insertion and deletion events in bacterial Hsp70.....38

M. GALA

SC 2 Supramolecular assembly of the pathological light chain under reducing conditions.....39

V. DŽUPPONOVÁ, G. ŽOLDÁK

SC 3 Production of Viral Proteins and Their Characterisation.....41

A. POLÁK, M. BENKO, A. BITALA, M. NEMČOVIČ, I. NEMČOVIČOVÁ

SC 4 Quenching of singlet oxygen in intracellular environment.....43

A. HOVAN, V. PEVNÁ, V. HUNTOŠOVÁ, P. MIŠKOVSKÝ, G. BÁNÓ

SC 5 Why analytical ultracentrifugation to investigate biomolecules?.....45

I. GARAGUSO, L. EHRARDT, A. BHATTACHARYA

SC 6 Modern Methods for the Analysis and Characterization of Biomolecules.....47

K. KOLKOVÁ

SC 7 Allosteric regulation of 14-3-3 protein family by Norharmane. Effects on adipogenic differentiation of 3T3L1 cells.....48

L. RIVERA, S. MULLER, E. BARRERA, M. UHART, D.M. BUSTOS

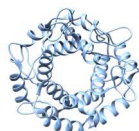
SC 8 Herbal extracts' effect on protein amyloid aggregation - individual vs pooled constituents50

M. GANČÁR, E. KURIN, Z. BEDNARIKOVA, J. MAREK, S. BITTNER FIALOVA, S. DOKUPILOVA, P. MUCAJI, M. NAGY, Z. GAZOVA

SC 9 Self-assembly of spider protein-DNA hybrids.....51

V. FEDOROVA, T. BIRO, K. SIPOSOVA, M. HUMENIK

SC 10 Fibril-based carrier systems for bioactive molecules.....53



Y.-Y. YANG, Y.-R. LAI, S.-C. HOW, S.S.S. WANG

SC 11 Development of Multi-Dimensional Whey Protein Amyloid Fibril-Based Composite Materials for Various Engineering Applications.....54

Y.-R. LAI and S.S.S. WANG

SC12 Synthesis of Poly(Acrylic acid)-Whey Protein Isolate Amyloid Fibril-Based Hydrogel Membranes for Drug Delivery.....56

C.-Y. CHANG and S.S.S. WANG

POSTERS

PO 1 Unique structural conformations affect the overall catalytic process of the phosphopantetheine adenylyltransferase in a highly virulent ESKAPE pathogen.....58

N. AHMAD, P. SHARMA, S. SHARMA, T. P. SINGH

PO 2 Hofmeister anions' influence on the amyloid aggregation of α -lactalbumin.....60

A. ANTOSOVA, M. GANCAR, J. MAREK, Z. GAZOVA

PO 3 Isolation and HPLC identification of fengycin isolated from Bacillus coagulans strain 9FT27 from Equine skin.....62

Z. BEDLOVIČOVÁ, E. STYKOVÁ, N. ŠURÍN HUDÁKOVÁ, M. MAĐAR

PO 4 Monomerization of 14-3-3 ζ proteins modulates the aggregation of β -amyloid peptides.....63

Z. BEDNARIKOVA, A. KOZELEKOVA, J. HRITZ, Z. GAZOVA

PO 5 Sugar as a cure – understanding the anti-amyloid potential of carbohydrate-amino acid hybrids?.....64

B. BOROVSÁ, M. TVRDOŇOVÁ, Z. BEDNÁRIKOVÁ, Z. GAŽOVÁ

PO 6 Effect of boceprevir on the lipid mesophases.....66

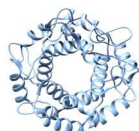
A. ČELKOVÁ, A. BÚCSI, M. KLACSOVÁ, J.C. MARTÍNEZ, D. UHRÍKOVÁ

PO 7 Determination of kinetics stabilizers reducing the formation of light chain protein deposits in multiple myeloma.....68

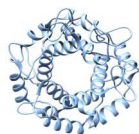
V. DEMČÁKOVÁ, G. ŽOLDÁK

PO 8 Ionic liquids as a powerful amyloid formation-inducing tool70

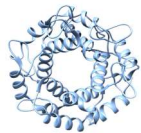
D. FEDUNOVÁ, V. VANÍK, A. ANTOŠOVÁ, Z. BEDNÁRIKOVÁ, J. MAREK, M. GANČÁR, M. GUNCHEVA, Z. GAŽOVÁ



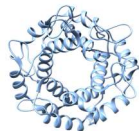
- PO 9 Functionalization of β -casein micelles with fluorescently-labeled DNA aptamers for targeting cancer cells.....72**
Z. GARAIOVÁ, I. KRÁLOVÁ, M. ZVARÍK, M. VELÍSKOVÁ, T. HIANIK
- PO 10 Archaeal FKBP: Peculiarities in structure and function.....74**
A. M. GOEL
- PO 11 Spectroscopic elucidation of the binding mechanism between novel 2,6,9-trisubstituted acridine derivatives and calf thymus DNA.....75**
A. GUCKÝ, O. OZHELEVSKA, J. KORÁBEČNÝ, M. KOŽURKOVÁ
- PO 12 Examination of “high-energy” metastable state of the oxidized bovine cytochrome c oxidase: proton uptake and reaction with H₂O₂.....77**
D. JANCURA, A. TOMKOVÁ, T. SZTACHOVÁ, V. BERKA, M. FABIAN
- PO 13 Molecular design of novel papain-like protease inhibitors with potential antiviral activity against SARS-CoV-2.....79**
L. KERTI, V. FREČER
- PO 14 Effect of Remdesivir on the Exogenous Pulmonary Surfactant.....81**
A. KESHAVARZI, A. Asi SHIRAZI, M. KLACSOVÁ, J.C. MARTÍNEZ, D. UHRÍKOVÁ
- PO 15 A fluorescence study of algal-based ghost vesicles as potential gene delivery systems.....83**
M. KLACSOVÁ, D. UHRÍKOVÁ, L. HORVAT, T. MIŠÍČ RADIĆ, N. IVOŠEVIĆ DENARDIS
- PO 16 Thinking outside the binding-pocket: in silico design of novel allosteric regulators of 14-3-3.....85**
S. MULLER, L. RIVERA, M. UHART, D.M. BUSTOS, E. BARRERA
- PO 17 Detection of cytochrome c aggregates with polyanions using thioflavin T87**
J. OLAJOŠ, R. VARHAČ, M. ANTALÍK
- PO 18 Triterpenoid-based ionic liquids with enhanced antitumor potency.....89**
P. OSSOWICZ-RUPNIEWSKA, J. KLEBEKO, I. GEORGIEVA, S. APOSTOLOVA, R. TZONEVA, M. GUNCHEVA
- PO 19 Adenine nanolayers on model metal oxide surfaces: XPS and NEXAFS study.....91**
N. POPOVYCH, N. TSUD, K. VELTRUSKA, V. MATOLIN, V. RIZAK



- PO 20 Exciton transfer between LH1 antenna complex and photosynthetic reaction center dimer93**
M. PUDLÁK, R. PINČÁK
- PO 21 Strategies for SERS detection of selected (biomacro)molecules with key importance for human health and environmental protection: nucleic acids and glyphosate.....94**
F. FUENZALIDA SANDOVAL, B. VARCHOLOVÁ, P. MIŠKOVSKÝ, S. SÁNCHEZ-CORTÉS, Z. JURAŠEKOVÁ
- PO 22 Effect of Polymyxin B on the Pulmonary Surfactant Bilayer.....96**
A. Asi SHIRAZI, N. KRÁLOVIČ, A. KESHAVARZI, M. KLACSOVÁ, J.C. MARTÍNEZ, D. UHRÍKOVÁ
- PO 23 New ferrocene-containing pyrazole/pyrimidine analogues of curcumin as inhibitors of amyloid- β peptide aggregation.....98**
K. SIPOSOVA, V. KOVAC
- PO 24 Photopolymer microstructures for intercellular drug transport studies.....100**
C. SLABÝ, J. KUBACKOVÁ, V. PEVNÁ, V. HUNTOŠOVÁ, A. STREJČKOVÁ, Z. TOMORI, G. BÁNO
- PO 25 Fatty acids in the bovine serum albumin structure influence binding parameters in its interaction with fungicide prothioconazole101**
J. STANIČOVÁ, V. VEREBOVÁ
- PO 26 Characterisation and purification of staphylokinase variants developed by ribosome display103**
M. ŠTULAJTEROVÁ, M. TOMKOVÁ, E. SEDLÁK
- PO 27 Study of the interaction of casein micelles with curcumin by fluorescence spectroscopy and dynamic laser scattering105**
V. ŠUBJAKOVÁ, Z. GAGARIOVÁ, T. HIANIK
- PO 28 Thermodynamic properties of the F type ferryl intermediate of the cytochrome *c* oxidase.....106**
A. TOMKOVÁ, T. SZTACHOVÁ, M. FABIÁN, D. JANCURA
- PO 29 Conformation changes of bovine serum albumin caused by binding of fungicide prothioconazole with regard to the presence of fatty acids in the protein molecule.....107**
V. VEREBOVÁ, J. STANIČOVÁ



PLENARY LECTURES



Protein Folding and Dimerization on Ribosomes

Mai Suan Li

Institute of Physics, Polish Academy of Science, Al. Lotnikow 32/46, 02-668 Warsaw, Poland

e-mail: masli@ifpan.edu.pl

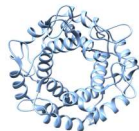
In this talk I will discuss the following problems:

1. Ribosome is a molecular machine for protein synthesis which involves four phases of translation - initiation, elongation, termination and ribosome recycling. This process is an area of intense research due to the essential role of proteins to life. Recently we have shown that electrostatic interactions govern extreme nascent protein ejection times from ribosomes and can delay ribosome recycling [1].
2. The hydrophobic interaction, which plays a key role in protein folding, was well studied in the aqueous environment. However, the water-mediated hydrophobic interaction inside the ribosome exit tunnel has been poorly understood. Using molecular dynamics simulation and umbrella sampling we showed that the hydrophobic effect is weaker in the vestibule. These findings mean that nascent proteins pass through a ribosome vestibule environment that can destabilize folded structures, which has the potential to influence co-translational protein folding pathways, energetics, and kinetics [2].
3. Using coarse-grain simulations of protein synthesis we showed that synonymous mutations can influence the protein dimerization in solution. The structural and kinetic origin of this effect is associated with misfolded states containing non-covalent lasso-entanglements, many of which structurally perturb the dimer interface, whose probability of occurrence depends on translation speed [3].

[1] D. A. Nissley, Q. V. Vu, F. Trovato, N. Ahmed, Y. Jiang, M. S. Li, and E. P. O'Brien, *J. Am. Chem. Soc.* 142, 13, 6103-6110 (2020).

[2] Q. V Vu, Y. Jiang, M. S. Li, E.P. O'Brien, *Chemical Science* 12, 11851 (2021).

[3] L. P. Dang, D. A. Nissley, I. Sitarik, Q. V. Van, Y. Jiang, M. S. Li, E. P. O'Brien, Synonymous mutations can alter protein dimerization through localized interface misfolding involving self-entanglements, doi: <https://doi.org/10.1101/2021.10.26.465867>.



PL 02

PLENARY LECTURES

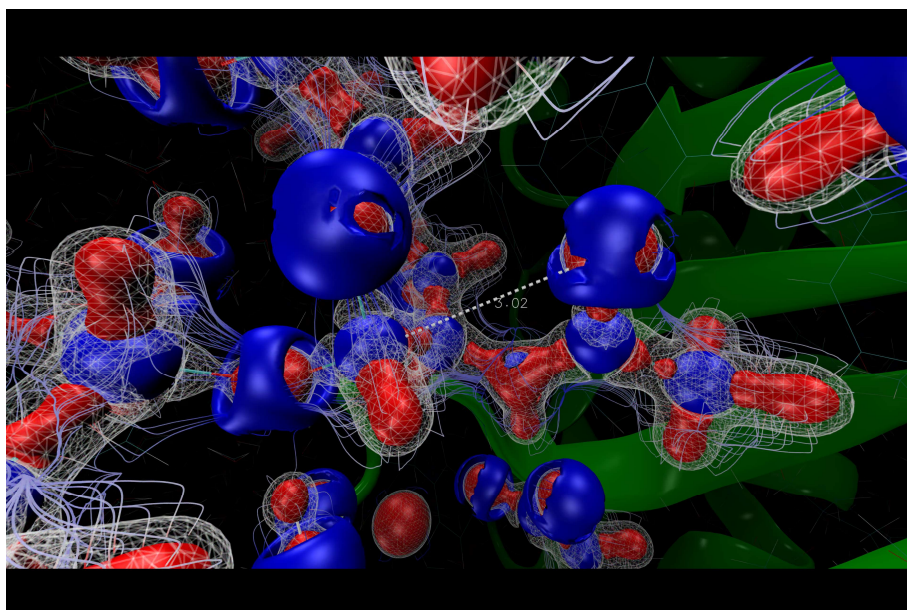
The importance of deep insight into discrete structural features of a target for successful drug design

^aG. WIECZOREK, ^bD. NIEDZIALEK

^a*Molecure S.A. Warsaw, Poland (<https://molecure.com/>)*

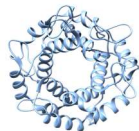
^b*Laboratory of Molecular Basis of Biological Activity, Institute of Biochemistry and Biophysics, Polish Academy of Sciences, Warsaw, Poland*

The understanding of the catalytic process of a targeted enzyme might be a very important step of successful drug design process. Having an experimentally resolved structure is a must. Yet, it is merely a starting point of the way towards understanding the full picture of the enzyme's mechanism of action. I would like to show you a difficult case study [1], when unraveling the enzyme's mode of action led to questioning the current knowledge about its sole purpose.



References

[1] Koralewski, R., Dymek, B., Mazur, M., Sklepkiwicz, P.,..., Olczak, J., Golebiowski, A. (2020). Discovery of OATD-01, a First-in-Class Chitinase Inhibitor as Potential New Therapeutics for Idiopathic Pulmonary Fibrosis. *J. Med. Chem.* 63 (24) 15527



PL 03

PLENARY LECTURES

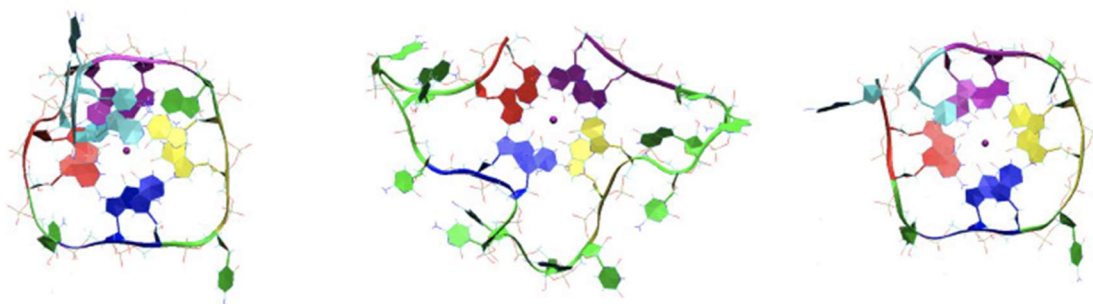
The importance of proper treatment of electrostatics in biomolecular modelling and drug design

^aD. NIEDZIALEK, ^bG. WIECZOREK

^aLaboratory of Molecular Basis of Biological Activity, Institute of Biochemistry and Biophysics, Polish Academy of Sciences, Warsaw, Poland

^bMolecure S.A. Warsaw, Poland (<https://molecure.com/>)

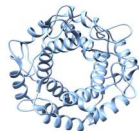
There are several levels of theory we can use for studying biomolecules. For example, in case of RNAs and their interactions with molecular partners, the classical models fail to properly estimate electrostatics that is crucial in highly polarized nucleic acid systems [1]. I would like to show you how to overcome these limitations by using a combination of polarizable force field models and quantum mechanical calculations.



Acknowledgment: This work was supported by the OPUS16 grant 2018/31/B/ST4/03809, funded by the National Science Centre.

References

[1] Göç, Y.B., Poziemski, J., Smolińska, W., Suwała, D., Wieczorek, G., Niedzialek, D. (2022) Tracking Topological and Electronic Effects on the Folding and Stability of Guanine-Deficient RNA G-Quadruplexes. Engineered with a New Computational Tool for De Novo Quadruplex Folding. *Int. J. Mol. Sci.* 23, 10990



Interrogating chaperones by force

G. ŽOLDÁK^{a,b}

^aCenter for Interdisciplinary Biosciences, Technology and Innovation Park, Pavol Jozef Šafárik University, Košice, Slovakia

^bCenter for Interdisciplinary Biosciences, Cassovia New Industry Cluster, CNIC, Košice, Slovakia

Protein stability plays a crucial role in ensuring the proper functioning of proteins within biological systems. When the stability of proteins is compromised, it can result in their unfolding and the formation of harmful aggregates in the body, often leading to serious diseases. The information on protein stability and integrity of protein substructures can be obtained using different techniques.

To gain insights into the mechanical aspects of proteins, I have been employing single-molecule force spectroscopy over the last decade [1-5]. This technique has recently utilized magnetic and laser optical tweezers to investigate chaperones and their interactions with protein clients. By employing mechanical probing strategies, we can uncover various facets of chaperone-client interactions. Firstly, when a chaperone is subjected to external forces, it becomes possible to examine the intricate mechanisms through which the chaperone interacts with and assists the client protein. This allows for a deeper understanding of the inner workings of chaperones during their interactions with client proteins. Secondly, by applying forces to protein clients, scientists can scrutinize the precise actions of chaperones during the folding process. This approach enables detailed investigations into the foldase, unfoldase, and holdase activities of chaperones in real time. These studies provide direct observation of chaperones' roles in facilitating the folding of client proteins.

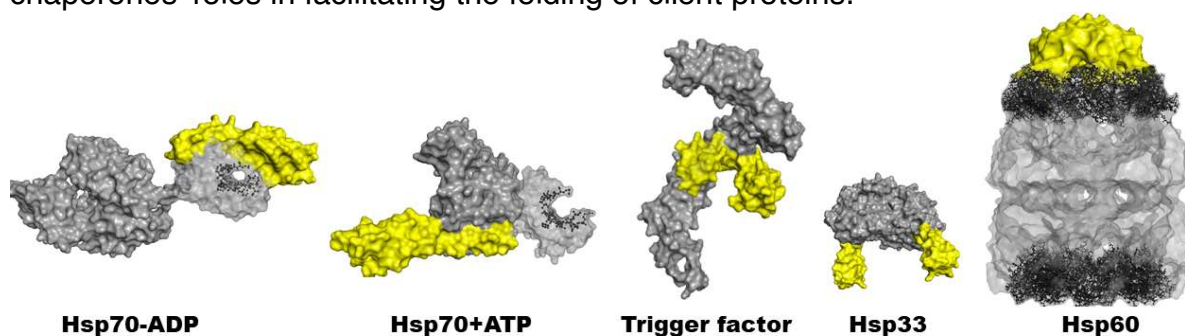
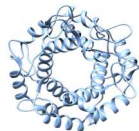


Figure 1: 3D structures of a few selected chaperones, from left to right: *E. coli* Hsp70 in the ADP/ATP form, helical lid shown in yellow, residues involved in peptide binding are shown as ball-and-sticks (PDB codes: 2KHO, NMR-RDC/x-ray structure hybrid, 4B9Q) *E. coli* trigger factor and its touching arms in yellow (PDB code: 1W26), the dimeric form of *Bacillus subtilis* Hsp33 with yellow C-terminal redox sensing domain (PDB code: 1VZY), and *E. coli* Hsp60 and yellow Hsp10 aka GroEL/GroES structure with highlighted apical domain, residues 191–376, as ball-and-sticks.

In my talk, I will present an overview of the various single-molecule mechanical techniques employed in studying proteins. I also summarize recent investigations into

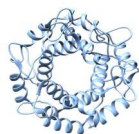


the mechanical aspects of heat shock proteins, chaperone-mediated folding on the ribosome, folding of SNARE proteins, and the involvement of chaperones in the folding of membrane proteins. Additionally, we offer insights into the potential directions for significant advancements in this field in the future.

Acknowledgment. This work was supported by research grants Slovak research and development agency (No. APVV-18-0285), the Slovak Grant Agency VEGA No 1/0024/22, EU H2020 TWINNING program GA. No. 952333 project CasProt, BioPickmol, ITMS2014+: 313011AUW6 supported by the Operational Programme Integrated Infrastructure, funded by the ERDF, and Open scientific community for modern interdisciplinary research in medicine (OPENMED), ITMS2014+: 313011V455 supported by the Operational Programme Integrated Infrastructure, funded by the ERDF.

References

1. Singh A., et al., Biophysical Journal, 2022, 121(23), 4729-4739
2. Žoldák G., Rief M., Biophysics Reviews, 2022, 3, 041301
3. Žoldák G. Nanomaterials, 2022, 12, 3524
4. Žoldák G., et al., Proc. Natl. Acad. Sci USA, 2013, 110, 18156-18161
5. Žoldák G., Rief M., Curr. Opinion Struct. Biol. 2013, 23, 48-57



Insights into the Alzheimer's disease specific pre-aggregation fold of tau proteins using conformational antibodies

^aO. CEHLAR*, ^aS. NJEMOGA, ^{a,b}J. PIESTANSKY, ^cZ. BEDNARIKOVA, ^aR. SKRABANA, ^{d,f}R. CRHA, ^{d,e}J. HRITZ, ^dP. KADERAVEK, ^aL. FIALOVA, ^aB. KOVACECH

^a Institute of Neuroimmunology, Laboratory of Structural Biology of Neurodegeneration, Slovak Academy of Sciences, Bratislava, Slovakia

^b Faculty of Pharmacy, Department of Galenic Pharmacy, Comenius University, Bratislava, Slovakia

^c Institute of Experimental Physics, Department of Biophysics, Kosice, Slovakia

^d CEITEC MU, Brno, Czech Republic

^e Faculty of Science, Department of Chemistry, Masaryk University, Brno, Czech Republic

^f Institute of Molecular Modeling and Simulation (MMS), BOKU, Wien, Austria

A key yet unresolved question of the pathogenesis of Alzheimer's disease (AD) and other tauopathies is the cause and the mechanism of the transition from the unstructured monomeric tau protein to the insoluble filaments deposited in the brain tissue. In the physiological state, tau protein exists as a conformational ensemble of interconverting structures and on the scale of transition from monomeric through oligomeric and filamentous species we can observe conformations reacting with specific antibodies, mainly with DC11, which is able to specifically discriminate between tau proteins isolated from healthy brain and tau proteins isolated from the brain of AD patient. The antibody recognizes also the recombinant truncated tau proteins up to the shortest fragment tau321-391 [1].

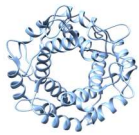
It was found that conformational antibodies DC11 and MN423 have catalytic pro-aggregatory effects in tau aggregation assay, whereas the antibody DC8E8 has inhibitory effects on tau filament formation [2]. This may imply possible mechanism of induction of pathological tau conformation, in which the antibody prepared against pathological tau imprints the pathological conformation into the physiological tau proteins in solution and therefore speeds up the tau aggregation. The information about conformational epitopes of these antibodies are therefore of high significance.

To further uncover the binding mode of the conformational antibody DC11, we have performed NMR epitope mapping using ¹³C,¹⁵N labeled tau321-391 and recombinantly prepared Fab fragment of DC11 antibody. The overlay of HSQC spectra showed the region of tau between residues 370-390 to be affected by the binding of DC11, i.e. its C-terminal region. However, previous studies suggest the importance of region 321-325 for the interaction of tau with DC11 antibody.

We have crystallized the Fab fragment of DC11 (Fig. 1) and used it for in silico docking of tau peptides.

Moreover, we have shown the ability of tau321-391 to aggregate despite the lack of aggregation prone VQIxxK hexapeptide regions.

The results highlight the importance of the R¹ region of tau, that was recently shown to be important also for tau interaction with microtubules [3]. This sequence



forms the interface of rigid filament core and flanking fuzzy C terminal segment in solved tauopathy filaments.

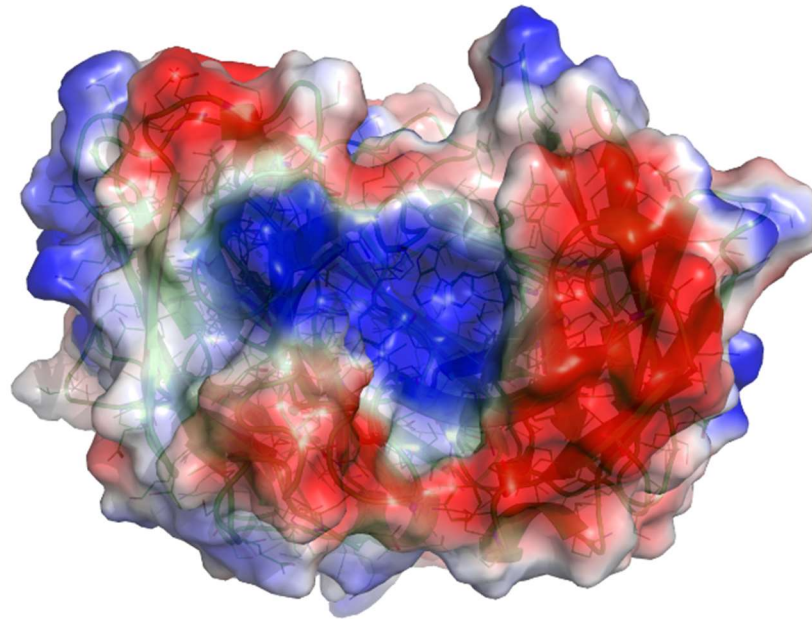
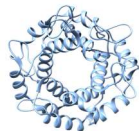


Figure 1 paratope of DC11 Fab fragment shown as a transparent surface colored according to the electrostatic potential.

Acknowledgment. This work was supported by research grants APVV 21-0479, VEGA 2/0125/23 and 2/0141/23, MSCA-RISE 873127, and by iNEXT-Discovery, grant number 871037, and MSCA-RISE 873127, both funded by the Horizon 2020 program of the European Commission.

References

1. Vechterova, L.; Kontsekova, E.; Zilka, N.; Ferencik, M.; Ravid, R.; Novak, M. (2003). DCII: a novel monoclonal antibody revealing Alzheimer's disease-specific tau epitope. *Neuroreport*, 14 (1), 87-91;
2. Kontsekova, E.; Zilka, N.; Kovacech, B.; Skrabana, R.; Novak, M. (2014). Identification of structural determinants on tau protein essential for its pathological function: novel therapeutic target for tau immunotherapy in Alzheimer's disease. *Alzheimers Res Ther*, 6 (4), 45. <https://doi.org/10.1186/alzrt277>.
3. El Mammeri, N., Dregni, A. J., Duan, P., Wang, H. K., Hong, M. (2022) *Sci. Adv.*, 8, 4459 <https://doi.org/10.1126/sciadv.abo4459>



Identifying a new aggregation hotspot in Alzheimer's disease: Opportunities for drug discovery

^{a,b}M. NEMERGUT

^aCenter for Interdisciplinary Biosciences, Technology and Innovation Park, P. J. Safarik University in Kosice, Trieda SNP 1, 04011 Kosice, Slovakia

^bLoschmidt Laboratories, Department of Experimental Biology, Faculty of Science, Masaryk University, Kamenice 5, 625 00 Brno, Czech Republic

Apolipoprotein E (ApoE) $\epsilon 4$ genotype is the most prevalent risk factor for late-onset Alzheimer's Disease (AD) [1]. Although ApoE4 differs from its non-pathological ApoE3 isoform only by the C112R mutation, the molecular mechanism of its proteinopathy is unknown. Here, we reveal the molecular mechanism of ApoE4 aggregation using a combination of experimental and computational techniques, including X-ray crystallography, site-directed mutagenesis, hydrogen-deuterium mass spectrometry (HDX-MS), static light scattering and molecular dynamics simulations. Treatment of ApoE $\epsilon 3/\epsilon 3$ and $\epsilon 4/\epsilon 4$ cerebral organoids with tramiprosate was used to compare the effect of tramiprosate on ApoE4 aggregation at the cellular level [2].

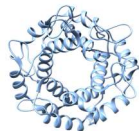
We found that C112R substitution in ApoE4 induces long-distance (>15 Å) conformational changes leading to the formation of a V-shaped dimeric unit that is geometrically different and more aggregation-prone than the ApoE3 structure. AD drug candidate tramiprosate and its metabolite 3-sulfopropanoic acid induce ApoE3-like conformational behavior in ApoE4 and reduce its aggregation propensity. Analysis of ApoE $\epsilon 4/\epsilon 4$ cerebral organoids treated with tramiprosate revealed its effect on cholesteryl esters, the storage products of excess cholesterol.

Our results connect the ApoE4 structure with its aggregation propensity, providing a new druggable target for neurodegeneration and ageing.

Acknowledgment. This work was supported by research grants Slovak research and development agency (No. APVV-18-0285), EU H2020 TWINNING program GA. No. 952333 project CasProt, BioPickmol, ITMS2014+: 313011AUW6 supported by the Operational Programme Integrated Infrastructure, funded by the ERDF.

References

1. Sadigh-Eteghad S, Talebi M, Farhoudi M. Association of apolipoprotein E epsilon 4 allele with sporadic late onset Alzheimer's disease. A meta-analysis. *Neurosciences (Riyadh)*. 2012;17:321–6.
2. Nemergut M, Marques SM, Uhrík L, Vanova T, Nezvedova M, Gadara DC, et al. Domino-like effect of C112R mutation on ApoE4 aggregation and its reduction by Alzheimer's Disease drug candidate. *Molecular Neurodegeneration*. 2023;18:38.



Occurrence and use of non-canonical nucleic acid structural motifs in nanotechnology

V. VÍGLASKÝ, L. TRIZNA

Department of Biochemistry, Institute of Chemistry, Faculty of Sciences, Pavol Jozef Šafárik University, 04001 Košice, Slovakia

Nucleic acids are capable of taking on different secondary structures, which depend mainly on their sequence. Due to their unique properties, these structural forms play a key role in gene expression in living cells. Therefore, the identification and prediction of sequences forming non-canonical motifs in regulatory regions of the genome is essential, for example, to find the specific target molecule that influences the formation of such a motif. An alternative approach to search for sequences forming non-canonical motifs has recently been developed in our laboratory [1,2]. In addition, non-canonical motifs contain many aptamers that are applied in biomedical research as sensing molecules and have recently been used to functionalize next-generation nanoparticles.

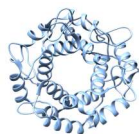
In addition, non-canonical motifs contain many aptamers, which are applied in biomedical research as sensor molecules and have recently been used to functionalize next-generation nanoparticles.

Our recent advances in the structural stability of tetrahelical non-canonical forms of nucleic acids and DNA nanorings and three-way junctions consisting of non-canonical motifs will be presented, as well as a completely new motif predicted by us.

Acknowledgment. This work was supported by the Slovak Grant Agency (1/0347/23), and an internal university grant (VVGS-PF-2022-2122). Funding for open access charge: Slovak Grant Agency.

References

1. Trizna L, Osif B, Víglaský V. (2023). G-QINDER Tool: Bioinformatically Predicted Formation of Different Four-Stranded DNA Motifs from (GT)_n and (GA)_n Repeats. *Int J Mol Sci.* 24, 7565
2. Víglaský V. (2022). Hidden Information Revealed Using the Orthogonal System of Nucleic Acids. *Int J Mol Sci.* 23, 1804



Study of the Dynamics of Flexible Subunits of RNA Polymerase from *Bacillus subtilis*

^aD. TUŽIŇČIN, ^bN. SALVI, ^aV. ZAPLETAL, ^aZ. JASEŇÁKOVÁ, ^cM. ZACHRDLA, ^dP. PADRTA, ^aS. NARASIMHAN, ^eT. MARQUARDSEN, ^fJ.-M. TYBURN, ^gH. ŠANDEROVÁ, ^gA. RABATINOVÁ, ^aK. BENDO VÁ, ^gL. KRÁSNÝ, ^aL. ŽÍDEK, ^bM. BLACKLEDGE, ^cF. FERRAGE, ^dP. KADERÁVEK

^aNational Centre for Biomolecular Research, Faculty of Science and Central European Institute of Technology, Masaryk University, Brno, Czech Republic

^bInstitut de Biologie Structurale (IBS), CEA, CNRS, University Grenoble Alpes, Grenoble, France

^cLaboratoire des Biomolécules, LBM, Département de chimie, École normale supérieure, PSL University, Sorbonne Université, CNRS, Paris, France

^dCentral European Institute of Technology, Masaryk University, Brno, Czech Republic

^eBruker BioSpin GmbH, Rheinstetten, Germany,

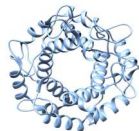
^fBruker BioSpin, Wissembourg Cedex, France

^gLaboratory of Microbial Genetics and GeneExpression, Institute of Microbiology, Czech Academy of Sciences, Prague, Czech Republic

The RNA polymerase found in Gram-positive bacteria is composed of multiple subunits, some of which exhibit interesting dynamic behaviors at various timescales. Nuclear magnetic resonance (NMR) is known as a unique technique capable of delivering insights into protein motions with atomic resolution. While analyzing the internal motion of structured proteins within the picosecond to nanosecond timescale relies on a well-established approach involving relaxation rate measurements and analysis [1], investigating the dynamics of intrinsically disordered proteins (IDPs) proves notably more challenging task for multiple reasons (complexity of motions, signal overlaps in NMR spectra, etc.).

This study presents an exploration of the C-terminal domain of the delta subunit of RNA polymerase, which represents a disorder region posing particular investigative challenges. In order to obtain detailed information about significant, slower segmental motions occurring within the nanosecond timescale, a specialized NMR methodology called high-resolution relaxometry [2] was employed. This approach resulted in a collection of unprecedented amounts of data covering the relaxation of backbone amides under a broad range of magnetic fields spanning two orders of magnitude. In order to validate the analysis process, a novel NMR experiment was devised, enabling the measurement of relaxation rates at an exceptionally low magnetic field strength (0.33 T)[3] using a unique two-field NMR spectrometer [4]. This experiment successfully confirmed the applied protocol and analysis methods.

Beyond its ability to study rapid picosecond-to-nanosecond motions, NMR enables the exploration of slower structural rearrangements through the analysis of relaxation dispersion experiments [5]. These experiments provide access to motions at the microsecond-to-millisecond timescale. Such motions are typically associated



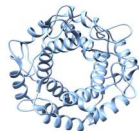
with important biological functions of biomolecules and they were detected also within domain 1.1 of the sigma subunit of the RNA polymerase.

Analyzing the results of relaxation dispersion experiments revealed that the studied domain naturally inclines toward adopting a more disordered state, even at room temperature. By extending the study to multiple temperatures, the thermodynamic parameters associated with this transition were determined, and an increasing significance of the observed event with rising temperatures was predicted. Complementing the investigation was a functional characterization of domain 1.1 and results clearly proved the biological importance of the identified phenomena.

This work was supported by the Czech Science Foundation grant Nos. GJ18-04197Y and 22-12023S, from European Regional Development Fund-Project MSCA-fellow2@MUNI (No. CZ.02.2.69/0.0/0.0/18 070/0009846) and grant no. ANR-18-CE29-0003 (NANO-DISPRO), provided by Agence Nationale de la Recherche. In addition, the project National Institute of Virology and Bacteriology (Programme EXCELES, ID ProjectNo. LX22NPO5103) — Funded by the European Union—Next Generation EU is acknowledged.

References

1. Korzhnev, D.M., Billeter, M., Arseniev, A.S., & Orekhov, V.Y. (2001). NMR studies of Brownian tumbling and internal motions in proteins. *Progress in Nuclear Magnetic Resonance Spectroscopy*, 38 (3), 197-266.
2. Redfield A.G. (2003). Shuttling device for high-resolution measurements of relaxation and related phenomena in solution at low field, using a shared commercial 500 MHz NMR instrument. *Magnetic Resonance in Chemistry*, 41(10), 753-768
3. Jaseňáková Z., Zapletal V., Padrta P., Zachrdla M., Bolik-Coulon N., Marquardsen T., Tyburn J., Žídek L., Ferrage F., Kadeřávek P. (2020). Boosting the resolution of low-field ¹⁵N relaxation experiments on intrinsically disordered proteins with triple-resonance NMR. *Journal of Biomolecular NMR*, 74(2-3), 139-145
4. Cousin S.F., Charlier C., Kadeřávek P., Marquardsen T., Tyburn J.M., Bovier P.A., Ulzega S., Speck T., Wilhelm D., Engelke F., Maas W., Sakellariou D., Bodenhausen G., Pelupessy P., Ferrage F. (2016). High-resolution two-field nuclear magnetic resonance spectroscopy. *Physical Chemistry Chemical Physics*, 18(48), 33187–33194
5. Sekhar A., Kay L.E. (2013). NMR paves the way for atomic level descriptions of sparsely populated, transiently formed biomolecular conformers. *The Proceedings of the National Academy of Sciences*, 110(32), 12867-12874



Short-range folding of intrinsically disordered proteins

^aR. SKRABANA, ^aK. MARTONOVA, ^aO. CEHLAR, ^bM. HRICOVINI, ^bM. HRICOVINI,
^aK. MESKOVA, ^cP. KADERAVEK, ^aS. NJEMOGA, ^aK. TOMKOVA

^a *Institute of Neuroimmunology, Laboratory of Structural Biology of Neurodegeneration, Slovak Academy of Sciences, Bratislava, Slovakia*

^b *Institute of Chemistry, Analytical Department and Department of Structure and Function of Saccharides, Slovak Academy of Sciences, Bratislava, Slovakia*

^c *CEITEC MU, Brno, Czech Republic*

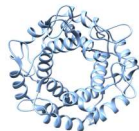
Phenomenon of protein intrinsic disorder is gaining an increasing attention for the past two decades [1]. In water solutions, intrinsically disordered (ID) proteins (IDPs) and ID protein regions contain no stable three-dimensional structure. ID polypeptide chain is nearly completely hydrated and highly flexible; therefore, IDP conformations are composing a conformational ensemble (CE). Individual members of CE are separated by a small energy barrier and easily interconvert [2].

Conformational and folding properties of proteins are dictated by the pattern of hydrogen bonds created by them. Globular proteins have the polypeptide backbone largely protected from solution; hydrogen bonds involving their main-chain atoms are in majority intramolecular, forming well-known structural elements of beta sheets and alpha helices. In contrast, IDPs satisfy hydrogen-bonding potential of their main chain almost exclusively by intermolecular hydrogen bonding to the solvent molecules. It is not yet clear how important could be hydrogen bonds if formed within the IDP molecules.

Working with IDP tau we found some intramolecular hydrogen bonds between side chain and main chain atoms, which may be important for the tau protein function. We can observe these bonds in crystal structure of tau complexes [3]. They are formed locally and create small 9-15 membered ring structures. Results of simulations indicate that these rings are stable only for short periods of time and frequently renew their existence. Quantum mechanics calculations revealed the proportion of rings in the local CE; experiments on cell lines showed indications of their potential biological significance

We identified in the literature various types of possible small hydrogen bond rings and we are presenting their overview. The ring structures can be found in the solved X-ray structures and/or detected experimentally on small dipeptides and tripeptides, mostly in the gas phase.

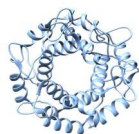
For these structures we coined the name SPuRs – Side chain Propelled Rings. It is hypothesized that these small ring structures influence the composition of IDP CE and may regulate corresponding biological activity. In the future work we aim to examine the SPURS also in other IDPs.



Acknowledgment. This work was supported by research grants APVV 21-0479, VEGA 2/0125/23 and 2/0141/23, and MSCA-RISE 873127 funded by the Horizon 2020 program of the European Commission.

References

1. J. Habchi, P. Tompa, S. Longhi, and V. N. Uversky, "Introducing protein intrinsic disorder," *Chem Rev*, vol. 114, no. 13, pp. 6561–6588, Jul. 2014, doi: 10.1021/cr400514h.
2. F. E. Thomassen and K. Lindorff-Larsen, "Conformational ensembles of intrinsically disordered proteins and flexible multidomain proteins," *Biochem Soc Trans*, vol. 50, no. 1, pp. 541–554, Feb. 2022, doi: 10.1042/BST20210499.
3. O. Cehlar, O. Bagarova, L. Hornakova, and R. Skrabana, "The structure of the unstructured: mosaic of tau protein linear motifs obtained by high-resolution techniques and molecular simulation," *Gen Physiol Biophys*, vol. 40, no. 6, pp. 479–493, Nov. 2021, doi: 10.4149/gpb_2021031.



Effects of photobiomodulation on oxidative stress and α -synuclein in 2D model of Parkinson's disease

^aK. STROFFEKOVA, ^aE. WETTER, ^aS. TOMKOVA

^aDepartment of Biophysics, Institute of Physics, PJ Safarik University, Kosice, Slovakia

According to the World Health Organization (WHO), the proportion of the world's population over 60 years will nearly double from 12% to 23% by 2050. With this in mind, neurodegenerations are projected to show up to a 66% increase, which poses a great socio-economic impact. The etiology of the most neurodegenerations is not clear, however, interactions between genetic and environmental factors, lifestyles and dietary factors were shown to play a role in Parkinson's (PD), Alzheimer (AD) diseases and ALS (amyotrophic lateral sclerosis). Long-term/low dose exposure to metals, pesticides, solvents, and petrochemicals are indicated as environment risk factors in PD, AD and ALS [1]. Parkinson's disease (PD) is a progressive neurodegenerative disorder characterized by the loss of dopaminergic neurons in the *substantia nigra pars compacta* (SNc) and accumulation of insoluble cytoplasmic protein inclusions, including α -synuclein (α SNC), referred to as Lewy bodies [2]. It is now widely accepted that oxidative stress, impairment of mitochondrial dynamics and function, calcium overload and balance disruption between apoptosis and autophagy are the key mechanisms underlying the pathogenesis of both sporadic and familial PD. PD was positively associated with two groups of pesticides, including rotenone (ROT) and paraquat (PAR) [2]. The ROT and PQ are used extensively in *in vitro* and *in vivo* PD models. Photobiomodulation (PBM) by low-level near infrared (NiR) radiation was shown to have positive effects in cell repair processes and proliferation, in wound healing, muscle repair, and angiogenesis. In last decade, there are reports of the PBM beneficial effects in PD and AD, and in treatment of traumatic brain injuries including stroke. PBM was shown to prevent mitochondrial dysfunction and dopamine loss in Parkinson's disease patients [3].

The aim of the present work was to study the PBM effects on oxidative stress and α SNC in 2D cellular model of Parkinson's disease (PD). First, we have established 2D model of PD by using human neuroblastoma cell line SH-SY5Y and ROT treatment. To model long term low concentration exposure, we treated SH-SY5Y cells 48 hrs with increasing ROT concentration gradient from 100nM to 10 μ M. The SH-SY5Y viability decreased with increasing ROT concentration. Cell viability decreased down to 50 \pm 3% at the concentrations above 500nM. For our PD model, we have then used 200nM ROT, where SH-SY5Y viability was 77 \pm 1%. As a next step, we determined that the PBM irradiation dose of 1J/cm² at wavelength 808 nm had the most desirable effect on cell viability, it increased the ROT treated cell viability by 20%. With the established framework of our model and PBM dose (200nM Rot for 48hr, NiR 1J/cm²), we then investigate key aspects of PD in cells. We have shown that ROT treatment induced mitochondria dysfunction and fragmentation, and that PBM prompted mitochondria fusion. In the next step, we had investigated oxidative stress in mitochondria and in whole cell in ROT treated cells. The chronic ROT treatment (200nM Rot for 48hr) significantly increased level of superoxide in mitochondria, detected by specific fluorescent probe MitoSOXRed, whereas PBM treatment decreased oxidative stress in cells exposed to ROT comparable with the antioxidant N-acetylcystein (NAC) (Fig.1).

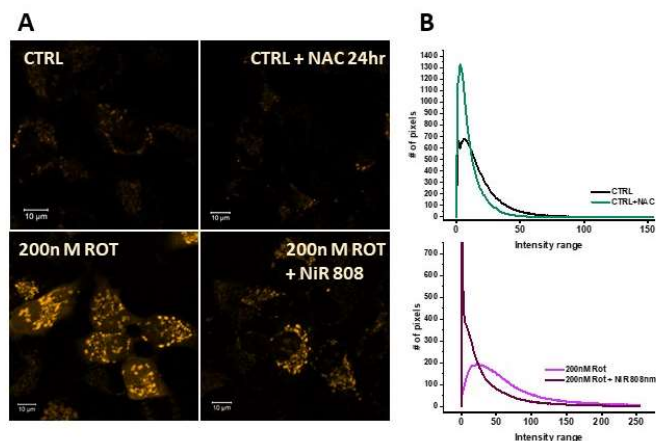
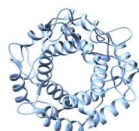


Figure 1. PBM effect on ROT induced mitochondrial oxidative stress in SH SY5Y cells

It has been shown previously that the ROT PD models replicated clinical pathological features such as dopaminergic cell loss and alpha-synuclein (aSN) inclusions (Lewy bodies and neurites) [2]. Therefore, we have looked at level of α -synuclein (α SNC) in our cells. We have aimed to look at the levels of α SNC monomer

and aggregates with specifically designed antibodies, respectively (ab138501, ab209538; Abcam). Our results show that control SH-SY5Y cells have a low level of α SNC monomer. ROT treatment increased α SNC monomer level. PBM further increased α SNC monomer level in both, control and ROT cells. Level of α SNC aggregates are appreciably higher than α SNC monomer in control and ROT treated cells. However, in contrast with α SNC monomer, PBM treatment notably decreased level of α SNC aggregates in both, control and ROT cells (Fig.2). This effect is most likely caused by autophagy activation, however, we have to do some more investigation in this matter.

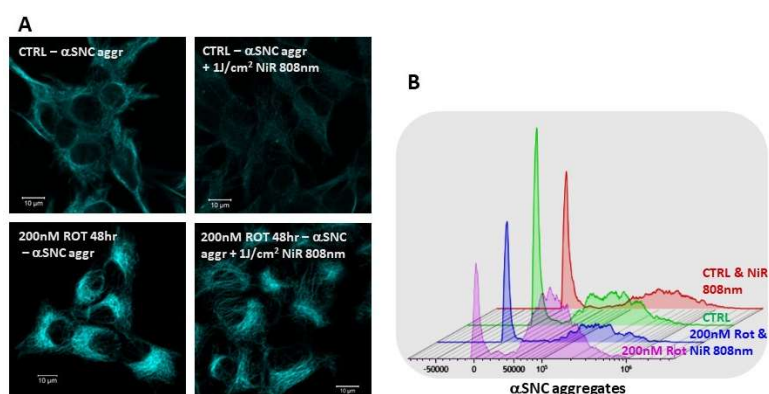


Figure 2. PBM effect on ROT α SNC aggregates in SH SY5Y cells.

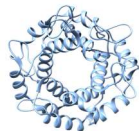
In conclusion, we have established ROT induced 2D PD model using SH-SY5Y cells, which displays increased oxidative stress, impairment of mitochondrial dynamics and function, and α SNC aggregates. We have shown that PBM treatment can alleviate PD

symptoms at the cellular level. These results can be the groundwork for a PBM therapy research in more complex systems such as 3D organoids, in the animal model in vivo, followed by possible preclinical studies.

Acknowledgment. This work was supported by the EU ERDF grant OPENMED (ITMS2014+: 313011V455), by the Slovak Grant Agency VEGA 1/0421/18;1/0557/20 and 1/0187/23; and by the Slovak Research and Development Agency APVV-21-0333.

References

1. Baltazar MT, Dinis-Oliveira RJ, de Lourdes Bastos M, Tsatsakis AM, Duarte JA, Carvalho F. (2014) Pesticides exposure as etiological factors of Parkinson's disease and other neurodegenerative diseases--a mechanistic approach. *Toxicol Lett.* 230(2), 85-103
2. Rocha EM., De Miranda B., Sanders LH. (2018) Alpha-synuclein: Pathology, mitochondrial dysfunction and neuroinflammation in Parkinson's disease, *Neurobiology of Disease*, 109(B), 249-257
3. Hamblin, M.R., & Huang, Y. (Eds.). (2013). *Handbook of Photomedicine* (1st ed.). CRC Press. <https://doi.org/10.1201/b15582>



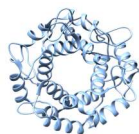
Ion-Specific Effects in Biological Systems

M. KHAJEHPOUR, I. ASAKEREH, B. T. SHARAKI, H. REZASOLTANI

Department of Chemistry, University of Manitoba, Winnipeg, Manitoba, Canada State

The addition of salt to aqueous solvent affects the thermodynamics of bio-molecules in an ion specific manner. The most well-known of these effects is seen in the salt induced precipitations of proteins, where the rank ordering of ions in terms of their precipitation efficacy results in the Hofmeister series. In addition to protein precipitation, ion-specific effects are also observed in protein folding, protein aggregation and enzyme kinetics. In this talk, we demonstrate a general methodology for analyzing salt effects on bio-molecular processes through introducing salt specific effects on folding and catalysis in a few model protein systems (RNase A, Melittin and Paratox), and also suggest interaction mechanisms that may contribute to the observed ion specificity.

Acknowledgment: This work was supported by NSERC-Canada research grant number 5933-217.



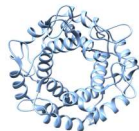
Ryanodine receptor inactivation by divalent ions

A. ZAHRADNÍKOVÁ, J. PAVELKOVÁ, I. ZAHRADNÍK

Department of Cellular Cardiology, Institute of Experimental Endocrinology, Biomedical Research Center, Slovak Academy of Sciences, Bratislava, Slovakia

Ryanodine receptors play a central role in the excitation-contraction coupling of skeletal and cardiac muscle cells, where upon cell excitation they release calcium from the sarcoplasmic reticulum into the cytosol, and so trigger contractile response. The skeletal isoform RyR1 and the cardiac isoform RyR2 differ in the physiological mechanism of activation (voltage- vs calcium-dependent) but their regulation by small cytosolic molecules (ATP, xanthines) and ions (Ca^{2+} , Mg^{2+}) is qualitatively similar. Also, their molecular architecture is almost identical despite their overall sequence identity of only 60% [1], and amino acid residues constituting the binding sites for the activators Ca^{2+} , ATP, and xanthines are conserved between isoforms [2]. At a low Ca^{2+} concentration in *in vitro* experiments, magnesium ions increase the EC_{50} of Ca^{2+} -dependent activation of both RyR isoforms. At high Ca^{2+} concentrations, both ions cause RyR inactivation, supposedly by binding to an inhibition site. Both divalent ions seem to have equal inhibitory potency at both RyR isoforms [3], but the RyR1 isoform is inactivated at much lower concentrations than RyR2. This observation was attributed to a lower sensitivity of the RyR2 inhibition site compared to that of RyR1 [2]. The respective inhibition sites, that is, positions of divalent ions in the inactivated RyR structures, were not resolved yet in either RyR isoform. There are indications, however, that the EF-hand region, containing the EF-hand motifs EF1 and EF2, as well as the cytosolic segment between membrane helices S2 and S3 (S2S3 segment), are involved in RyR inhibition by divalent ions. Functional studies based on scrambling of the ion-coordinating residues of EF1 or introducing mutations leading to malignant hyperthermia to the S2S3 residues F4732, G4733, or R4736 revealed that these interventions decreased the sensitivity of RyR1 to inactivation, in some cases down to the same level as observed in RyR2 [4,5]. However, the S2S3 residues are conserved between RyR1 and RyR2; therefore, their contribution to the differences between inactivation of RyR1 and RyR2 is not clear. Several cryo-EM structures of RyR1 in the inactivated state are available, in which the EF-hand region and the S2S3 segment are in close contact; however, Ca atoms were not observed there even when Ca^{2+} concentration in the reconstitution medium was very high. At the same time, Ca atoms were observed at the activation site and in the ATP-binding cavity [6].

To elucidate the mechanism of RyR inactivation we have analyzed Ca^{2+} binding to the EF-hands EF1 and EF2 in RyR1 and RyR2 using bioinformatics, and compared the published structures of RyR1 and RyR2 in the closed, primed, open, and inhibited conformations. We found that a stronger binding of Ca^{2+} to EF1 and EF2 is predicted to occur in RyR2 than in RyR1, contrary to expectations. We hypothesize that the different sensitivity of RyR1 and RyR2 to divalent ion-induced inactivation is not caused

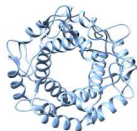


by differences in ion binding but is very likely caused by a different transmission of the inhibitory signal between the inhibition site and the channel gate. An additional pathway should be present in RyR1, in which the occupied inhibition site promotes inactivation directly by transmitting the signal from the EF-hand region to the gating site via the S2S3 segment.

Acknowledgment. This work was supported by research grants JRP/2019/836/RyRinHeart, ERA-CVD_JTC2019-055, VEGA 2/20182/21, and APVV-21-0443.

References

1. Sorrentino, V. & Volpe, P. (1993). Ryanodine receptors: how many, where and why? Trends in Pharmacological Sciences, 14, 98-103
2. Meissner, G. (2017). The structural basis of ryanodine receptor ion channel function. Journal of General Physiology 149(12), 1065-1089
3. Laver, D.R., Baynes, T.M. & Dulhunty, A.F. (1997). Magnesium inhibition of ryanodine-receptor calcium channels: Evidence for two independent mechanisms. Journal of Membrane Biology 156, 213-229
4. Gomez, A.C. & Yamaguchi, N. (2014). Two regions of the ryanodine receptor calcium channel are involved in Ca(2+)-dependent inactivation. Biochemistry, 53(8), 1373-9
5. Gomez, A.C., Holford, T.W. & Yamaguchi, N. (2016). Malignant hyperthermia-associated mutations in the S2-S3 cytoplasmic loop of type 1 ryanodine receptor calcium channel impair calcium-dependent inactivation. American Journal of Physiology, 311(5), C749-C757
6. Nayak, A.R. & Samsó, M. (2022) Ca(2+) inactivation of the mammalian ryanodine receptor type 1 in a lipidic environment revealed by cryo-EM. eLife, 11, e75568



The effect of the central-helix mutations on the stability and dynamic motion of the N-terminal domain of the human ryanodine receptor 2

V. BAUEROVA-HLINKOVÁ, T. HROMÁDKOVÁ, E. KUTEJOVÁ, J. A. BAUER

Institute of Molecular Biology Slovak Academy of Sciences, Dúbravská cesta 21, 845 51 Bratislava, Slovakia

Regular heart activity is one of the requirements of human life. Ryanodine receptor 2 (hRyR2) plays a key role in this process. hRyR2 is a large homotetramer (MW ~ 2.3 MDa) in which each subunit consists of nearly 5000 amino acids [1]; it is expressed primarily in cardiac muscle. hRyR2 is a multidomain transmembrane protein (Fig. 1A) localized to the sarcoplasmic reticulum (SR) membrane, where it provides excitation-contraction coupling through a mechanism known as Ca²⁺-induced Ca²⁺ release (CICR) [1; 2]. hRyR2 dysfunction, which is often caused by point mutations in its gene, is associated with several arrhythmias, including CPVT1, SCD, ARVC/D2, SIDS, and heart failure; it is also associated with colorectal cancer (<https://www.hgmd.cf.ac.uk/ac/gene.php?gene=RYR2>). The causes of these diseases and their molecular mechanisms are, in many cases, unknown.

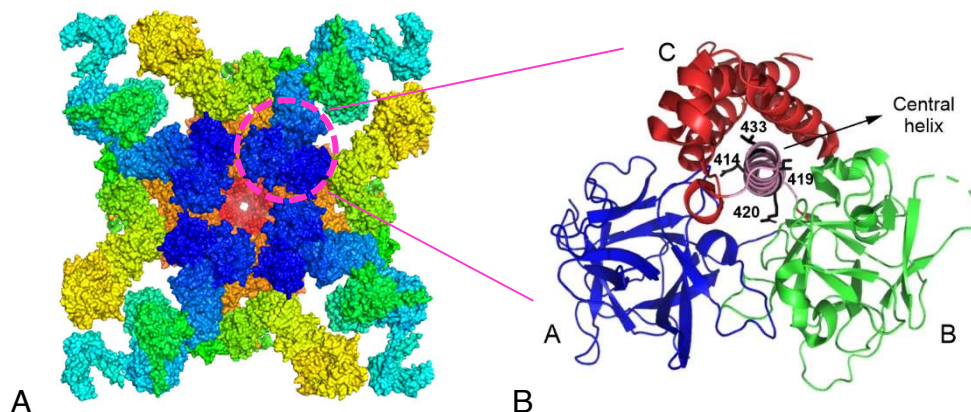
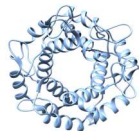


Fig. 1. A. Homotetrameric structure of human RyR2 determined by cryo-electron microscopy. View from the cytoplasmic side. The N-terminal domain (NTD) is shown in blue and circled. B. Crystal structure of the hRyR2 NTD determined by X-ray crystallography (PDB 4JKQ). The NTD consists of three subdomains: A, B and C. The central helix (salmon) together with the residues whose mutations are associated with cardiac arrhythmias are indicated.

The structure of the entire RyR2 homotetramer has been determined by electron microscopy (Fig.1A) in both open and closed conformations [3] as well as in complex with several modulators that regulate RyR2's gating [4, 5, 6]. The structure of the N-terminal domain of hRyR2 (NTD) was also determined by X-ray crystallography (Fig.1B) [7] where an important role was revealed for the central helix in NTD stability. In the central helix there are several residues – R414, I419, R420 [8] and L433 (Fig.1B)

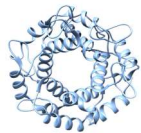


– whose mutations are associated with the diseases listed above. Our biophysical and molecular dynamics studies showed that mutations in these residues can cause substantial differences in the dynamic motion of the NTD subdomains, which might, at least in part, modify the dynamics of the whole hRyR2 and in this way contribute to cardiac arrhythmias.

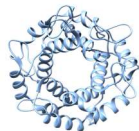
Acknowledgment. This work was financially supported by the Slovak Grant Agency VEGA, grant 2/0131/20 and Interreg SK-AT StruBioMol ITMS: 305011X666.

References

- Otsu K., Willard H.F., Khanna V.K., Zorzato F., Green N.M., MacLennan D.H. 1990. *J. Biol. Chem.* 265: 13472-13483
- Nakai J, Imagawa T, Hakamat Y, Shigekawa M, Takeshima H, Numa S. *FEBS Lett.* 1990 Oct 1;271(1-2):169-77. doi: 10.1016/0014-5793(90)80399-4
- Peng W., Shen H., Wu J., Guo W., Pan X., Wang R., Chen S.R., Yan N. 2016. *Science* 354: 301
- Chi X., Gong D., Ren K., Zhou G., Huang G., Lei J., Zhou Q., Yan N. *Proc Natl Acad Sci U S A.* 2019 Dec 17;116(51):25575-25582. doi: 10.1073/pnas.1914451116
- Gong D., Chi X., Wei J., Zhou G., Huang G., Zhang L., Wang L., Lei J., Chen S.R.W., Yan N. *Nature.* 2019 Aug;572(7769):347-351. doi: 10.1038/s41586-019-1377-y
- Dhindwal S, Lobo J, Cabra V, Santiago DJ, Nayak AR, Dryden K, Samsó M. *Sci Signal.* 2017 May 23;10(480):eaai8842. doi: 10.1126/scisignal.aai8842
- Borko Ľ., Bauerová-Hlinková V., Hostinová E., Gašperík J., Beck K., Lai F.A., Zahradníková A., Ševčík J. 2014. *Acta Cryst. D70:* 2897-2921
- Bauer J.A., Borko Ľ., Pavlović J., Kutejová E., Bauerová-Hlinková V. 2020. *J Biomol Struct Dyn.* 2020 Mar;38(4):1054-1070. doi: 10.1080/07391102.2019.1600027



SHORT COMMUNICATIONS



Computational evolutionary analysis of insertion and deletion events in bacterial Hsp70

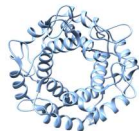
^aM. GALA, ^bG. ŽOLDÁK

^a*Department of Biophysics, Institute of Physics, P. J. Šafárik University, Košice, Slovakia*

^b*Center for Interdisciplinary Biosciences, Technology and Innovation Park, P.J. Šafárik University, Košice, Slovakia*

Heat shock proteins 70 (Hsp70) are molecular chaperones that comprise a nucleotide-binding domain (NBD) and a substrate-binding domain (SBD), the latter of which is responsible for binding protein clients. Upon ATP binding to the NBD, the interface between the α/β subdomains of the SBD undergoes conformational changes, resulting in its opening and subsequent docking onto the NBD. The stabilization of allosteric effects is facilitated by the interdomain contacts between the NBD and SBD that have recently been established. Here, we investigate the impact of Hsp70 evolution on the formation of subdomain interfaces and their subsequent opening. Insertion and deletion events, commonly referred to as indels, can significantly impact mechanical events. This is due to the fact that such changes introduce a collective shift in the pairing interactions at communicating interfaces. Through an analysis of multiple sequence alignment data obtained from the Swiss-Prot/UniProt database, a number of indel-free regions (IFR) have been identified within Hsp70. The two most sizable IFRs are situated in interdomain regions that engage in allosteric conformational changes. We speculate that the reduced probability of indel occurrence in these regions can be attributed to the disruptive effects of indel events on the mechanical balance of the protein, leading to functional impairment. The rational design of functional allosteric machines necessitates the incorporation of a notion of balance among structural components.

Acknowledgment. This work was supported by APVV-18-0285, EU H2020 TWINNING program GA. No. 952333 project CasProt, BioPickmol, ITMS2014+: 313011AUW6 supported by the Operational Programme Integrated Infrastructure, funded by the ERDF.



Supramolecular assembly of the pathological light chain under reducing conditions

^{a,b}V. DŽUPPONOVÁ, ^bG. ŽOLDÁK

^a*Department of Biophysics, Faculty of Science, Pavol Jozef Šafárik University, Košice, Slovakia*

^b*Center for Interdisciplinary Biosciences, Technology and Innovation Park, Pavol Jozef Šafárik University, Košice, Slovakia*

Protein stability is an important property necessary for correct functioning in biological systems. When the stability is low, protein can misfold, which can lead to the formation of aggregates that are often toxic for the cell. Protein misfolding can result in serious diseases. Examples of such diseases include amyloidosis and multiple myeloma of the immunoglobulin light chain. Multiple myeloma (MM) is haematological malignancy characterized by the abnormal proliferation of plasma cells, which produce excessive amounts of the monoclonal parts of antibodies known as light chains. These light chains pass into the bloodstream and form extracellular deposits in vital organs, causing significant damage. Understanding the molecular mechanisms underlying protein aggregation and the influence of the physicochemical environment on the conversion of functional proteins into harmful aggregates is crucial for developing effective strategies to reduce the morbidity associated with these leukemic diseases. Furthermore, identifying the critical steps involved in the aggregation process would allow for the targeted development of drugs that can inhibit the formation of toxic aggregates [1-3].

In our study [4], we investigated the aggregation mechanism and structures of pathological aggregates formed by the human multiple myeloma light chains (hLC) after disrupting stabilizing disulfide bonds using different reducing agents. We measured the aggregation kinetics in the presence of three commonly used disulfide reducers (TCEP, DTT, and glutathione) and visualized the resulting aggregates using a combination of light microscopy and advanced imaging techniques such as confocal and super-resolution STED microscopy. Our findings revealed that the aggregation kinetics could be described by two macroscopic rate constants based on the Finke-Watzky model, which are associated with the nucleation and growth processes, respectively. Surprisingly, we observed decreased growth rate constants at higher protein concentrations. We interpret this observation as the involvement of an aggregation-active monomer particle that becomes progressively depleted at high concentrations due to shifts in the monomer/dimer equilibrium. By employing three-dimensional visualization techniques at the submicrometer resolution, we observed distinct branched morphologies of the final aggregates, specific to the reducing agents used. These branched aggregates exhibited non-trivial fractal dimensions. Consequently, disrupting the stabilizing disulfide bonds in hLC leads to forming large, branched aggregates through a monomer-addition mechanism with unique structural fingerprints (Fig. 1).

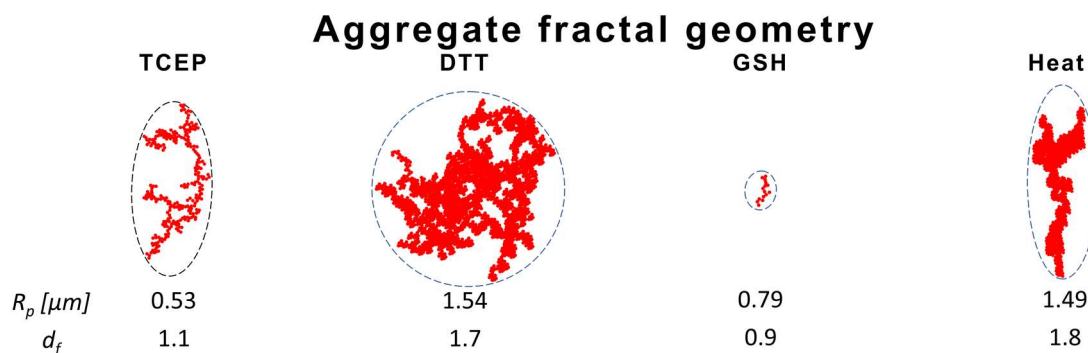
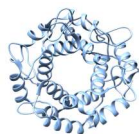
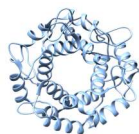


Figure 2: 3D morphologies of light chain aggregates formed after reducing disulfide bonds using different chemical reducing agents: TCEP, DTT, GSH or temperature. 3D morphologies were obtained by the fluorescent labeling of LC with Abberior STAR RED dye and visualized by the STEDYCON microscope.

Acknowledgment. This work was supported by research grants Slovak research and development agency (No. APVV-18-0285), the Slovak Grant Agency VEGA No 1/0024/22, Internal Scientific Grants System (VVGs) of Faculty of Science UPJŠ No vvg-s-pf-2021-2072, EU H2020 TWINNING program GA. No. 952333 project CasProt, BioPickmol, ITMS2014+: 313011AUW6 supported by the Operational Programme Integrated Infrastructure, funded by the ERDF, and Open scientific community for modern interdisciplinary research in medicine (OPENMED), ITMS2014+: 313011V455 supported by the Operational Programme Integrated Infrastructure, funded by the ERDF.

References

1. Andrich K., et al., Journal of Biological Chemistry, 2016, 292(6), 2328-2344
2. Chiti F., Dobson C. M., Annual Review of Biochemistry, 2017, 86, 27-68
3. Blancas-Mejia L. M., et al., Chemical Communications, 2018, 54, 10664-10674
4. Džupponová V., Žoldák G., Colloids and Surfaces B: Biointerfaces, 2023, 221, 112983



Production of Viral Proteins and Their Characterisation

^{a,b,c}A. POLÁK, ^aM. BENKO, ^aA. BITALA, ^dM. NEMČOVIČ, ^aI. NEMČOVIČOVÁ

^a*Biomedical Research Center, Institute of Virology, Department of Viral Immunology, Slovak Academy of Sciences, Dúbravská cesta 9, 845 05 Bratislava, Slovak Republic*

^b*Faculty of Natural Sciences, Department of Molecular Biology, Comenius University in Bratislava, Mlynská dolina, Ilkovičova 6, 842 15 Bratislava, Slovak Republic*

^c*Institute of Neuroimmunology, Laboratory of Structural Biology of Neurodegeneration, Slovak Academy of Sciences, Dúbravská cesta 9, 845 10 Bratislava*

^d*Institute of Chemistry, Department of Glycobiology, Slovak Academy of Sciences, Dúbravská cesta 9, 845 38 Bratislava, Slovak Republic*

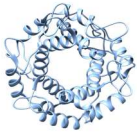
The immunomodulatory protein UL144 is encoded in UL/b' locus of cytomegaloviruses (CMV). The main function of viral immunomodulatory proteins is to escape host immune system, which may lead to severe infections. The infections are primarily threatening immune-deficient patients and pregnant women (1). Estimated mean prevalence of CMV infections reached up to 83% of serum-positive patients in 2009 (2). Despite this, a specific therapy targeting human CMV infection has not been fully developed yet. The main goal of our work was the preparation of UL144-wt (wild type) protein and its glycosylation-deficient mutants since glycosylation has been found to significantly alter UL144 binding affinity (3). Our next goal was the characterisation of UL144 proteins binding to specific human receptors.

The produced proteins included: human CMV UL144-wt protein, RhUL144 protein from Rhesus CMV and two mutant proteins, UL144-dg (glycosylation-deficient mutant) and UL144-N91 protein with mutation in position 91, abolishing glycosylation on this site. We also produced two ligands to UL144-proteins: CD160 and BTLA glycoproteins. All proteins have been detected by polyacrylamide electrophoresis (SDS-PAGE) and Western blot method. Further identification was ensured using tandem mass spectrometry (fig. 1). Two produced proteins, UL144-wt and RhUL144 had suitable concentration for protein crystallization. We used sitting-drop method for their crystallization.

The main outcome was an estimation of binding affinity of mentioned proteins. The binding of highly glycosylated UL144-wt was expected only to BTLA, whereas the less-glycosylated RhUL144 proteins were expected to bind both BTLA and CD160. Since UL144-dg and UL144-N91 glycosylation-deficient mutants have similar glycosylation profile as RhUL144, similar binding was also expected (fig. 2).

We produced all studied proteins using Sf9-baculovirus expression system. Surface plasmon resonance (SPR) method was used to estimate the binding affinity. Our preliminary results confirmed the formation of UL144-wt-CD160 protein complex as well as formation of RhUL144-CD160 and RhUL144-BTLA complexes. In case of UL144-N91 protein, both complexes were observed but with low affinity. We did not manage to confirm expected binding between UL144-dg protein to either of the glycoprotein ligands.

Our preliminary results are promising but require further study. The understanding of mechanism underlying the interaction between viral



immunomodulatory proteins and human immune system is of a high importance. These data are crucial to develop better targeted strategies against viral infections.

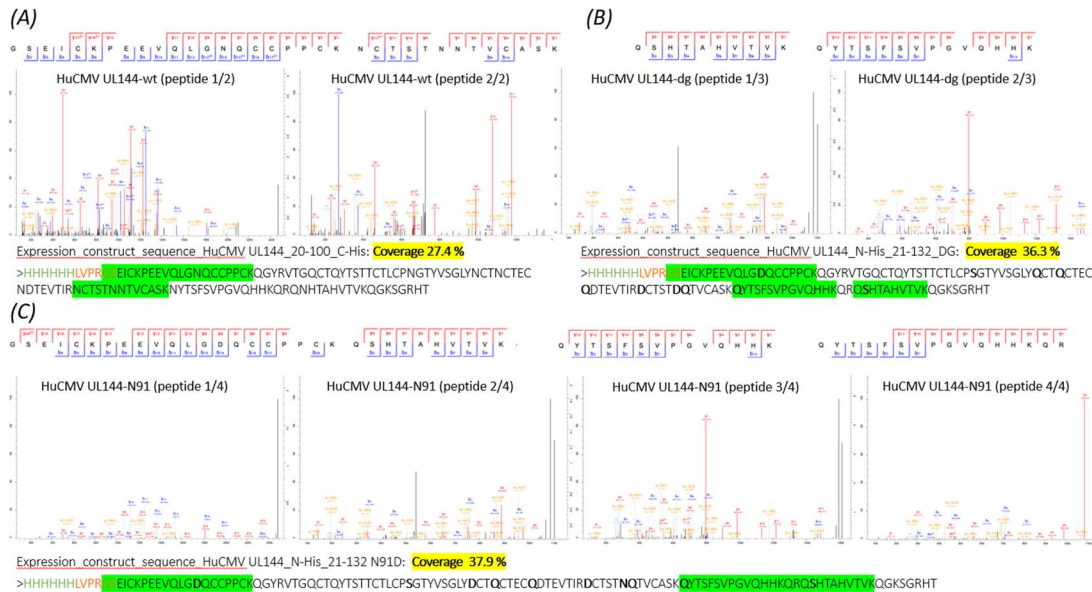


Fig. 1: Tandem mass spectrometry (MS/MS) of produced proteins with highlighted coverage. A – UL144-wt, B – UL144-dg, C – UL144-N91. No data was obtained for RhUL144 protein, however, RhUL144 was clearly identified using other methods.

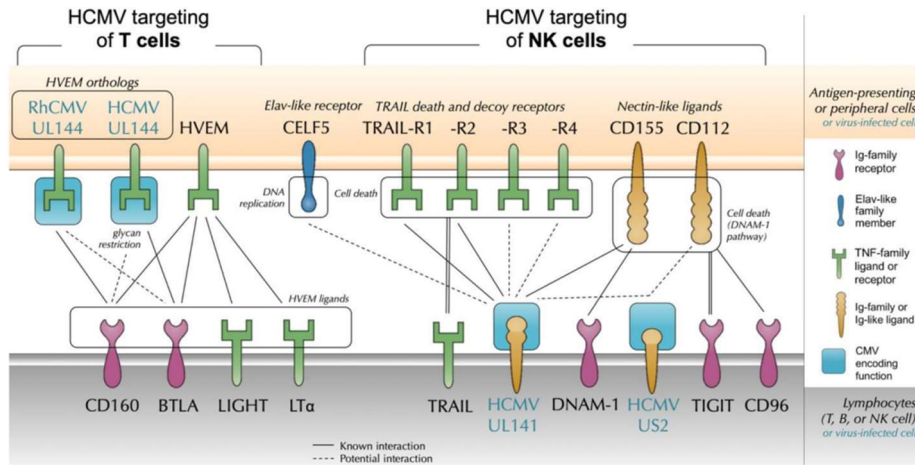
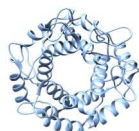


Fig. 2: UL144 cytomegalovirus proteins and their binding to human glycoproteins.

Acknowledgement: This project was funded by the VEGA grant 02/0026/22. Participation at SSB2023 conference was covered by the grant APVV 21-0479.

References:

- Nogalski, M. T. et al., (2014). Overview of human cytomegalovirus pathogenesis. *Methods in molecular biology (Clifton, N.J.)*, 1119, 15–28.
- Zuhair, M., et al., (2019). Estimation of the worldwide seroprevalence of cytomegalovirus: A systematic review and meta-analysis. *Reviews in medical virology*, 29(3)
- Bitra, A., et al., (2019). Structure of human cytomegalovirus UL144, an HVEM orthologue, bound to the B and T cell lymphocyte attenuator. *The Journal of biological chemistry*, 294(27)



Quenching of singlet oxygen in intracellular environment

^aA. HOVAN, ^aV. PEVNÁ, ^bV. HUNTOŠOVÁ, ^cP. MIŠKOVSKÝ, G. BÁNÓ

^aDepartment of Biophysics, Institute of Physics, P. J. Šafárik University in Košice, Košice, Slovakia

^bCenter for Interdisciplinary Biosciences, Technology and Innovation Park, P. J. Šafárik University in Košice, Košice, Slovakia

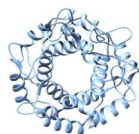
^cCassovia New Industry Cluster, Košice, Slovakia

Singlet oxygen, which is the lowest excited state of molecular oxygen, plays a crucial role in photodynamic therapy [1]. The process of singlet oxygen quenching within the cellular environment has been extensively studied for many years. The primary objective of this research was to determine the lifetime of singlet oxygen, which would then allow the definition of an action radius [2-5]. Even though a lot of effort was put into this research, there was no scientific consensus on the singlet oxygen lifetime in cells. In this study, we tried to minimize the problematic parts of the previous studies and we examined the quenching of singlet oxygen in U87MG glioblastoma cells at various stages of apoptosis, utilizing hypericin as a photosensitizer. Through the utilization of time-resolved singlet oxygen phosphorescence in conjunction with transient absorption measurements, we observed changes in the quenching of singlet oxygen at different phases of apoptosis. Additionally, we were able to identify two distinct populations of hypericin, each exhibiting different triplet state lifetimes and contributions to singlet oxygen phosphorescence. One population was localized within the cellular environment, while the other was present in the plasma membrane and membrane blebs that occur during apoptosis. The singlet oxygen lifetime corresponding to the intracellular environment of U87MG cells was determined to be 0.4 μ s, with an increase observed as the level of apoptosis increased.

Acknowledgment. This work was supported by research grants VEGA 1/0557/20, APVV-21-0333, internal grant of Faculty of Science UPJS in Košice vvg-2022-2184 and BioPickmol, ITMS2014+: 313011AUW6 from the Operational Program Integrated Infrastructure funded by the ERDF.

References

1. Ogilby, P. R. (2010). Singlet oxygen: there is indeed something new under the sun. *Chemical Society Reviews*, 39(8), 3181-3209.
2. Hatz, S., Lambert, J. D. C., & Ogilby, P. R. (2007). Measuring the lifetime of singlet oxygen in a single cell: addressing the issue of cell viability. *Photochemical & Photobiological Sciences*, 6(10), 1106-1116.
3. Skovsen, E., Snyder, J. W., Lambert, J. D. C., & Ogilby, P. R. (2005). Lifetime and diffusion of singlet oxygen in a cell. *Journal of Physical Chemistry B*, 109(18), 8570-8573.
4. Schlothauer, J., Hackbarth, S., & Roder, B. (2009). A new benchmark for time-resolved detection of singlet oxygen luminescence - revealing the evolution of lifetime in living cells with low dose illumination. *Laser Physics Letters*, 6(3), 216-221.
5. Niedre, M., Patterson, M. S., & Wilson, B. C. (2002). Direct near-infrared luminescence detection of singlet oxygen generated by photodynamic therapy in cells in vitro and tissues in vivo. *Photochemistry and Photobiology*, 75(4), 382-391.



Why Analytical Ultracentrifugation to Investigate Biomolecules?

^aI. GARAGUSO, ^aL. EHRARDT, ^bA. BHATTACHARYA

^a Beckman Coulter GmbH, Krefeld, Germany

^b Beckman Coulter Life Sciences, Loveland, CO, US

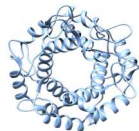
The Analytical ultracentrifugation (AUC) is a biophysical technique that uses centrifugal force to separate molecules dissolved in solution according to their size, buoyancy density and anisotropy. The compounds are then detected by UV-visible absorbance and Rayleigh interference or fluorescence. The AUC combines a wide dynamic range, high particle-size resolution with high statistical accuracy as well as sensitivity. Being a first-principle technique, AUC, does not require standards. The main variables determined by AUC experiments are sedimentation, diffusion coefficients and partial concentrations. Furthermore, the AUC provides information on the size and shape of biomolecules in their native state as they exist in solution with virtually no limits on the nature of the sample or solvent, i.e. any substance whose absorbance (or refractive index) differs from that of the solvent can be analysed¹. Thus, AUC is a widely applicable technology providing relevant information for the study of thermodynamics and macromolecular characteristics of nanoparticles, colloidal systems, dispersions, emulsions and biopolymers. This technology have been used to characterize proteins, nucleic acids, carbohydrates², and is well suited to determine the molar mass, particle size, particle density, shape, stoichiometry³⁻⁵ extinction coefficient⁶ as well as interaction parameters such as association constants and bonding properties⁷. In addition, the wide dynamic range of measurement of the AUC can be applied to compounds ⁸ with molecular masses ranging from a few hundred units, such as sucrose ⁹; up to several millions such as organelles¹⁰ and viral particles ^{11,12} requiring small amounts of sample (18 to 450 μ L) even at low concentrations (down to 0.01g/L).

Although there has been a rapid development of both computational power and tools for AUC analysis, this technology is definitely underutilised, considering capabilities and potential, in the fields of biochemistry and molecular biology. Here we present an overview of applications and case studies on the determination of chemical-physical properties and interactions of biological macromolecules of common interest such as Proteins, nucleic acids, drugs, Liposomes and viral vectors. Addressing practical questions and highlighting the power of AUC for a reliable and robust analysis of biomacromolecules.

Contact:

Ignazio Garaguso, Sr. Sales Specialist AUC Europe

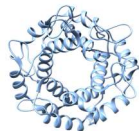
Beckman Coulter GmbH
Europark Fichtenhain B 13 – D-47807 Krefeld, DE
T: +49 1743799785



E: igaraguso@beckman.com
W: beckman.com

References

1. Demeler B. Measuring molecular interactions in solution using multi-wavelength analytical ultracentrifugation: combining spectral analysis with hydrodynamics. *The Biochemist*. 2019;41(2):14-18. doi:10.1042/BIO04102014
2. Lebowitz J, Lewis MS, Schuck P. Modern analytical ultracentrifugation in protein science: A tutorial review. *Protein Sci*. 2009;11(9):2067-2079. doi:10.1110/ps.0207702
3. Yang TC, Catalano CE, Maluf NK. Analytical Ultracentrifugation as a Tool to Study Nonspecific Protein–DNA Interactions. *Methods Enzymol*. 2015;562:305-330. doi:10.1016/bs.mie.2015.04.009
4. Unzai S. Analytical ultracentrifugation in structural biology. *Biophys Rev*. 2017;10(2):229-233. doi:10.1007/s12551-017-0340-0
5. Cole JL, Lary JW, Moody T, Laue TM. Analytical Ultracentrifugation: Sedimentation Velocity and Sedimentation Equilibrium. *Methods Cell Biol*. 2008;84:143-179. doi:10.1016/S0091-679X(07)84006-4
6. Hoffmann A, Grassl K, Gommert J, Schlesak C, Bepperling A. Precise determination of protein extinction coefficients under native and denaturing conditions using SV-AUC. *Eur Biophys J*. 2018;47(7):761-768. doi:10.1007/s00249-018-1299-x
7. Van Holde KE, Weischet WO. Boundary analysis of sedimentation-velocity experiments with monodisperse and paucidisperse solutes. *Biopolymers*. 1978;17(6):1387-1403. doi:10.1002/bip.1978.360170602
8. Scott DJ, Winzor DJ. Characterization of Intrinsically Disordered Proteins by Analytical Ultracentrifugation. In: *Methods in Enzymology*. Vol 562. Elsevier; 2015:225-239. doi:10.1016/bs.mie.2015.06.034
9. Van Holde KE, Baldwin RL. Rapid Attainment of Sedimentation Equilibrium. *J Phys Chem*. 1958;62(6):734-743. doi:10.1021/j150564a025
10. Duong P, Chung A, Bouchareychas L, Raffai RL. Cushioned-Density Gradient Ultracentrifugation (C-DGUC) improves the isolation efficiency of extracellular vesicles. Hancock R, ed. *PLOS ONE*. 2019;14(4):e0215324. doi:10.1371/journal.pone.0215324
11. Mullins EK, Powers TW, Zobel J, et al. Characterization of Recombinant Chimpanzee Adenovirus C68 Low and High-Density Particles: Impact on Determination of Viral Particle Titer. *Front Bioeng Biotechnol*. 2021;9:753480. doi:10.3389/fbioe.2021.753480
12. Richter K, Wurm C, Strasser K, et al. Purity and DNA content of AAV capsids assessed by analytical ultracentrifugation and orthogonal biophysical techniques. *Eur J Pharm Biopharm*. Published online May 16, 2023. doi:10.1016/j.ejpb.2023.05.011



SC 06

SHORT COMMUNICATIONS

Modern Methods for the Analysis and Characterization of Biomolecules

K. KOLKOVÁ

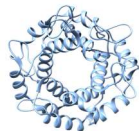
SPECION, s.r.o., Budějovická 1998/55, 140 00 Prague, Czech Republic

In our company presentation, we will introduce the latest trends and innovative methods in the analysis and characterization of biomolecules. Our comprehensive portfolio offers state-of-the-art solutions for biomolecular research, including protein stability measurement, sample characterization and distribution, biomolecular structure elucidation, and interaction studies.

Quality and the generation of significant datasets play a crucial role in our research. Efficient data collection in a short time frame and with minimal resource consumption has become a key objective. We will present solutions in the field of biotechnology that feature a high degree of automation, low consumable material costs, and allow operation without the need for deep knowledge of a single technique. These solutions also generate extensive datasets, often through a platform-based measurement approach.

Distinguished companies such as Refeyn, Applied Photophysics, Redshift, Symcel, and Horiba will be showcased at the conference, presenting advanced technologies including Mass Photometry, Circular Dichroism, Differential Scanning Fluorimetry, Microfluidic Modulation Spectroscopy, and others.

Attendees of our presentation will gain insight into cutting-edge modern technologies, with an invitation to follow for demonstrations and webinars of selected technologies.



SC 07

SHORT COMMUNICATIONS

Allosteric regulation of 14-3-3 protein family by Norharmane Effects on adipogenic differentiation of 3T3L1 cells

^aL. RIVERA, ^aS. MULLER, ^aE. BARRERA, ^aM. UHART, ^{a,b}D.M. BUSTOS

^aLaboratorio de Integración de Señales Celulares, IHEM (CONICET-UNCuyo), Mendoza, Argentina

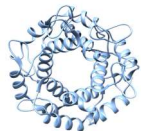
^bFCEN, UNCuyo, Mendoza, Argentina

14-3-3 proteins constitute a family of seven mammalian paralogs that participate in a plethora of cellular processes mainly through protein-protein interactions. It is estimated that more than 10% of the human proteome could participate as target proteins. Even though 14-3-3 targets don't share any defined structural motif, our analysis show that intrinsic structural disorder and the presence of phosphorylated Ser or Thr residues are common and needed elements for binding [1, 2, 3, 4, 5, 6]. A recent breakthrough in our research has unveiled an allosteric site governing two distinct conformations (open/closed) of 14-3-3. These conformations exhibit differing affinities towards phosphorylated partners. Through virtual screening of this region, we identified a family of compatible ligands named β -carbolines, which prompt the protein to adopt the closed state. To validate our bioinformatics approach, we conducted a pull-down experiment using one such ligand, Norharmane (9H-Pyrido[3,4-B]indole). Results revealed that the 14-3-3 partner R18 exhibited increased binding only when Norharmane was added post incubation of 14-3-3 and R18. Pre-incubation of 14-3-3 with Norharmane obstructed R18's interaction. Furthermore, we explored the impact of Norharmane on 14-3-3 activity in a biological process. Drawing from previous findings indicating 14-3-3 γ 's inhibitory effect on adipogenic differentiation of 3T3L1 cells [7, 8], we assessed adipogenic potential under Norharmane treatment with or without reduced 14-3-3 γ expression. Norharmane-treated 3T3L1 cells exhibited reduced lipid droplet accumulation, an effect absent in 14-3-3 γ knockdown cells. This suggests Norharmane's potential to influence adipogenic differentiation via 14-3-3 γ modulation. Our findings provide initial evidence about a novel allosteric regulatory mechanism of 14-3-3 proteins by Norharmane and reveal new concepts about 14-3-3 nature.

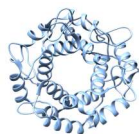
Acknowledgment. This work is being supported by research grant CONICET (National Scientific and Technical Research Council - Argentina) and Marie Skłodowska Curie Action RISE (Research and Innovation Staff Exchange) grant.

References

1. Sluchanko, N. N., & Bustos, D. M. (2019). Intrinsic disorder associated with 14-3-3 proteins and their partners. *Progress in Molecular Biology and Translational Science*, 166, 19–61.
2. Masone, D., Uhart, M., & Bustos, D. M. (2017). On the role of residue phosphorylation in 14-3-3 partners: AANAT as a case study. *Scientific Reports*, 7(1), 1–9.
3. Uhart, M., & Bustos, D. M. (2014). Protein intrinsic disorder and network connectivity. The case of 14-3-3 proteins. *Frontiers in Genetics*, 5, 10.



4. Bustos, D. M. (2012). The role of protein disorder in the 14-3-3 interaction network. *Molecular BioSystems*, 8(1), 178–184.
5. Uhart, M., Iglesias, A. A., & Bustos, D. M. (2011). Structurally constrained residues outside the binding motif are essential in the interaction of 14-3-3 and phosphorylated partner. *Journal of Molecular Biology*, 406(4), 552–557.
6. Bustos, D. M., & Iglesias, A. A. (2006). Intrinsic disorder is a key characteristic in partners that bind 14-3-3 proteins. *PROTEINS: Structure, Function, and Bioinformatics*, 63(1), 35–42.
7. Frontini-López, Y. R., Gojanovich, A. D., Del Veliz, S., Uhart, M., & Bustos, D. M. (2021). 14-3-3b isoform is specifically acetylated at Lys51 during differentiation to the osteogenic lineage. *Journal of Cellular Biochemistry*, 122(12), 1767–1780.
8. Gojanovich, A. D., Bustos, D. M., & Uhart, M. (2016). Differential expression and accumulation of 14-3-3 paralogs in 3T3-L1 preadipocytes and differentiated cells. *Biochemistry and Biophysics Reports*, 7, 106-112.



Herbal extracts' effect on protein amyloid aggregation - individual vs. pooled constituents

^aM. GANCAR, ^bE. KURIN, ^aZ. BEDNARIKOVA, ^aJ. MAREK, ^bS. BITTNER FIALOVA,
^bS. DOKUPILOVA, ^bP. MUCAJI, ^bM. NAGY, ^aZ. GAZOVA

^aDepartment of Biophysics, Institute of Experimental Physics Slovak Academy of Sciences,
Watsonova 47, 040 01, Kosice, Slovakia

^bDepartment of Pharmacognosy and Botany, Faculty of Pharmacy, Comenius University Bratislava,
Odbojarov 10, 832 32, Bratislava, Slovakia

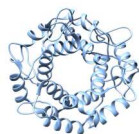
The propensity of proteins to aggregate into amyloid structures is a pressing concern in various health disorders. Notably, insulin, a crucial therapeutic for diabetes, undergoes aggregation, resulting in undesired fibrillar deposits and iatrogenic injection amyloidosis. Seeking innovative avenues for mitigating amyloidosis is essential. Herbal extracts, with their diverse molecular components, offer promise for effective treatments.

This comprehensive investigation explored the anti-amyloidogenic potential of seven distinct compounds sourced from *Camellia sinensis* and *Origanum vulgare*, encompassing their equimolar combinations against insulin amyloid aggregation. Our evaluation employed a multifaceted approach, integrating the thioflavin T fluorescence assay, infrared spectroscopy, atomic force microscopy imaging, and *in silico* calculations.

Our results demonstrate the pronounced anti-amyloid activity of *Origanum vulgare* extracts, evident through their lower effective concentrations required for inhibiting insulin amyloid aggregation. However, limited synergistic interactions were noted among the compounds within this extract. Conversely, constituents from *Camellia sinensis* notably delayed the onset of insulin amyloid aggregation under specified conditions, revealing multiple potentiating synergies. Molecular docking studies further provided insights into the mechanistic foundations of our *in vitro* observations.

In summary, our study identifies specific bioactive compounds with individual efficacy in counteracting insulin amyloid aggregation. We elucidate their modulatory impacts on the aggregation process and decode the intricate interplay of synergistic and antagonistic interactions stemming from their equimolar combinations. This research enriches our understanding of the potential of natural compounds sourced from *Camellia sinensis* and *Origanum vulgare* as therapeutic agents for amyloid-related disorders, illuminating their underlying molecular mechanisms. The findings underscore the promise of these compounds for future therapeutic interventions.

Acknowledgement: This work was supported by the Slovak Research and Development Agency under Contracts no. APVV 18-0284 and APVV SK-TW-21-0004; Slovak Grant Agency VEGA grants: 1/0284/20, 1/0226/22, 2/0164/22 and 2/0176/21.



Self-assembly of spider protein-DNA hybrids

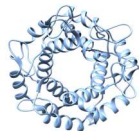
^aV. FEDOROVA, ^bT. BIRO, ^aK. SIPOSOVA, ^cM. HUMENIK

^aDepartment of Biophysics, Institute of Experimental Physics, Slovak Academy of Sciences, Kosice, Slovakia

^bDepartment of Biophysics, Institute of Physics, P. J. Safarik University in Kosice, Kosice, Slovakia

^cDepartment of Biomaterials, Faculty of Engineering Science, Universität Bayreuth, Bayreuth, Germany

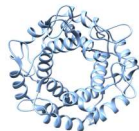
Protein self-assembly is a spontaneous process based on non-covalent interactions between molecular subunits without the requirement of external energy sources, resulting in the formation of highly organized aggregates [1]. Such self-assembled molecules forming numerous structures, e.g. fibrous, helical, or tubular, include pathological and functional amyloid proteins sharing typical cross- β structures arranging perpendicularly along the axis of the amyloid fibril [2,3]. Moreover, the possibility of chemical modification by attaching functional ligands, e.g. oligonucleotides with specific functions, to peptides or proteins and further alteration of physical and chemical conditions which stimulate self-assembly of the proteins, enables us to form bio-inspired nanomaterials with desired structure and programmable function by the ordered self-assembly process [4]. Among amyloid proteins, spider silk fibers stand out for their extraordinary properties, including mechanical strength, biocompatibility, and biodegradability alongside the absence of immune response in living organisms predetermining them for practical use in different industries. However, since spiders are known for their often cannibalistic behaviour, a way of producing recombinant spider silk proteins in commonly used host organism *E. coli* has been introduced. Here, the recombinant spider protein eADF4(C16) derived from the functional protein ADF4 of the dragline fibroin 4 from the European garden spider *Araneus diadematus*, which possesses 16 repetitions of module C has been used [5,6]. Using the „click-chemistry“ reaction approach, the spider protein has been coupled by the thrombin-binding oligonucleotides TBA15 and TBA29, respectively. Phosphate ions has been proven to trigger the formation of protein fibrils [4], while K^+ ions are essential for the proper composition of secondary structures of DNA oligomers, which Na^+ stabilizes [7]. Therefore, we focus on monitoring the kinetics of the self-assembly of the DNA-modified eADF4(C16) protein in order to evaluate the effect of different experimental conditions and the presence of ions on the self-assembly process and morphology of fibrils as well using a combination of biophysical/biochemical techniques. Detailed understanding of the self-assembly process of amyloid proteins and their structure will allow us to fabricate hybrid protein-DNA fibrils that are able to form self-organized highly ordered structures with specific binding sites able to attach relevant ligands, for instance, biomacromolecules including enzymes or drugs that could be controllably released.



Acknowledgment: This work was supported by the grants: PPP SK-DAAD and VEGA 2/0034/22.

References

1. Solomonov, A., & Shimanovich, U. (2020). Self-assembly in protein-based bionanomaterials. *Israel Journal of Chemistry*, 60(12), 1152-1170
2. Naleway, S. E., Porter, M. M., McKittrick, J., & Meyers, M. A. (2015). Structural design elements in biological materials: application to bioinspiration. *Advanced materials*, 27(37), 5455-5476
3. Knowles, T. P., & Buehler, M. J. (2011). Nanomechanics of functional and pathological amyloid materials. *Nature nanotechnology*, 6(8), 469-479
4. Humenik, M., & Scheibel, T. (2014). Nanomaterial building blocks based on spider silk–oligonucleotide conjugates. *ACS nano*, 8(2), 1342-1349
5. Huebnerich, D., Helsen, C. W., Quedzuweit, S., Oschmann, J., Rudolph, R., & Scheibel, T. (2004). Primary structure elements of spider dragline silks and their contribution to protein solubility. *Biochemistry*, 43(42), 13604-13612
6. Scheibel, T. (2004). Spider silks: recombinant synthesis, assembly, spinning, and engineering of synthetic proteins. *Microbial cell factories*, 3, 1-10
7. Macaya, R. F., Schultze, P., Smith, F. W., Roe, J. A., & Feigon, J. (1993). Thrombin-binding DNA aptamer forms a unimolecular quadruplex structure in solution. *Proceedings of the National Academy of Sciences*, 90(8), 3745-3749



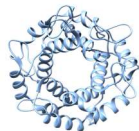
Fibril-based carrier systems for bioactive molecules

^aYu-Yuan YANG, ^aYou-Ren LAI, ^bSu-Chun HOW and ^aSteven S.-S. WANG

¹ *Department of Chemical Engineering, National Taiwan University, Taipei 10617, Taiwan*

² *Department of Chemical Engineering and Biotechnology, Tatung University, Taipei 104, Taiwan*

The connection between amyloid fibril buildup and a range of disorders, such as Alzheimer's, Parkinson's, Huntington's, type II diabetes, and prion diseases, is widely acknowledged. Evidence has indicated the importance of protofibrillar assemblies and oligomers, rather than the fibrils themselves, in causing tissue damage. Additionally, amyloid fibrils have been found to possess physiological functions across diverse organisms. Moreover, the unique properties (e.g., remarkable stability, resilience, and multifaceted) of amyloid fibrils make them promising candidates for various applications in biomedicine and biotechnology. We have made attempts to develop diverse carrier systems, such as hydrogels and microcapsules, with amyloid fibrils derived from the milk proteins, β -lactoglobulin (β -LG) and whey protein isolate (WPI), via different methods. We have not only characterized the structural properties but also examined the key features and relevant functions of the as-synthesized amyloid fibril-based carriers. Our results have demonstrated that these carriers are able to efficiently encapsulate bioactive molecules, particularly those with hydrophobic and lipophilic traits. Our research work has highlighted the potential of amyloid fibril-based hybrid materials as carriers/matrices to encapsulate or delivery drug and/or bioactive molecules.



Development of Multi-Dimensional Whey Protein Amyloid Fibril-Based Composite Materials for Various Engineering Applications

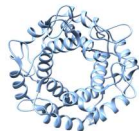
You-Ren LAI and Steven S.-S. WANG*

Department of Chemical Engineering, National Taiwan University, Taipei 10617, Taiwan

sswang@ntu.edu.tw

Food protein wastes have been identified as one of the contributing factors to climate change. Recent research indicates that the adverse environmental impacts of food protein wastes include a high carbon footprint, chemical pollution, and biodiversity loss [1]. Approximately 240 million tons of whey are produced globally each year. The surplus of whey proteins is a crucial issue for the dairy industry due to environmental concerns caused by its high biological oxygen demand [2]. Therefore, efforts have been directed toward exploring sustainable and eco-friendly approaches for valorizing food protein wastes into advanced sustainable materials. Amyloid fibril formation is a generic property of all polypeptides. Under appropriate conditions, proteins can form amyloid fibrils by self-assembly. Moreover, amyloid fibrils of proteins (including food proteins) exhibit remarkable characteristics, such as high aspect ratio, high charge density, excellent stiffness, outstanding chemical stability, good biocompatibility and biodegradability, and diversity of functional groups [3, 4]. These features make them promising advanced materials in the applications of biomedical engineering, environmental engineering, and nanotechnology [3, 4]. Therefore, amyloid fibril formation is considered an attractive strategy for reinforcing food protein function and valorizing food protein wastes.

Our research is aimed at synthesizing multi-dimensional amyloid-based materials (e.g., one-dimensional composites, two-dimensional membranes, and three-dimensional aerogels) using whey protein, a by-product of the dairy industry. Additionally, our work explores the applications of amyloid fibrils as functional materials in relevant biochemical and environmental engineering fields, such as nanocatalyst carriers, electrode surface modifiers, drug delivery vehicles, heavy metal adsorption films, and oil-water separation aerogels. For example, one-dimensional silver nanoparticle-decorated whey protein amyloid fibrils (AgNP/WPI-AF) composites were synthesized using photochemical/chemical routes and used as catalysts for the chemical catalytic reduction of methylene blue [4]. The AgNP/WPI-AF composites were also utilized as the electrode surface modifiers for the electrochemical detection of environmental pollutants (e.g., p-nitrophenol). The two-dimensional carboxymethyl cellulose/whey protein amyloid fibril (CMC/WPI-AF) membranes were fabricated using chemical crosslinking coupled with phase inversion and used as the drug delivery vehicles for the *in vitro* release of cationic and hydrophobic drugs [5]. The CMC/WPI-AF membranes were also utilized as adsorbents for the physical adsorption/removal of heavy metal ions. Through polysaccharide modification, we have prepared three-

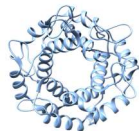


dimensional chitosan-modified whey protein amyloid fibril aerogels, which could be applied in the oil-water separation and water-in-oil (W/O) emulsion separation. In our research, amyloid fibrils derived from food proteins were employed to create eco-friendly and sustainable composites, membranes, and aerogels. We believe the outcome from our research may contribute to the circular economy.

Acknowledgment. This work was supported by the grants from the National Science and Technology Council (NSTC), Taiwan.

References

1. Peydayesh, M., Bagnani, M., Soon, W. L., & Mezzenga, R. (2022). Turning food protein waste into Sustainable Technologies. *Chemical Reviews*, 123(5), 2112-2154
2. Carvalho, F., Prazeres, A. R., & Rivas, J. (2013). Cheese whey wastewater: Characterization and treatment. *Science of the total environment*, 445, 385-396
3. Cao, Y., & Mezzenga, R. (2019). Food protein amyloid fibrils: Origin, structure, formation, characterization, applications and health implications. *Advances in colloid and interface science*, 269, 334-356
4. Lai, Y. R., Lai, J. T., Wang, S. S. S., Kuo, Y. C., & Lin, T. H. (2022). Silver nanoparticle-deposited whey protein isolate amyloid fibrils as catalysts for the reduction of methylene blue. *International Journal of Biological Macromolecules*, 213, 1098-1114
5. Lai, Y. R., Wang, S. S. S., Hsu, T. L., Chou, S. H., How, S. C., & Lin, T. H. (2023). Application of Amyloid-Based Hybrid Membranes in Drug Delivery. *Polymers*, 15(6), 1444



SC 12

SHORT COMMUNICATIONS

Synthesis of Poly(Acrylic acid)-Whey Protein Isolate Amyloid Fibril-Based Hydrogel Membranes for Drug Delivery

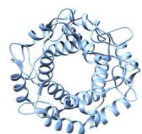
Chia-Yu CHANG and Steven S.-S. WANG*

Department of Chemical Engineering, National Taiwan University, Taipei 10617, Taiwan

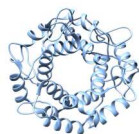
sswang@ntu.edu.tw

The unique structural characteristics and biocompatibility of amyloid fibrils make them promising biomaterials, which can be used in a variety of applications in the fields of Biotechnology and Engineering. In this study, poly(Acrylic acid) (PAA) and whey protein isolate amyloid fibril (WPI-F) were utilized to synthesize the hydrogel membranes, which serve as carriers for both cationic and anionic drugs, such as vitamin C (VitC) and metformin (MEF). The fibrillar structure of WPI-F was verified using ThT binding assay, Congo red binding assay, FTIR, and TEM. The formation of PAA-WPI-F hydrogel membranes through graft polymerization was confirmed via FTIR analysis. Zeta potential measurements showed the negatively charged nature of the hydrogel membranes. In addition, compression test revealed that the presence of WPI-F could enhance the mechanical strength of as-synthesized hydrogel membranes. The drug-loaded PAA-WPI-F hydrogel membranes were subjected to *in vitro* drug release test and the drug release kinetics was examined using UV-visible spectrophotometry. Four different models (e.g., First order, Higuchi, Korsmeyer-Peppas (KP), and Peppas–Sahlin (PS) models) were employed to fit and analyze the *in vitro* drug release data. Furthermore, the relevant rate constants and parameters were determined accordingly.

Acknowledgment. This work was supported by the grants from the National Science and Technology Council (NSTC), Taiwan.



POSTERS



PO 01

POSTERS

Unique structural conformations affect the overall catalytic process of the phosphopantetheine adenylyltransferase in a highly virulent ESKAPE pathogen

N. AHMAD, P. SHARMA, S. SHARMA, T. P. SINGH

Department of Biophysics, All India Institute of Medical Sciences, New Delhi, India, 110029

Email: nabbu1412@gmail.com

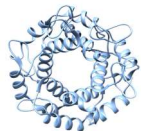
Keywords: coaD, PPAT, Coenzyme-A biosynthesis, ESKAPE pathogens.

Klebsiella pneumoniae is a gram-negative non-motile, encapsulated, lactose-fermenting, facultatively anaerobic, rod-shaped, pathogenic bacterium which is a leading cause of hospital-acquired infections. It is an opportunistic pathogen which colonizes the mucosal surfaces causing serious infections including pneumonia, UTIs, and bloodstream infections in hospitalized and immunocompromised individuals. Because of the rapid emergence of the multidrug-resistant strains of the species, it is the need of the hour to identify potential drug targets.

Coenzyme-A (CoA) is required as an essential cofactor in several metabolic reactions. The biosynthesis of CoA in bacteria occurs in five steps which are catalysed by four different enzymes. Pantothenate kinase (PanK), Phosphopantothenoyl-cysteine decarboxylase (PPCS) (catalysing the second and third steps), Phosphopantetheine adenylyltransferase (PPAT), and Dephospho-CoA kinase (DPCK). PPAT catalyzes the penultimate step of the pathway and involves the transfer of an adenylyl group from Adenosine-triphosphate (ATP) to 4'-phosphopantetheine (PhP) yielding 3'- dephospho-coenzyme A (dPCoA) and pyrophosphate (PP_i). Though PanK is a master regulator of CoA biosynthesis, PPAT is involved in the pathway regulation when regulation at the PanK step is circumvented by the feedback-resistant mutation thereby, making it an effective drug target.

We have determined the crystal structure of the PPAT enzyme from *Klebsiella pneumoniae* (*KpPPAT*) at 2.59 Å resolution. The crystals belonged to tetragonal space group P4₁2₁2 with cell dimensions of a=b=72.82 Å and c=200.37 Å. The asymmetric unit shows the presence of three crystallographically independent molecules A, B, and C. The structure determination shows that each *KpPPAT* molecule folds into six α-helices, and five β-helices arranged as β1-α1-β2-α2-β3-α3-β4-η1-α4-β5-α5-α6. This arrangement leaves a narrow cleft that extends deep into the centre of the molecule which represents the substrate binding site.

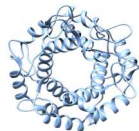
A key difference in the structure of *KpPPAT* when compared with those from other species is the position of the side chain of Met74 in the substrate binding site. This unique conformation adopted by Met74 due to its stabilization by neighbouring residues, prevents the binding of PhP in the same orientation as that in *EcPPAT* due to steric clashes. Also, the PhP binding in the active site region cannot be stabilised owing to the different orientations of Lys42, Pro40, and Pro44. These unique structural



constraints prevent the proper alignment of the phosphate group of the PhP molecule between two positively charged amino acids, Lys42 and Arg88.

Overall, we conclude that due to these unique structural conformations in *KpPPAT*, the overall catalytic process of the enzyme is affected, thereby, making the coenzyme-A pathway less relevant. This could be due to the adaptation of the bacterium to fulfil its demand for coenzyme-A through other means. Also, the feedback inhibition process seems to suffer because the structural constraints remain true during the binding of CoA and dPCoA.

Acknowledgment. This work was supported by research grants from Indian Council of Medical Research, New Delhi, India.



PO 02

POSTERS

Hofmeister anions' influence on the amyloid aggregation of α -lactalbumin

A. ANTOSOVA, M. GANCAR, J. MAREK, Z. GAZOVA

Institute of Experimental Physics Slovak Academy of Sciences, Watsonova 47, 040 01 Kosice, Slovakia

Calcium binding, globular whey protein α -lactalbumin (α -LA) gained attention in drug, vitamin, and bioactive compound delivery. α -LA is a unique protein from which many nanostructures (such as nanoparticles, nanotubes, nanodisks, and nanofibers) can be derived for different applications in food science and technology or drug delivery [1, 2].

Our goal was to study the influence of selected anions (SO_4^{2-} , CH_3COO^- , H_2PO_4^- , Br^- , NO_3^- , ClO_4^-) in the form of sodium salts on the α -lactalbumin amyloid aggregation to prepare specific amyloid fibrils for their further biotechnological applications. The aggregation kinetics, morphology of prepared amyloid fibrils and secondary/tertiary structures of native α -LA and α -LA fibrils have been studied using ThT fluorescence, ATR-FTIR and CD spectroscopy, and AFM. We have observed selected anions affecting the characteristics mentioned above of α -LA fibrils differently. The effect of studied anions on kinetic parameters of α -LA amyloid formation (t_{LAG} , t_{HALF}) strongly correlates to their position in the Hofmeister series (HS). t_{LAG} and t_{HALF} prolonged but followed the anions' order in HS, except for the t_{LAG} and t_{HALF} in the case of large and strongly hydrated $\text{H}_2\text{PO}_4^{2-}$ and CH_3COO^- , respectively. Distinctly shortest lag and half phases were observed for strongly hydrated anion SO_4^{2-} . α -LA aggregates formed in the presence of studied salts were visualised using AFM. The presence of CH_3COONa (Fig. 1), NaH_2PO_4 and NaBr resulted in many long fibrils. Furthermore, fibrils formed in the presence of CH_3COONa have the highest β -sheets content and the least amount of random secondary structure. Smaller amounts of shorter fibrils were formed in the presence of Na_2SO_4 (Fig. 1), NaNO_3 and NaClO_4 . This may be related to the fact that the tertiary structure of α -lactalbumin was intensively altered in the presence of these anions (Fig. 1). Discussed tertiary structure changes are described by a high WSD value obtained from weighted spectral difference analysis. Except for Na_2SO_4 , the fibril β -sheets content obtained by ATR-FTIR decreases, corresponding to the position of the anions in HS - from CH_3COONa to NaClO_4 . These findings are essential to clarify the mechanism of α -LA amyloid assembly and the possible application of its fibrils in biotechnology.

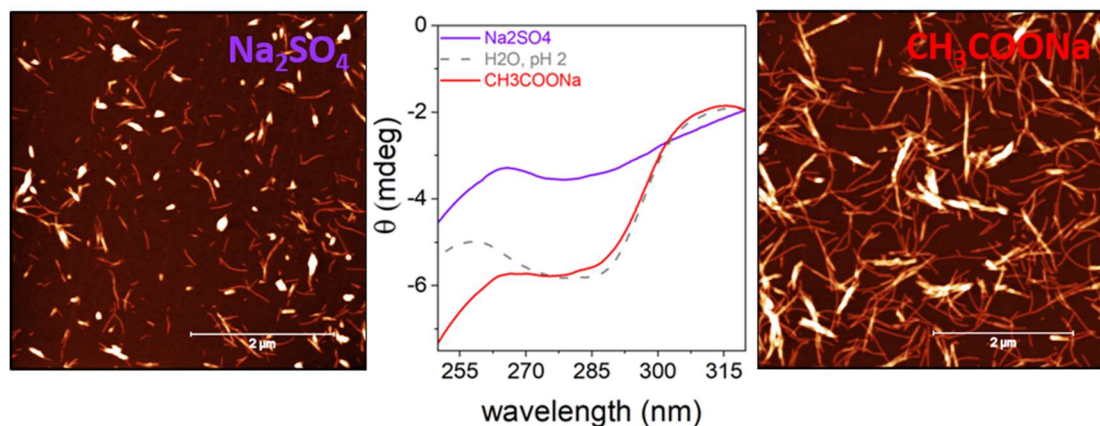
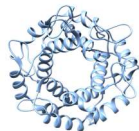
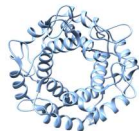


Fig. 1. AFM images of 10 μM α -LA fibrils prepared in the presence of Na_2SO_4 and CH_3COONa . Near-UV CD spectra of native 90 μM α -LA in the presence of 300 mM Na_2SO_4 (violet line) and CH_3COONa (red line) at pH 2.0. α -LA dissolved in the water at pH 2.0 (dotted grey line) served as a control.

Acknowledgement: This work was supported by research grants from the Slovak Research and Development Agency under the Contract no. APVV-18-0284, APVV-22-0598 and Slovak Grant Agency VEGA 2/0176/21, 02/0164/22 and BIOVID-19 (ITMS2014+ 313011AVG3) supported by OPII and funded by the ERDF.

References

1. Permyakov, E. A (2020). α -Lactalbumin, amazing calcium-binding protein. *Biomolecules*, 10, 1210
2. Jiménez-Cruz, E., Cuevas-Gómez, A., Unsworth, L., Cornejo-Mazón, M., Arroyo-Maya, I., Hernandez, H. (2021). Poly-L -lysine-coated α -lactalbumin nanoparticles: Preparation, effect of pH and stability under in vitro simulated gastrointestinal conditions. *Journal of Chemical Technology and Biotechnology*, 97, 1597–1603.



PO 03

POSTERS

Isolation and HPLC identification of fengycin isolated from *Bacillus coagulans* strain 9FT27 from Equine skin

^aZ. BEDLOVIČOVÁ, ^bE. STYKOVÁ, ^cN. ŠURÍN HUDÁKOVÁ, ^cM. MAĐAR

^aDepartment of Chemistry, Biochemistry and Biophysics, University of Veterinary Medicine and Pharmacy, Komenského 73, 041 81, Košice, Slovakia

^bEquine Clinic, University of Veterinary Medicine and Pharmacy, Komenského 73, 041 81, Košice, Slovakia

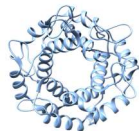
^cDepartment of Microbiology and Immunology, University of Veterinary Medicine and Pharmacy, Komenského 73, 041 81, Košice, Slovakia

Fengycin is the surface-active biosurfactant compound produced by various microorganisms including the genus *Bacillus*. Biosurfactants in general possess biological activities, *e. g.* antimicrobial, antibiofilm or antiadhesive properties leading to applications as antiinfective agents [1]. The strain 9FT 27 was isolated from the equine skin of a healthy broodmare of Norik breed Muráň Plain type, that was kept on pasture in the Center of Horse breeding in Dobšiná, Slovak Republic. The 16S rRNA gene of this bacteria was submitted to the GenBank database and published under the accession number *Bacillus coagulans* 9FT27 (AN: MN559543). The strain was deposited in Czech Culture Collection of Microorganisms (Brno, MUNI) as *Bacillus coagulans* Biocenol™ 9FT27 CCM 9014 under the Budapest treaty [2]. The aim of this study was to isolate and identify the lipopeptide biosurfactant fengycin. For isolation of fengycin was used standard methods described in our previous study [3]. For identification of fengycin the UHPLC with DAD detection was used.

Acknowledgment. This work was supported by the Slovak Research and Development Agency under the contract No. APVV-16-0203 and by the project of the Ministry of Education, Science, Research and Sport of the Slovak Republic VEGA 1/0372/22.

References

1. Roy, A. (2017) A review on the biosurfactants: Properties, types and its applications. *J. Fundam. Renew. Energy Appl.*, 8, 1–5
2. Styková, E., Nemcová, R., Maďar, M., ... & Domenech, F. R. (2022). Antibiofilm Activity of *Weissella* spp. and *Bacillus coagulans* Isolated from Equine Skin against *Staphylococcus aureus*. *Life*, 12, 2135
3. Englerová, K., Bedlovičová, Z., Nemcová, R., ... & Reiffová, K. (2021). *Bacillus amyloliquefaciens*—Derived Lipopeptide Biosurfactants Inhibit Biofilm Formation and Expression of Biofilm-Related Genes of *Staphylococcus aureus*. *Antibiotics*, 10, 1252.



PO 04

POSTERS

Monomerization of 14-3-3 ζ proteins modulates the aggregation of β -amyloid peptides

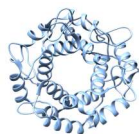
^aZ. BEDNARIKOVA, ^bA. KOZELEKOVA, ^bJ. HRITZ, ^aZ. GAZOVA

^a*Department of Biophysics, Institute of Experimental Physics, Slovak Academy of Sciences, Kosice, Slovakia*

^b*CEITEC MU, Brno, Czech Republic; Department of Chemistry, Faculty of Science, Masaryk University, Brno, Czech Republic*

Pathophysiology of Alzheimer's disease is tightly associated with intracellular tau protein and extracellular A β peptide deposits consisting of insoluble amyloid fibrils formed by these poly/peptides. The 14-3-3 proteins are one of the most abundant adaptor proteins expressed in the brain. They can be found extracellularly in the exosomes and cerebrospinal fluid of people with neurodegenerative diseases. Emerging studies describe 14-3-3 interactions with amyloidogenic proteins having a protective role through the sequestration of toxic, pathological proteins or chaperone-like activities. Most of these studies focus on amyloidogenic proteins with 14-3-3 binding motifs, such as tau protein or α -synuclein. On the other hand, studies about the impact of 14-3-3 proteins on A β peptide aggregation are very limited. Therefore, the A β anti-aggregation potential of 5 recombinant 14-3-3 ζ proteins was tested by in vitro Thioflavin T (ThT) fluorescence, infrared spectroscopy (FTIR), and atomic force microscopy (AFM). The IC₅₀ values (the concentration of 14-3-3 protein with 50 % inhibitory potential) determined from dose-dependent curves and the kinetics of fibril formation were used to assess the 14-3-3s potency. We have shown that phosphorylated monomeric mutant pS58 and monomeric mutant LEMK have the most substantial anti-aggregation potential. Our data suggest that dimer dissociation to monomers and increased hydrophobicity may be crucial in the anti-aggregation potential of 14-3-3 proteins.

Acknowledgment. This work was supported by the Slovak Research and Development Agency under the Contract no. APVV-22-0598; Slovak Grant Agency VEGA 02/0176/21; and MVTS-COST CA21160.



PO 05

POSTERS

Sugar as a cure – understanding the anti-amyloid potential of carbohydrate-amino acid hybrids

^aB. BOROVSÁ, ^bM. TVRDOŇOVÁ, ^aZ. BEDNÁRIKOVÁ, ^aZ. GAŽOVÁ

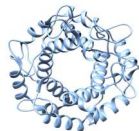
^aDepartment of Biophysics, Institute of Experimental Physics, Slovak Academy of Sciences, Košice, Slovakia

^bDepartment of Organic Chemistry, Institute of Chemical Sciences, Faculty of Science, P. J. Šafárik University, Košice, Slovakia

Amyloid fibrils are highly ordered and stable protein aggregates with high content of β -sheets in hydrogen-bonded cross- β conformation. *In vivo*, such structures can accumulate in cells and tissues, causing cell death, tissue and organ malfunction, often with fatal outcomes. Currently, more than 50 amyloid-related diseases are incurable and have unclear origins. Therefore, great scientific attention is directed towards understanding the mechanism of amyloid formation and designing molecules with the potential to either prevent amyloid formation or break down the amyloid aggregates into structures with as low side effects as possible. One of the mainly described anti-amyloid mechanisms is the disruption of the amyloid stabilizing elements such as hydrophobic, hydrogen and π -stacking interactions [1]. Previously, we showed that tripeptides composed of aromatic amino acids destroy $A\beta_{40}$ amyloid fibrils [2]. Similarly, the sugar-amino acid derivatives act like β -breakers; destabilize the amyloid fibrils by binding to their hydrophobic core [3].

Based on these results, we designed 12 carbohydrate-amino hybrids consisting of furanoid sugar and aromatic amino acids: furanoid sugar with amino acid moiety at the position C-3 or C-4 of the furanose skeleton (α - and β -amino acids) (1st group), conjugates of furanose with single aromatic amino acid (2nd group) or with aromatic dipeptides (3rd group). We studied the potential of these compounds to destroy the amyloid fibrils of intrinsically disordered $A\beta_{40}$ peptide ($A\beta_{40}F$) and HEW lysozyme amyloid fibrils (LAF). The Thioflavin-T fluorescence assay and atomic force microscopy (AFM) assessed the destroying potential of carbohydrate-amino acid conjugates. The potential of the studied molecules as drug candidates was predicted by *in silico* ADMET factors.

The studied hybrids were more prone to destroy the $A\beta_{40}F$ while were inactive towards LAF. The highest destruction potential on $A\beta_{40}F$ displayed compounds of the 1st group, while the destroying activity of the 2nd group did not show any significance. On the other hand, the effect of 3rd group's compounds was profoundly dependent on the amino acid composition. Furanoid sugar α -amino acid **1** and its dipeptide derivatives **8** (Trp-Trp) and **11** (Trp-Tyr) were the most potent anti- $A\beta$ fibrils compounds decreasing the number of amyloid fibrils by approx. 70 %. The ADMET calculations showed that the furanoid amino acids (1st group) and compounds **4** and **7** (2nd group) also satisfy the drug-likeness rule.

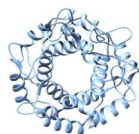


We have found that furanoid sugar-amino acid conjugates interfere with amyloid fibrils of A β ₄₀ peptide and lysozyme differently. Our results emphasize the importance of the structural elements of potent inhibitors. Conjugated aromatic rings and hydroxyl groups of tyrosine are essential features in destroying amyloid fibrils of the A β ₄₀ peptide.

Acknowledgements. This work was supported by Slovak Research and Development Agency under the Contract no. APVV-22-0598, Slovak Grant Agency VEGA 02/0176/21, Operational Programme Integrated Infrastructure, the project “NANOVIR”, ITMS: 313011AUW7 and “BIOVID”, ITMS: 313011AVG3, and the project implementation: Open scientific community for modern interdisciplinary research in medicine “OPENMED”, ITMS 2014+: 313011 V455 co-funded by ERDR.

References

1. Dorgeret, B.; Khemt' emourian, L.; Correia, I.; Soulier, J.L.; Lequin, O.; Onger, S., (2011) Eur. J. Med. Chem. 46 (2011) 5959–5969.
2. Viet, M.H.; Siposova, K; Bednarikova, Z; Antosova, A; Nguyen, T.T.; Gazova, Z; Li, M.S., (2015) J. Phys. Chem. B 119, 5145–5155
3. Levy-Sakin, M.; Shreberk, M.; Daniel, Y.; Gazit, E. (2009) Islets. 1:3, 210-215.



Effect of boceprevir on the lipid mesophases

^aA. ČELKOVÁ, ^aA. BÚCSI, ^aM. KLACSOVÁ, ^bJ.C. MARTÍNEZ and ^aD. UHRÍKOVÁ

^aDepartment of Physical Chemistry of Drugs, Faculty of Pharmacy, Comenius University Bratislava, SK-832 32, Odbojárov 10, Bratislava, Slovakia

^bBL-11 NCD beamline, Alba Synchrotron, Carrer de la Llum 2-26, 08290 Cerdanyola del Vallès, Barcelona, Spain

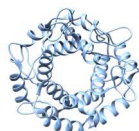
COVID-19 is an infectious disease caused by the virus SARS-CoV-2. According to WHO statistics, COVID-19 caused nearly 7 000,000 casualties, and the number is still growing even today. The available vaccines are effective in prevention, but their effectiveness is reduced by mutations in the spike protein. When prevention fails, treatment is necessary. Only two antivirals are authorised in the European Union (remdesivir and a combination nirmatrelvir/ritonavir) and one antiviral is being evaluated for market authorisation, molnupiravir [1].

In our study, we focus on boceprevir, an M^{Pro} inhibitor, as a potential SARS-CoV-2 antiviral. Boceprevir (BCP) is a repurposed peptidomimetic drug and was used to derive inhibitors with higher potency, including nirmatrelvir [2]. We studied the effect of boceprevir on two different types of membrane phospholipids: phosphatidylcholine (PC) and phosphatidylethanolamine (PE). The molecule of PC has a cylindrical shape, PCs are preferentially packed in bilayers forming a lamellar phase one dimensional periodical structure. A smaller headgroup of PE and unsaturated acyl-chains leads to a conical shape of the molecule with tendency to aggregate into nonlamellar phases, particularly inverted hexagonal phase H_{II}. H_{II} is a two-dimensional periodical structure, consists of lipid tubules with the headgroups oriented toward the interior; tubules are arranged in a hexagonal symmetry. H_{II} phase can serve as a simple model of membrane fusion. Membrane fusion is an essential for the main cell processes, such as endocytosis and exocytosis.

1,2-dimyristoyl-*sn*-glycero-3-phosphocholine (DMPC) was selected from PCs for the study. At 35°C, DMPC forms a lamellar liquid-crystalline phase L_α, which is natural state of the biological membrane. Egg yolk phosphatidylethanolamine (EYPE) selected for the study, forms L_α and H_{II} phase in the studied temperature range from 40 to 80°C.

The structural and thermodynamic properties of the DMPC-BCP system were monitored by small-angle X-ray scattering (SAXS) and differential scanning calorimetry (DSC). The diffractograms show typical peaks for the lamellar phase in the liquid-crystalline state L_α with repeat distance $d = 6.32 \pm 0.02$ nm for molar ratios BCP/DMPC ≤ 0.01 mol/mol. At higher content of the drug, two lamellar phases were detected with slightly different repeat distances, and different thermodynamic profiles: DSC revealed one peak with similar T_m as for pure DMPC and the second one is shifted to lower temperatures.

The formation of the H_{II} phase of our model BCP/EYPE was investigated in the temperature range 40-80°C. EYPE shows 3 sharp peaks at $t < 54^\circ\text{C}$, typical for a lamellar phase L_α, we found the repeat distance $d \sim 5$ nm. The onset of the L_α → H_{II} transition for EYPE was detected at 54°C. With an increasing molar ratio BCP/EYPE, the onset temperature was shifted to a higher value with maximum 64°C, at molar ratio 0.1 mol/mol. After reaching the maximum, the onset temperature drops to 57°C for the



highest studied molar ratio 0.5 mol/mol. With increasing temperature to 70°C, the system shows a coexistence of lamellar L_α and hexagonal phase H_{II} for BCP/EYPE < 0.1 mol/mol. In addition, we detected the coexistence of a lamellar, hexagonal and a cubic phase in mixtures of BCP/EYPE ≥ 0.1 mol/mol (Fig. 1 left). From the positions of the peaks, we resolved the structure as a cubic $Pn3m$ phase. Further heating of the system (80°C) caused vanishing of the lamellar phase (Fig. 1 right).

BCP is insoluble in water, the drug incorporates into the lipid bilayer and induces thermodynamic and structural changes. In the bilayer containing DMPC, we observed a fluidizing effect of the drug. On the other hand, BCP stabilises the lamellar packing of the EYPE membrane, and the onset of H_{II} phase is shifted to the higher temperature. Moreover, the formation of a cubic phase was detected in mixtures BCP/EYPE ≥ 0.1 mol/mol. Bicontinuous cubic phases (like $Pn3m$) attract attention because of their ability to facilitate transport through the biological membrane, and in the formulation of sustained-release dosage forms.

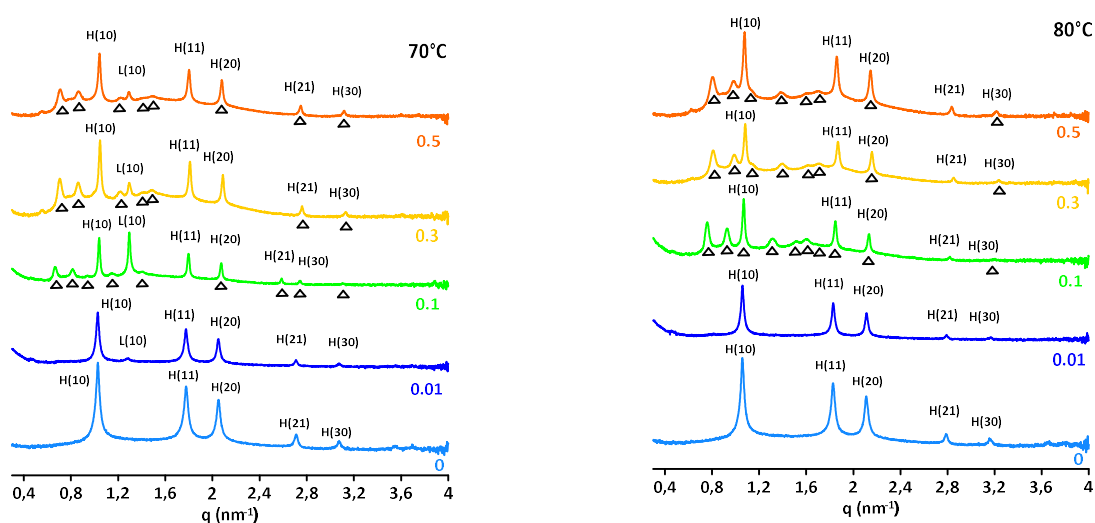
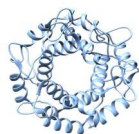


Figure 1. SAXS patterns at 70°C (left) show the coexistence of lamellar and non-lamellar phases at molar ratios higher than 0.1 mol/mol included. We observed the complete transition from lamellar phase to non-lamellar phases at 80°C (right). Black triangles denote reflexions of the cubic phase.

Acknowledgement: SAXS experiments were performed at BL11-NCD beamline at Alba Synchrotron with the collaboration of Alba staff. This work was supported by projects VEGA 1/0223/20, APVV-21-0108 and UK/369/2023.

References

1. European Medicines Agency: COVID-19 treatment: authorized, (2023). <https://www.ema.europa.eu/en/human-regulatory/overview/public-health-threats/coronavirus-disease-covid-19/treatments-vaccines/treatments-covid-19/covid-19-treatments-authorized> (accessed July 18, 2023).
2. Y.R. Alugubelli, Z.Z. Geng, K.S. Yang, N. Shaabani, K. Khatua, X.R. Ma, E.C. Vatanserver, C.C. Cho, Y. Ma, J. Xiao, L.R. Blankenship, G. Yu, B. Sankaran, P. Li, R. Allen, H. Ji, S. Xu, W.R. Liu, A systematic exploration of boceprevir-based main protease inhibitors as SARS-CoV-2 antivirals, *Eur J Med Chem.* 240 (2022) 1–11.



PO 07

POSTERS

Determination of kinetics stabilizers reducing the formation of light chain protein deposits in multiple myeloma

^aV. DEMČÁKOVÁ, ^bG. ŽOLDÁK

^aDepartment of Biophysics, Institute of Physics, Pavol Jozef Šafárik University, Košice, Slovakia

^bCenter for Interdisciplinary Biosciences, Technology and Innovation Park, Pavol Jozef Šafárik University, Košice, Slovakia

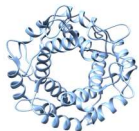
Multiple myeloma is the second most common oncohematological disease characterized by the accumulation of neoplastic plasma cells in the bone marrow. Malignant plasma cells produce increased levels of abnormal forms of immunoglobulin or only a part of them called M-protein. In 15% of multiple myeloma cases neoplastic plasma cells overexpress only free abnormal light chains (LC) of immunoglobulin G without the presence of a heavy chain [1]. Most LCs would be excreted by the kidneys. However, due to misfolding pathological forms of the LCs show lower stability and tend to form protein deposits in vital organs, for example heart or kidneys. Deposits of the immunoglobulin light chain are highly resistant to proteolysis, which allows them to accumulate and makes them difficult to remove from organs [2]. Additionally, these deposits are highly toxic to cells and cause organ dysfunction or even organ failure [3].

Current therapy primarily focuses on the eradication of malignant clones of plasma cells. However, the treatment primarily uses cytotoxic chemotherapy, which is often poorly tolerated by MM patients. Nevertheless, the potential strategy could involve the reduction of the formation of light chain deposits by “kinetic stabilizers”. They are small molecules able to interact with LCs, stabilize the native structure and prevent their misfolding [4]. This strategy was successfully used to reduce the formation of deposits in transthyretin amyloidosis (TTR). TTR stabilizers (tafamidis) decreased the mortality of patients with transthyretin amyloid cardiomyopathy [5] [6]. Finding molecules that would stabilize light chain structure and prevent the formation of its protein deposits could be used as a potential treatment for patients with light chain multiple myeloma.

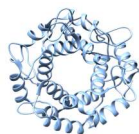
Acknowledgment. This work was supported by research grants Slovak research and development agency (No. APVV-18-0285), the Slovak Grant Agency VEGA No 1/0024/22, EU H2020 TWINNING program GA. No. 952333 project CasProt, BioPickmol, ITMS2014+: 313011AUV6 supported by the Operational Programme Integrated Infrastructure, funded by the ERDF.

References

1. Zhang, J., Sun, W., Huang, Z., Chen, S., Zhong, Y., Hu, Y., An, N., Shen, M., & Li, X. (2014). Light chain multiple myeloma, clinic features, responses to therapy and survival in a long-term study. *World Journal of Surgical Oncology*, 12:234.
2. Brumshtein, B., Esswein, S. R., Salwinski, L., Phillips, M. L., Ly, A. T., Cascio, D., Sawaya, M. R., & Eisenberg, D. S. (2015). Inhibition by small-molecule ligands of formation of amyloid fibrils of an immunoglobulin light chain variable domain. *eLIFE*, 4:e10935.



3. Morgan, G. J., Usher, G. A., & Kelly, J. W. (2017). Incomplete Refolding of Antibody Light Chains to Non-Native, Protease-Sensitive Conformations Leads to Aggregation: A Mechanism of Amyloidogenesis in Patients? *Biochemistry*, 56(50), 6597–6614.
4. Morgan, G. J., Yan, N. L., Mortenson, D. E., Rennella, E., Blundon, J. M., Gwin, R. M., Lin, C. Y., Stanfield, R. L., Brown, S. J., Rosen, H., Spicer, T. P., Fernandez-Vega, V., Merlini, G., Kay, L. E., Wilson, I. A., & Kelly, J. W. (2019). Stabilization of amyloidogenic immunoglobulin light chains by small molecules. *Proceedings of the National Academy of Sciences of the United States of America*, 116(17), 8360–8369.
5. Maurer, M. S., Schwartz, J. H., Gundapaneni, B., Elliott, P. M., Merlini, G., Waddington-Cruz, M., Kristen, A. V., Grogan, M., Witteles, R., Damy, T., Drachman, B. M., Shah, S. J., Hanna, M., Judge, D. P., Barsdorf, A. I., Huber, P., Patterson, T. A., Riley, S., Schumacher, J., ... Rapezzi, C. (2018). Tafamidis Treatment for Patients with Transthyretin Amyloid Cardiomyopathy. *New England Journal of Medicine*, 379(11), 1007–1016.
6. Rosenblum, H., Castano, A., Alvarez, J., Goldsmith, J., Helmke, S., & Maurer, M. S. (2018). TTR (Transthyretin) Stabilizers Are Associated with Improved Survival in Patients with TTR Cardiac Amyloidosis. *Circulation: Heart Failure*, 11(4).



Ionic liquids as a powerful amyloid formation-inducing tool

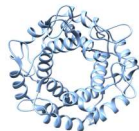
^aD. FEDUNOVA, ^aV. VANIK, ^aA. ANTOSOVA, ^aZ. BEDNARIKOVA, ^aJ. MAREK,
^aM. GANCAR, ^bM. GUNCHEVA, ^aZ. GAZOVA

^a*Department of Biophysics, Institute of Experimental Physics, Slovak Academy of Sciences, Kosice, Slovakia*

^b*Institute of Organic Chemistry with Centre of Phytochemistry, Bulgarian Academy of Sciences, Sofia 113, Bulgaria*

The amyloid fibrils have been gaining interest as potential novel biomaterials due to their high stability, strength, elasticity or resistance against degradation. The great effort is focused on developing strategies to regulate amyloid aggregation *in vitro* in order to optimize amyloid fibril fabrication as well as to contribute to the understanding of the fundamental principles of amyloid aggregation. Among the crucial conditions affecting the protein self-assembly into amyloid fibrils are solvent properties [1]. Ionic liquids (ILs) are novel solvents consisting of organic cation and organic/inorganic anion. ILs are called “designer solvents” due to the tunability of their physico-chemical properties based on the variability of their composition.

In this work, we have studied the effect of several series of ILs containing imidazolium- or cholinium-based cations and amino acid-based or Hofmeister series anions on the amyloid aggregation of insulin (IN) and lysozyme (LZ). Using the combination of spectroscopic, calorimetric and microscopic methods along with docking calculations, we have characterized the effect of ILs on the kinetics of formation and morphology of the amyloid fibrils. We have found that the kinetics of amyloid aggregation of both proteins depends on the ILs concentration, charge and hydrophobicity of used ions. Hofmeister series rank anions according to their effect on protein stability, solubility or activity. We have found that all selected Hofmeister anions were able to induce the formation of LZ amyloid fibrils or accelerate the kinetics of IN amyloid aggregation depending on concentration and anion type. Moreover, at higher concentrations, the kinetics parameters followed the reverse Hofmeister series ($[\text{HSO}_4^-] > [\text{CH}_3\text{COO}^-] > [\text{Cl}^-] > [\text{NO}_3^-] > [\text{BF}_4^-]$), pointing out the direct interactions of anions with protein surface mediating the effect along with non-specific electrostatic shielding. The important role of the electrostatic interactions was observed also for the amino acid-based anions. The most effective accelerators of IN amyloid aggregation kinetics were anions with an additional charge on the side chain (Lys, Glu) combined with either cation. On the other hand, ILs containing hydrophobic Trp anion inhibited the formation of insulin amyloid fibrils, which is in agreement with previous findings that an effective inhibitor might contain a planar aromatic ring capable of interfering with β -sheet-rich structures - an inherent composition of amyloid fibrils. The inhibiting effect was also observed in the presence of non-polar Ile anion. The interference with the hydrophobic protein core is an important factor modulating the amyloid aggregation kinetics of IN. ILs consisting of the n-alkyl imidazolium cations [$n = 4, 6, 8, 10$]



accelerated/inhibited kinetics of IN amyloid aggregation in dependence of concentration and n-alkyl chain length. ILs cations interact with the amyloidogenic (amyloid aggregation-prone) hydrophobic region of IN, with the affinity increasing with the increase of the n. These specific interactions, along with the non-specific interactions with the hydrophobic patches on the protein surface and electrostatic screening, may contribute to the change from promoting amyloid fibrillization to inhibiting it.

The studied ILs were able to modulate the morphology of obtained amyloid fibrils of LYS and IN. The formed fibrils possess needle-like morphology with different heights, lengths or ability to associate laterally or into big clusters in dependence on ILs concentration and composition. The variability of fibril morphology was not based on the changes in the secondary structure of proteins, but mainly on the number and arrangement of protofibrils into fibrils. The highest variability in fibril morphology was found in the presence of n-alkyl-imidazolium ILs producing fibrils with lengths varying from 212 to 1021 nm.

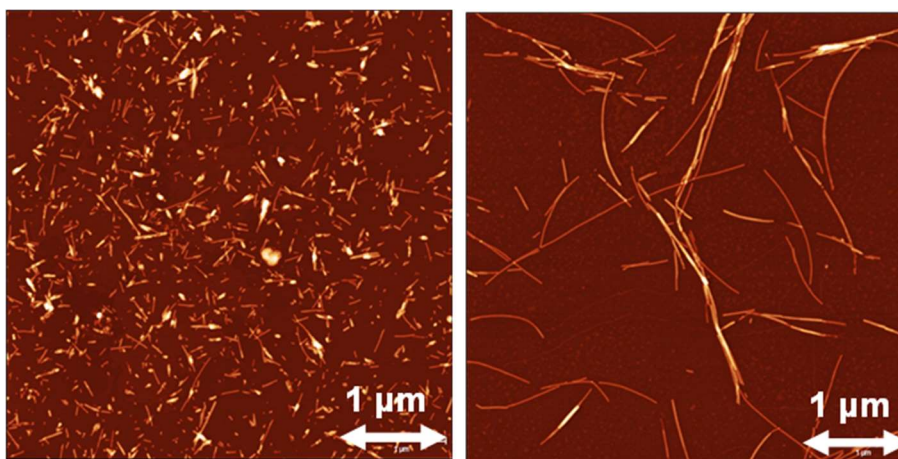


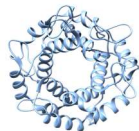
Figure: AFM image of the Insulin amyloid fibrils ($10 \mu\text{M}$) formed in: (left) water solution, pH 1.6; (right) 25 mM 1-octyl-3-methylimidazolium chloride.

We conclude that all of the examined ILs were able to modulate the amyloid fibrilization of selected proteins and produce morphologically different fibrils. The effect of ILs was specifically driven by a sensitive balance and interplay between specific protein-ion and ion-water interactions and non-specific long-range electrostatic shielding. The application of ILs as modulators of protein amyloid aggregation is beneficial for further utilization of fibrils in biotechnological applications and understanding the molecular mechanism of protein amyloid aggregation and stability in complex solvents such as ILs.

Acknowledgment. This work was supported by the Slovak Research and Development Agency under the Contract no. APVV-22-0598; Slovak Grant Agency VEGA 02/164/22, 02/0176/21 and the Operational Programme Integrated Infrastructure, the project „NANOVIR“, ITMS: 313011AUV7, co-funded by ERDF.

References

Almeida Z. L. & Brito R. M. (2020). Structure and Aggregation Mechanis in Amyloids. *Molecules*, 25(5), 1195.



PO 09

POSTERS

Functionalization of β -casein micelles with fluorescently-labeled DNA aptamers for targeting cancer cells

Z. GARAIOVÁ, I. KRÁĽOVÁ, M. ZVARÍK, M. VELÍSKOVÁ, T. HIANIK

*Department of Nuclear Physics and Biophysics, Faculty of Mathematics, Physics and Informatics,
Comenius University, Bratislava, Slovakia*

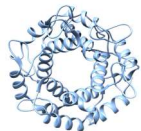
β -casein is an amphiphilic milk protein that can self-assemble into the micellar nanostructures. These structures are interesting for their potential drug delivery applications including cancer therapy [1,2].

Aptamers are short nucleic acid sequences which can fold into the unique structure and bind targets, e.g., oncomarker receptors, with high affinity and specificity [3]. Functionalization of casein structures with aptamers has not been studied in sufficient details so far.

We focused on the preparation and modification of β -casein micelles with sgc8c DNA aptamers that specifically bind to protein tyrosine kinase 7 (PTK7), which is highly expressed in the membranes of the leukemic cells [4]. The aptamers were fluorescently labeled (Atto542) and conjugated with a cholesteryl-TEG linker (Chol-sgc8c-Atto542). The micelles were prepared from β -casein (2 mg/ml) in sodium-phosphate buffer (10 mmol/l, pH 7) in the presence of CaCl_2 (10 mmol/l) or without CaCl_2 under constant stirring for 1.5 h at 25 °C, followed by filtration through a 0.2 μm pore size filter. The filtered micelles were modified with aptamers (2 $\mu\text{mol/l}$) under constant stirring for 2h at laboratory temperature (approx. 20 °C). The prepared formulations were analyzed by fluorescence measurements using a) microplate reading and b) size exclusion chromatography (SEC-HPLC) on a 30 nm size pore column.

The fluorescence signal ($\lambda_{\text{ex}} = 510 \pm 10$ nm, $\lambda_{\text{em}} = 580 \pm 30$ nm) from microplate reading was observed to be quenched upon the incubation of sgc8c with β -casein as well as with CaCl_2 . The fluorescent signal originated from the internal fluorescence of β -casein ($\lambda_{\text{ex}} = 295$ nm, $\lambda_{\text{em}} = 343$ nm) and from the Atto542-fluorescence of aptamer ($\lambda_{\text{ex}} = 540$ nm, $\lambda_{\text{em}} = 565$ nm) were obtained by SEC-HPLC. The fluorescence peak of β -casein had a 2-arm profile that eluted at 3.4 min and 5 min suggesting a presence of its different variants (A1, A2/B) or oligomeric forms. The fluorescent signal corresponding to shorter elution time of β -casein decreased for the complexed sample of β -casein + Chol-sgc8c-Atto 542, and the fluorescence signal from the aptamer was partly shifted to this region. Similar behaviour was observed for the complexed sample in the presence of CaCl_2 . In both cases, aptamers being not coeluted – signal at later retention times (6 min) was also observed, indicating the presence of unbound Chol-sgc8c-Atto 542, too.

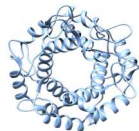
Obtained results suggest interaction of fluorescently labelled Chol-sgc8c-Atto 542 aptamer with β -casein, the most preferably with its slightly bigger variant/form possessing probably more hydrophobic regions that complement the hydrophobic nature of aptamer cholesteryl-moiety.



Acknowledgment. This work was supported by the Science Agency VEGA research grant, project No. 1/0554/23.

References

1. Li, M., Fokkink, R., Ni, Y., Kleijn, J.M. (2019). Bovine beta-casein micelles as delivery systems for hydrophobic flavonoids. *Food Hydrocolloids*, 96, 653-662.
2. Cuggino, J.C., Picchio, L.M., Gugliotta, A., Burgi, M., Ronco, L.I., Calderón, M., Etcheverrigaray, M., Alvarez Igarzabal, C.I., Minari, R.J., Gugliotta, L.M. (2021). Crosslinked casein micelles bound paclitaxel as enzyme activated intracellular drug delivery systems for cancer therapy. *European Polymer Journal*, 145, 110237.
3. Fu, Z., Xiang, J. (2020). Aptamer-Functionalized Nanoparticles in Targeted Delivery and Cancer Therapy. *International Journal of Molecular Sciences*, 21(23), 9123.
4. Poturnayová, A., Buríková, M., Bizík, J., Hianik, T. (2019). DNA Aptamers in the Detection of Leukemia Cells by the Thickness Shear Mode Acoustics Method. *Chemphyschem: a European journal of chemical physics and physical chemistry*, 20(4), 545-554.



Archaeal FKBP: Peculiarities in structure and function

Anchal Manisha GOEL

Department of Biophysics, University of Delhi, South Campus, New Delhi

Email: deshwal.anchal@gmail.com

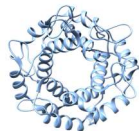
FKBPs are one of the classes of peptidyl prolyl cis–trans isomerases. *Cis–trans* isomerization of peptidyl-prolyl bonds is the rate limiting step in protein folding [1]. PPlases (EC 5.2.1.8) catalyse this step and thereby accelerate protein folding [2]. PPlase function has been studied in eukaryotes and bacteria, but very little is known about their role in archaeal organisms. Eukaryotes and bacteria often have multiple copies of various PPlase homologs with variation in functions from PPlase activity to receptor signalling and signal transfer [3].

The current study is an attempt to understand the mechanistic working of the archaeal FKBP. We studied the distribution of FKBP homologs in the five archaeal phyla. Subsequently we studied their phylogenetic evolution, conservation of functional amino acids residues, and structural variation in native states of proteins to throw light on their molecular function in comparison to other orthologs found in bacteria and eukaryotes. We have structurally and functionally characterized the FKBP from a halophile *Haloferax mediterranei*. It exhibits both PPlase and chaperone activity. Interestingly it also exhibits inhibition of β -amyloid formation. This is the first biophysical characterization of any archaeal FKBP. This will contribute to our understanding proteostasis in archaea and also serve as model system for understanding protein folding disease.

Acknowledgement: This work was supported by the research grant From Indian council for medical research (ICMR) and University of Delhi, South Campus.

References

1. Brandts JF, Halvorson HR, Brennan M. Consideration of the Possibility that the slow step in protein denaturation reactions is due to cis-trans isomerism of proline residues. *Biochemistry*. 1975 Nov 4;14(22):4953-63. doi: 10.1021/bi00693a026. PMID: 241393.
2. Göthel SF, Marahiel MA. Peptidyl-prolyl cis-trans isomerases, a superfamily of ubiquitous folding catalysts. *Cell Mol Life Sci*. 1999 Mar;55(3):423-36. doi: 10.1007/s000180050299. PMID: 10228556.
3. Kang CB, Hong Y, Dhe-Paganon S, Yoon HS. FKBP family proteins: immunophilins with versatile biological functions. *Neurosignals*. 2008;16(4):318-25. doi: 10.1159/000123041. Epub 2008 Jul 18. PMID: 18635947.



Spectroscopic elucidation of the binding mechanism between novel 2,6,9-trisubstituted acridine derivatives and calf thymus DNA

^aA. GUCKÝ, ^aO. OZHELEVSKA, ^bJ. KORÁBEČNÝ, ^aM. KOŽURKOVÁ

^a*Department of Biochemistry, Institute of Chemical Sciences, Faculty of Science, Pavol Jozef Šafárik University, Košice, Slovakia*

^b*Department of Toxicology and Military Pharmacy, Faculty of Military Health, University of Defence, Hradec Králové, Czech Republic*

Acridine derivatives represent one of the most versatile compounds in multiple fields of current pharmacotherapy. Their biological activity stems particularly from the ability of the planar azaheterocyclic ring to interact with various biomacromolecules. Nonetheless, this activity can be enhanced by structural modifications of the acridine moiety, mainly in position 9 as well as in other positions (e.g. 2,3,6). 9-substituted acridines exhibit anticancer, antibacterial, antiprotozoal, antioxidant, antimalarial, antifungal and numerous other pharmacologically important effects [1,2]. Acridine derivatives belong to the class of low-molecular-weight ligands, the most attractive modern chemotherapeutics. These small molecules tend to interact with DNA as their target biomacromolecule. Such interactions are of non-covalent nature and comprise three major binding modes – intercalation, groove binding and electrostatic interaction. The mechanisms of ligand-DNA interactions may be deciphered with the aid of various spectroscopic techniques and such investigation is advantageous in elucidating the binding parameters of a given molecule [3]. In our study, we have employed different spectroscopic methods to ascertain the mode of interaction between three novel 2,6,9-trisubstituted acridine derivatives **A1-A3** (Fig. 1) and calf thymus DNA (ctDNA). The UV-Vis absorption spectra of all studied compounds displayed hypochromic and bathochromic shifts upon addition of ctDNA and observed isosbestic points confirmed the formation of a complex between ctDNA and derivatives **A1-A3**. Fluorescence spectra measured at three different temperatures displayed a single emission band for each compound in the wavelength range of 480-495 nm and this fluorescence was gradually quenched as ctDNA was being added to the sample. Circular dichroism spectra of ctDNA exhibited considerable alterations in the intensity of both the positive and negative band upon interaction with the acridine derivatives **A1-A3**. Finally, thermal denaturation studies revealed significant alterations in T_m value of the used ctDNA sample that have arisen upon complex formation with the ligands **A1-A3** (4,89-6,44 °C). In summary, all of the aforementioned results seem to indicate that acridine derivatives **A1-A3** interact with ctDNA predominantly through an intercalative mechanism, which is also typical for numerous acridine-based compounds.

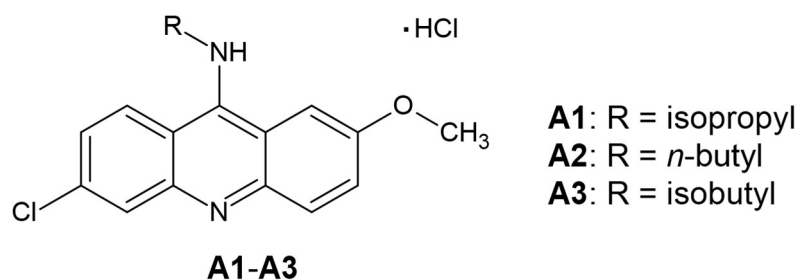
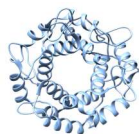
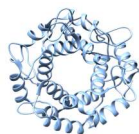


Fig. 1 Chemical structure of studied acridine derivatives **A1-A3**.

This work was supported by research grant VEGA no. 1/0037/22.

References

1. Kožurková, M., Sabolová, D., Kristian, P. (2021). A new look at 9-substituted acridines with various biological activities. *Journal of Applied Toxicology*, 41(1), 175-189.
2. Vilková, M., Hudáčková, M., Palušeková, N., Jendželovský, R., Almáši, M., Béres, T., Fedoročko, P., Kožurková, M. (2022). Acridine Based *N*-Acyldiazone Derivatives as Potential Anticancer Agents: Synthesis, Characterization and ctDNA/HSA Spectroscopic Binding Properties. *Molecules*, 27(9), 2883.
3. Rehman, S. U., Sarwar, T., Husain, M. A., Ishqi, H. M., Tabish, M. (2015) Studying non-covalent drug-DNA interactions. *Archives of Biochemistry and Biophysics*, 576, 49-60.



PO 12

POSTERS

Examination of “high-energy” metastable state of the oxidized bovine cytochrome c oxidase: proton uptake and reaction with H₂O₂

^aD. JANCURA, ^aA. TOMKOVÁ, ^aT. SZTACHOVÁ, ^bV. BERKA, ^cM. FABIAN

^aDepartment of Biophysics, Faculty of Science, University of P. J. Safarik, Jesenna 5, 041 54 Kosice, Slovak Republic

^b Department of Internal Medicine, University of Texas Health Science Center, 77030 Houston, Texas, USA

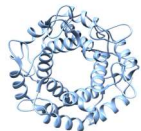
^cCenter for Interdisciplinary Biosciences, Technology and Innovation Park, University of P. J. Safarik, Jesenna 5, 041 54 Kosice, Slovak Republic.

Cytochrome c oxidase (CcO) catalyzes the electron transfer from ferrocyanochrome c to molecular oxygen and contributes to the formation of electrochemical proton gradient on inner mitochondrial membrane [1]. One of the current models of the proton pumping relies on the existence of a high-energy metastable **O_H** state, which is formed immediately after oxidation of the fully reduced CcO with the oxygen. In the absence of external electron donor, the high-energy **O_H** form should relax to the resting oxidized form (**O**) [2]. It was proposed that the catalytic heme *a*₃-Cu_B center of these two forms should differ in a protonation state and the transition of **O_H**-to-**O** is associated with a proton transfer into this center [3]. In this work, employing a stopped-flow and UV-Vis absorption spectroscopy, we investigated a proton uptake during the assumed relaxation of **O_H**. It is shown, using pH indicator phenol red, that from 100 ms up to ~10 minutes after reoxidation of the fully reduced CcO, there is no uptake of a proton from medium (pH 7.8). Moreover, ligation state and protonation of Tyr244, located at the vicinity of the catalytic center, were examined by interaction of **O** and **O_H** with H₂O₂. Identical kinetics of the interaction of H₂O₂ with both **O** and **O_H** indicate the same ligation state of the catalytic site and protonation state of Tyr244 in both forms of the oxidized CcO. These results together with previous findings [4] suggest that the ligation and protonation state of the catalytic center should be the same in both forms of the oxidized CcO, or relaxation of the catalytic center during the **O_H**-to-**O** transition occurs in few milliseconds.

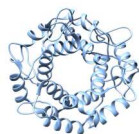
Acknowledgment. This work was supported by the project “Open scientific community for modern interdisciplinary research in medicine (OPENMED)-ITMS2014+: 313011V455” from the Operational Program Integrated Infrastructure funded by the ERDF and by the Slovak Grant Agency (VEGA 1/ 0028/22).

References

1. Wikstrom, M., R.B. Gennis, R.B. and P.R. Rich, P.R. (2023). Structures of the intermediates in the catalytic cycle of mitochondrial cytochrome c oxidase. *Biochim Biophys Acta Bioenerg*, 2023. 1864, : art. numb. 148933.
2. Verkhovsky, M.I., et al.(1999). Proton translocation by cytochrome c oxidase. *Nature* 400, 480-483.



3. Sharma, V. Karlin, K.D. and M. Wikstrom, M. (2013). Computational study of the activated O_H state in the catalytic mechanism of cytochrome c oxidase. PNAS 110, 16844-16849.
4. Jancura, D., et al. (2006). Spectral and kinetic equivalence of oxidized cytochrome c oxidase as isolated and "activated" by reoxidation. J Biol Chem. 281, 30319-30325.



PO 13

POSTERS

Molecular design of novel papain-like protease inhibitors with potential antiviral activity against SARS-CoV-2

^aL. KERTI, ^aV. FREČER

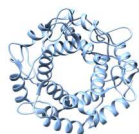
^a *Department of Physical Chemistry of Drugs, Faculty of Pharmacy, Comenius University Bratislava, Slovak republic*

The pandemic of the new coronavirus SARS-CoV-2, which causes the severe acute respiratory syndrome COVID-19, represents a long-term threat to the health of the population. The subject of this study is based on previous results in the development of SARS-CoV-2 inhibitors [1]. The topic lies in the computational molecular design and optimization of aminophenylethylbenzamides (APEB) and other potential inhibitors that bind to the papain-like protease PL^{pro} of the SARS-CoV-2 coronavirus and inhibit its proteolytic, deubiquitination, and deISGylation activity, which is directly related to the dramatic course of COVID-19 disease [2–5].

The objective of the study is to design and optimize novel chemical structures that are capable of inhibiting PL^{pro} protease and to predict inhibitory potencies and pharmacokinetic parameters of the proposed drug candidates. Other goals of the study are to clarify the detailed mechanism of action of APEB and to propose quantitative structure-activity relationships (QSAR) of PL^{pro} inhibitors based on inhibitory activity data from similar compounds taken from the literature that inhibit PL^{pro} of SARS-CoV-2 at micromolar concentrations. The most perspective compounds will be synthesized and evaluated later for inhibitory activities in enzyme inhibition assays. The most important contribution of our study is the improvement of the structures of known PL^{pro} inhibitors, which are expected to reach inhibitory concentrations at the nanomolar concentration scale.

The project uses rational structure-based drug design, molecular modeling, and computer simulation methods based on molecular mechanics, molecular dynamics, and quantum chemistry, which are available in the Small Molecule Discovery Suite software package (Schrödinger, Inc., USA). This software also offers an ideal graphical interface for working with protein structures, enzymes or receptors, their processing, and preparation, for demanding computational simulations, the design, and preparation of suitable ligands, and calculation of binding energies and other parameters of intermolecular interactions between a ligand and receptor. [6]

Based on the QSAR correlation between the calculated binding energies (ΔE_{bin}) and the observed inhibitory potencies IC_{50}^{exp} taken from the literature ($R^2 = 0.85$), we have designed a new series of PL^{pro} inhibitors of the class of APEB. In the first phase, we have generated a larger combinatorial library of inhibitors of PL^{pro} and screened them by docking to the active site of PL^{pro}. The calculated ΔE_{bin} and predicted inhibitory concentrations resulting from the QSAR model (IC_{50}^{pre}) were used to identify a dozen



new APEB molecules with stronger binding affinity to the target PL^{pro}. For the resulting best APEB analogues, the ADME properties were also predicted by means of the QikProp program (Schrödinger, Inc., USA). Taking all these steps into account, we discovered perspective APEBs with predicted IC₅₀^{pre} values in the micromolar to nanomolar concentration range with favorable pharmacokinetic properties.

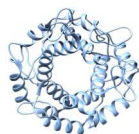
The results are consistent with the initial hypothesis that the extension of known APEB structures to reach the S₂ and S₁ pockets of the catalytic site of PL^{pro}, when also complemented by an electrophilic capping group capable of a strong interaction with catalytic cysteine residues, will enhance the binding affinity of APEB. Closure of the BL2 loop also plays a significant role in stabilizing the enzyme-inhibitor complex by covering the S₃ and S₄ pockets of the substrate channel.

These results provide a significant step towards the development of new specific and potent inhibitors of SARS-CoV-2 PL^{pro} and show that the APEB pharmacophore skeleton could be suitable for the design of potent inhibitors against coronaviruses.

Acknowledgment. This work was supported by a research grant from the Slovak Research and Development Agency APVV-21-0108.

References

1. Shen, Z., Ratia, K., Cooper, L., Kong, D., Lee, H., Kwon, Y., Li, Y., Alqarni, S., Huang, F., Dubrovskiy, O., Rong, L., Thatcher, G. R. J., & Xiong, R. (2022). Design of SARS-CoV-2 PL^{pro} Inhibitors for COVID-19 Antiviral Therapy Leveraging Binding Cooperativity. *Journal of Medicinal Chemistry*, 65(4), 2940–2955. <https://doi.org/10.1021/acs.jmedchem.1c01307>
2. Munnur, D., Teo, Q., Eggermont, D., Lee, H. H. Y., Thery, F., Ho, J., van Leur, S. W., Ng, W. W. S., Siu, L. Y. L., Beling, A., Ploegh, H., Pinto-Fernandez, A., Damianou, A., Kessler, B., Impens, F., Mok, C. K. P., & Sanyal, S. (2021). Altered ISGylation drives aberrant macrophage-dependent immune responses during SARS-CoV-2 infection. *Nature Immunology*, 22(11), Article 11. <https://doi.org/10.1038/s41590-021-01035-8>
3. Freitas, B. T., Durie, I. A., Murray, J., Longo, J. E., Miller, H. C., Crich, D., Hogan, R. J., Tripp, R. A., & Pegan, S. D. (2020). Characterization and Noncovalent Inhibition of the Deubiquitinase and delSGylase Activity of SARS-CoV-2 Papain-Like Protease. *ACS Infectious Diseases*, 6(8), 2099–2109. <https://doi.org/10.1021/acsinfecdis.0c00168>
4. Cao, X. (2021). ISG15 secretion exacerbates inflammation in SARS-CoV-2 infection. *Nature Immunology*, 22(11), Article 11. <https://doi.org/10.1038/s41590-021-01056-3>
5. Shin, D., Mukherjee, R., Grewe, D., Bojkova, D., Baek, K., Bhattacharya, A., Schulz, L., Widera, M., Mehdipour, A. R., Tascher, G., Geurink, P. P., Wilhelm, A., van der Heden van Noort, G. J., Ovaa, H., Müller, S., Knobloch, K.-P., Rajalingam, K., Schulman, B. A., Cinatl, J., ... Dikic, I. (2020). Papain-like protease regulates SARS-CoV-2 viral spread and innate immunity. *Nature*, 587(7835), 657–662. <https://doi.org/10.1038/s41586-020-2601-5>
6. Schrödinger Release 2023-2: Schrödinger, LLC, New York, NY, 2023.



Effect of Remdesivir on the Exogenous Pulmonary Surfactant

^aA. KESHAVARZI, ^aA. Asi SHIRAZI, ^aM. KLACSOVÁ, ^bJ.C. MARTÍNEZ, ^aD. UHRÍKOVÁ

^aDepartment of physical chemistry of drugs, Faculty of Pharmacy, Comenius University Bratislava, Bratislava, Slovakia

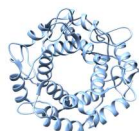
^bAlba synchrotron, 08290 Cerdanyola del Vallès, Barcelona, Spain

The severe acute respiratory syndrome coronavirus-2 (SARS-CoV-2), identified as the causal agent of Corona virus disease 2019 (COVID-19), exerted massive pressure on the healthcare system. To prevent development of respiratory failure, which is the leading cause of mortality in COVID-19, different strategies were employed to fight back COVID-19 such as: direct targeting SARS-CoV-2 infection, symptomatic treatment and supportive care.

SARS-CoV-2 infects different cells in the human body, including type II pneumocytes, cells responsible for the production of pulmonary surfactant (PS). PS is a complex of lipids (~90%) and proteins, covering the alveoli of the lungs, which reduces surface tension at the air-liquid interface and facilitates breathing. Severe case of SARS-CoV-2 infections causes a fatal condition called COVID-19-related acute respiratory distress syndrome (CARDS) due to decrease PS level and its altered composition [1]. PS could be highly beneficial for the treatment of COVID-19 for different reasons. The first reason is that CARDS pathophysiologically resembles neonatal respiratory distress syndrome [2] (the only case for which exogenous PS is currently indicated for), therefore, exogenous PS itself can be used as treatment. Another reason is that due to its nature and composition, it could carry membrane-impermeable drug molecules to the distal region of the breathing surface, which are alveoli.

Remdesivir (Rem), the first approved treatment for severe COVID-19, is a nucleoside analogue with broad-spectrum activity against RNA viruses. In SARS-CoV-2, Rem causes delayed chain termination after incorporation into the replicating RNA and, therefore, prevents transcriptional and translational processes in viral replication. Pulmonary delivery of Rem in addition to intravenous infusion increases clinical efficacy; however, it is crucial to analyse how the incorporation of Rem can affect PS properties.

We focused on the changes in the biophysical properties of the lipid bilayer of exogenous PS, Curosurf (porcine-derived, the only registered exogenous PS preparation in Slovakia) as a result of incorporation of Rem. Fig. 1 panel A indicates the DSC thermograms of Curosurf – Rem mixture. The temperature of the main phase transition (T_m) of Curosurf was found at 27.3 ± 0.1 °C. Increasing the content of Rem the mixture reduces the temperature of the main phase transition to $T_m = 24.2 \pm 0.1$ at molar ratio $n_{\text{Rem}}/n_{\text{Curosurf}} = 0.5$. The reported value for the partition coefficient K_p for Rem, $K_p \sim 100$ [3], indicates that the molecule affects the hydrophobic region of the lipid bilayer.



The structural changes of the Curosurf – Rem mixtures were studied in the presence of $2 \text{ mmol.l}^{-1} \text{ CaCl}_2$ in hydration medium ($\text{NaCl } 150 \text{ mmol.l}^{-1}$) to shield the negative surface charge of Curosurf. SAXS patterns indicate a lamellar phase at 20 and 50 °C. At 20 °C, the repeat distance of Curosurf $d = 8.10 \pm 0.01 \text{ nm}$ decreases by adding Rem up to $n_{\text{Rem}}/n_{\text{Curosurf}} = 0.3$ with $d = 7.48 \pm 0.01 \text{ nm}$ (Fig1. Panel B).

In conclusion, our study of the biophysical characteristic of Curosurf – Rem mixtures indicates that remdesivir does not destabilise the lamellar structure of PS; however, its high content affects the temperature of gel-to-liquid-crystalline phase transition.

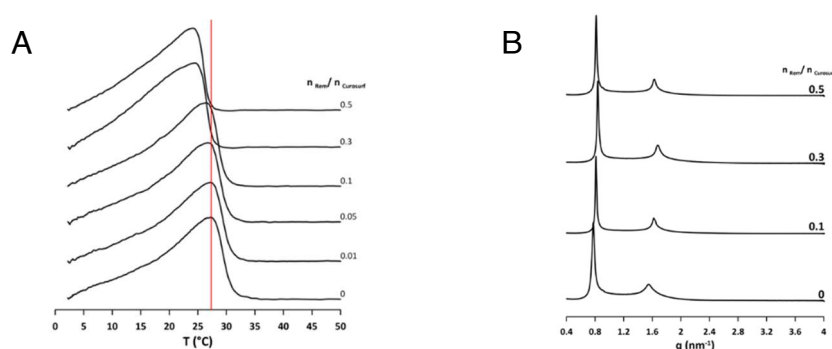
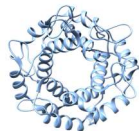


Fig1. Panel A: DSC profiles of Curosurf in presence of Rem as a function of Rem/Curosurf mole ratios. Panel B: SAXS patterns of Curosurf–Rem mixtures at 20 °C.

Acknowledgment. SAXD experiments were performed at BL11-NCD beamline (proposal 2021025016) at Alba Synchrotron with the collaboration of Alba staff. This work was supported by grants VEGA 1/0223/20; APVV 17-0250; APVV 21-0108 and FaF/27/2023

References

1. Wang, S., Li, Z., Wang, X., Zhang, S., Gao, P., & Shi, Z. (2021). The Role of Pulmonary Surfactants in the Treatment of Acute Respiratory Distress Syndrome in COVID-19. *Front Pharmacol*, 12.
2. Herman, L., De Smedt, S. C., & Raemdonck, K. (2022). Pulmonary surfactant as a versatile biomaterial to fight COVID-19. *J Control Release*, 342, 170–188.
3. Pashaei, Y. (2020). Analytical methods for the determination of remdesivir as a promising antiviral candidate drug for the COVID-19 pandemic. *Drug Discov Ther.*, 14(6), 273–281.



A fluorescence study of algal-based ghost vesicles as potential gene delivery systems

^aM. KLACSOVÁ, ^aD. UHRÍKOVÁ, ^bL. HORVAT, ^bT. MIŠIĆ RADIĆ, ^bN. IVOŠEVIĆ
DENARDIS

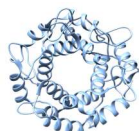
^aDepartment of Physical Chemistry of Drugs, Faculty of Pharmacy, Comenius University Bratislava, Bratislava, Slovakia

^bDivision for Marine and Environmental Research, Ruđer Bošković Institute, Zagreb, Croatia

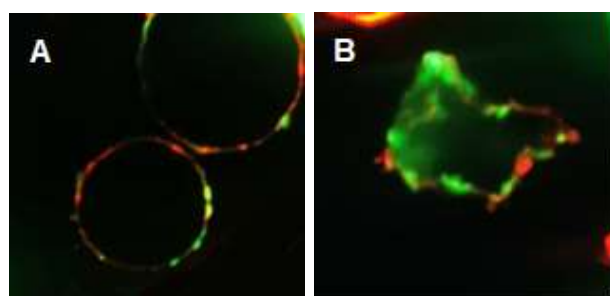
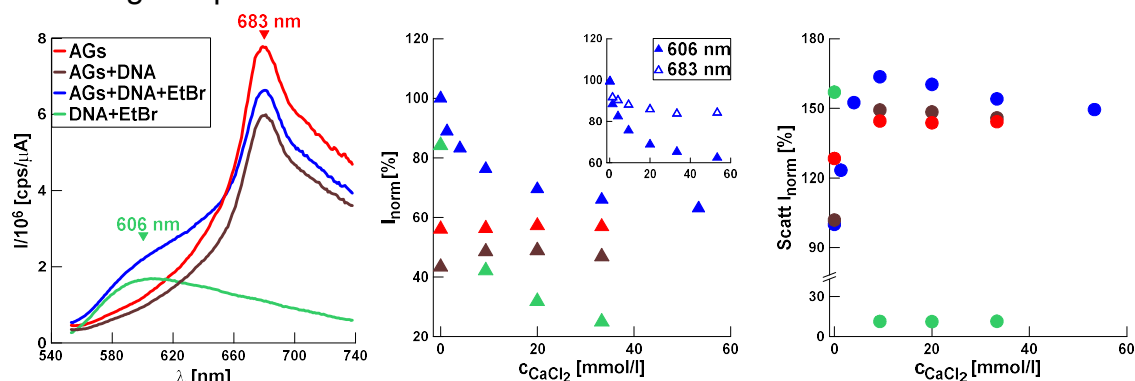
It is of biotechnological interest to develop delivery systems for the transport of a variety of bioactive molecules. Lipid-based synthetic vesicles (liposomes) have been extensively studied as gene delivery systems. The advantages of such delivery systems arise from their basic physicochemical properties - they consist of a lipid bilayer surrounding the aqueous core. This allows encapsulation and protection of active hydrophilic molecules such as nucleic acids. Their rapid excretion, toxicity, and immunogenicity limit clinical applications. Therefore, the search for alternative bioinspired materials that are freely available and fulfill environmental friendliness and sustainability is becoming increasingly important. The unicellular marine microalga *Dunaliella tertiolecta* with a thin elastic plasma membrane and a glycocalyx surface layer has been shown to be a suitable cell model for vesicle preparation [1]. The hypoosmotic shock of soft cells causes the cells to burst, the intracellular contents are released, and the membrane fragments are spontaneously reconstructed into vesicles that better mimic the complexity of natural biomembranes [1,2].

Our present fluorescence study aimed to (i) follow the condensation of DNA (calf thymus) by algal-based ghost vesicles (AGs), and (ii) visualize the interaction of AGs with DNA (pEGFP-N1 plasmid) using calcium ions as mediators of this interaction. For fluorescence spectroscopy, lyophilized AGs rehydrated with 5 mmol/l NaCl solution were used. Samples were prepared at a ratio of AGs/DNA = 5 wt/wt. After incubation with CaCl₂, ethidium bromide (EtBr, $\lambda_{\text{ex}} = 260$ nm), a DNA fluorescent probe, was added at DNA/EtBr = 6 mol/mol. Fluorescence intensity was measured at $\lambda_{\text{em}} = 606$ and 683 nm. To monitor the size of aggregates, side scatter was measured at $\lambda_{\text{ex}} = \lambda_{\text{em}} = 600$ nm. Data were corrected for the intensity of the blank sample (EtBr in solvent) and then normalized to the intensity of the reference sample without CaCl₂. All measurements were performed at 25 °C. For confocal imaging, AGs were stabilized with Tris-HCl buffer and MgCl₂ (both at a final concentration of 10 mM, pH 8.0). Plasmid was added at a ratio of AGs/plasmid = 800 wt/wt. After incubation with CaCl₂, fluorescent dye Dil was added at a final concentration of 2 $\mu\text{mol/l}$.

The fluorescence spectra of the samples show two maxima: at $\lambda_{\text{max}} = 606$ and 683 nm, corresponding to the emission of DNA+EtBr and residual chlorophyll in AGs [1], respectively (Fig. 1. left). When AGs interact with DNA, they create a steric barrier against intercalation of EtBr into DNA. This is manifested as a decrease of fluorescence intensity with increasing CaCl₂ concentration at both λ_{max} , but more pronounced at 606 nm (Fig. 1. middle). The reference samples, pure AGs and



AGs+DNA, show no pronounced dependence on CaCl_2 concentration. However, CaCl_2 itself condenses DNA significantly, with a decrease of I_{norm} almost threefold of the total decrease observed in samples with AGs. In the presence of AGs, $\sim 60\%$ of the DNA is still accessible to EtBr. The size of the aggregates formed increases up to $c_{\text{CaCl}_2} = 10 \text{ mmol/l}$ for all sets of samples examined, except for pure DNA, where the size decreases dramatically even at the lowest c_{CaCl_2} examined (Fig. 1, right). The highest values of scattered intensity were obtained for AGs+DNA+EtBr samples, indicating complexation of AGs with DNA.



↑ Fig. 1. Emission fluorescence spectra of selected samples (left). Normalized fluorescence emission intensity at 606 nm (middle) and normalized scattered light intensity (right) as a function of CaCl_2 concentration.

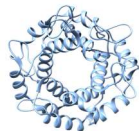
← Fig. 2. Overlapping confocal images of the Dil-stained AGs (red) + pEGFP-N1 plasmid (green) system at $c_{\text{CaCl}_2} = 30 \text{ mmol/l}$.

Fig. 2A shows confocal images of AGs (diameter: $4\text{--}5 \mu\text{m}$) complexed with plasmid DNA fluorescing green on the membrane, indicating that the concentration of 30 mmol/l CaCl_2 was sufficient to shade the electrostatic repulsion between two negatively charged moieties. In some cases, the spherical structure of the AGs was disrupted (Fig. 2B), which might indicate the initial formation of structures with long-range order, as previously described for various synthetic lipid+DNA systems [3].

Acknowledgment. This work was supported by International Visegrad Fund, grant No. 2222011.

References

1. Ivošević DeNardis, N., Pletikapić, G., Frkanec, R., Horvat, L., Vernier, P.T. (2020) From algal cells to autofluorescent ghost plasma membrane vesicles. *Bioelectrochemistry*, 134, 107524.
2. Levak Zorinc, M., Demir-Yilmaz, I., Formosa-Dague, C., Vrana, I., Gašparović, B, Horvat, L., Butorac, A., Frkanec, R., Ivošević DeNardis, N. (2023) Reconstructed membrane vesicles from the microalga *Dunaliella* as a potential drug delivery system. *Bioelectrochemistry*, 150, 108360.
3. Uhríková, D., Lengyel, A., Hanulová, M., Funari, S.S., Balgavý, P. (2007) The structural diversity of DNA–neutral phospholipids–divalent metal cations aggregates: a small-angle synchrotron X-ray diffraction study. *European Biophysical Journal*, 36(4-5), 363-375.



PO 16

POSTERS

Thinking outside the binding-pocket: *in silico* design of novel allosteric regulators of 14-3-3

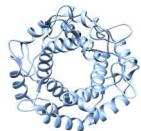
^aS. MULLER, ^aL. RIVERA, ^aM. UHART, ^aE. BARRERA, ^{a,b}D.M. BUSTOS

^aLaboratorio de Integración de Señales Celulares, IHEM (CONICET-UNCuyo), Mendoza, Argentina

^bFCEN, UNCuyo, Mendoza, Argentina.

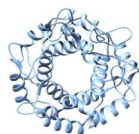
The 14-3-3 protein family, consisting of seven distinct mammalian paralogs, has emerged as a pivotal mediator in numerous cellular processes. Despite exhibiting some functional redundancy, recent evidence underscores their evolutionary and biochemical diversity. These proteins function by binding, either as a monomer or dimer, to phosphorylated Ser and Thr residues within disordered domains of partner proteins through a conserved amphipathic groove on their surface [1, 2, 3, 4, 5]. Consequently, 14-3-3 proteins have garnered significant attention as attractive targets for drug discovery. Various reports have explored the utilization of small molecules to achieve competitive inhibition or partner stabilization, focusing on the well-defined ligand binding groove [6]. In order to detect distinct druggable hot-spots, we decided to make a virtual screening of 2×10^6 compounds using ZINC database over a monomer of 14-3-3. For this, we used Autodock 4.0 for molecular docking and excluded the region that belongs to the canonical binding pocket. After manual selection of top docking poses, we detected a list of 50 compounds that belong to a family of β -carbolines with high affinity binding to a specific region located on the opposite face of the main binding groove of 14-3-3. We decided to use Norharmane (9H-Pyrido[3,4-B]indole) as a first approach for further *in silico* assays. Molecular dynamic simulations demonstrated that the amino acids that conform such cavity drive the dynamics of the whole protein. The presence of Norharmane induced a conformational shift, causing the protein to transition into a closed state. This conformational change obstructs partner accessibility to the primary groove. Further on, to obtain paralog specific compounds, a set of endogenous beta-carbolines were studied with a combination of pharmacophore based docking and enhanced molecular dynamics simulations, selecting candidates by binding affinities and residence times. Collectively, our findings underscore the existence of small molecules like members of the beta-carboline family with the potential to modulate 14-3-3 proteins through a novel allosteric site. The convergence of *in silico*, *in vitro*, and *in vivo* methodologies holds promise for the discovery and optimization of active agents that selectively target this site across distinct 14-3-3 paralogs. This novel regulatory mechanism adds a layer of complexity to the intricate network of 14-3-3 protein interactions, fueling the quest for innovative therapeutic interventions.

Acknowledgment. This work is being supported by research grant CONICET (National Scientific and Technical Research Council - Argentina) and Marie Skłodowska Curie Action RISE (Research and Innovation Staff Exchange) grant.



References

1. Sluchanko, N. N., & Bustos, D. M. (2019). Intrinsic disorder associated with 14-3-3 proteins and their partners. *Progress in Molecular Biology and Translational Science*, 166, 19–61.
2. Masone, D., Uhart, M., & Bustos, D. M. (2017). On the role of residue phosphorylation in 14-3-3 partners: AANAT as a case study. *Scientific Reports*, 7(1), 1–9.
3. Uhart, M., & Bustos, D. M. (2014). Protein intrinsic disorder and network connectivity. The case of 14-3-3 proteins. *Frontiers in Genetics*, 5, 10.
4. Uhart, M., Iglesias, A. A., & Bustos, D. M. (2011). Structurally constrained residues outside the binding motif are essential in the interaction of 14-3-3 and phosphorylated partner. *Journal of Molecular Biology*, 406(4), 552–557.
5. Bustos, D. M., & Iglesias, A. A. (2006). Intrinsic disorder is a key characteristic in partners that bind 14-3-3 proteins. *PROTEINS: Structure, Function, and Bioinformatics*, 63(1), 35–42.
6. Stevers, L. M., Sijbesma, E., Botta, M., MacKintosh, C., Obsil, T., Landrieu, I., ... & Ottmann, C. (2017). Modulators of 14-3-3 protein–protein interactions. *Journal of Medicinal Chemistry*, 61(9), 3755-3778.



PO 17

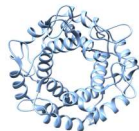
POSTERS

Detection of cytochrome c aggregates with polyanions using thioflavin T

J. OLAJOS̃, R. VARHAČ, M. ANTALÍK

*Department of Biochemistry, Institute of Chemistry, Pavol Jozef Šafárik University in Kosice,
Moyzesova 11, 040 01 Kosice, Slovakia*

Thioflavin T (ThT) is a fluorescence dye, generally used for staining amyloid tissues or detection of amyloid fibrils in solutions. The binding of ThT to amyloid aggregates causes the occurrence of fluorescence emission in the 475–600 nm region after excitation in the 440–450 nm region. In contrast, very low emission quantum yields of ThT are observed in the presence of native proteins as well as unfolded or partially folded monomeric protein conformations. Since ThT binding only slightly affects the early stages of fibrillization, this method is also suitable for in situ fibril detection and monitoring of kinetics of fibril formation. In spite of extensive study the precise mechanism of ThT interactions with biosystems is not understood in detail yet. Several studies on the mechanism of ThT-fibril interactions have been reported (1). β -sheets, as major components of amyloid fibrils, contain cavities and channels, which can serve as possible ThT binding sites. ThT emission changes after binding to amyloids were attributed to formation of highly fluorescent dimers, excimers, or micelles. Recent findings suggest another mechanism based on ThT behavior as molecular rotor. For the molecular rotors, fluorescence quantum yield significantly increases with increasing viscosity or rigidity of microenvironment due to the decreased torsional relaxation in the molecule. Thus, free rotation of benzothiazole and benzamidine rings around shared C-C bond is blocked in ThT-amyloid complexes, leading to significant increase of fluorescence yield. The fluorescent conformer was also observed in complex of ThT with an α -helical protein acetylcholinesterase, in which planarised conformation of ThT were formed due to the π - π stacking interactions with protein aromatic residues. The fluorescent conformer with lower quantum yield was also observed after binding to β -sheet structure of monomeric non-amyloid protein β 2-microglobulin (2). The entrapment of ThT molecules in amyloid fibrils leads to formation not only fluorescent conformers, but also to optically active conformers. This induced circular dichroism was for example observed for ThT complex with insulin amyloid fibrils. However, the induced optical activity of ThT was also found after binding to α -helical polyglutamic acid lacking the β -sheet structure or aromatic side-chains. Moreover, the polyglutamic acid binds ThT in conditions even before the polypeptide becomes fully α -helical. The authors suggest that docking interaction of ThT with different protein targets may be more unspecific as previously assumed. In order to test the possible variability of ThT interactions with other than regular secondary structures, we have studied the complexes of ThT with non-peptide chiral polyanions – heparin and nonchiral – polystyrene sulphonate (PSS)(3). These polyanions possess different charged groups, hydrophobicity and charge density. Heparin is glycosaminoglycan, consisting of sulphate and carboxylate groups and it is one of the

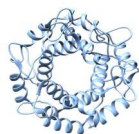


most negatively charged biomacromolecules without regular tertiary structure. The structurally related glycosaminoglycans such as heparan sulphates are part of blood coagulation pathways. They form stable complexes with thrombin and antithrombin protease systems and other proteins (4). True physiological role of heparin in the body remains still unclear. The potential role of heparin in transport of positively charged drugs or other biologically active compounds has been studied. Polystyrene sulphonate possess together with negatively charged sulphonate groups also hydrophobic styrene rings. This macromolecule is used as potassium binder for patients suffering from hyperkalaemia – abnormal high blood serum potassium levels. It has been shown that PSS forms complexes with ThT and enhances the formation of ThT excimer (5). Our aims was to obtain the best possible knowledge about the formation of the aforementioned aggregates and fibrils and their subsequent detection using ThT. We used different techniques such as spectrofluorimeter, zetasizer and electrophoresis.

Acknowledgment. This work was supported by the Grant Agency of Ministry of the Education, Science, Research and Sport of the Slovak Republic VEGA 1/0347/23.

References

1. Khurana R., Coleman C., Ionescu-Zanetti C., Carter S. A., Krishna V., Grover R. K., Roy R., Singh S. (2005): Mechanism of thioflavin T binding to amyloid fibrils. *J. Struct. Biol.* 151, 229–238.
2. Stsiapura V. I., Maskevich A. A., Kuzmitsky V. A., Uversky V. N., Kuznetsova I. M., Turoverov K. K. (2008): Thioflavin T as a molecular rotor: fluorescent properties of thioflavin T in solvents with different viscosity. *J. Phys. Chem. B* 112, 15893–15902.
3. Babenko V., Dzwolak W. (2011): Thioflavin T forms a non-fluorescent complex with α -helical poly-L-glutamic acid. *Chem. Commun.* 47, 10686–10688.
4. Rabenstein D. L. (2002): Heparin and heparin sulfate: structure and function. *Nat. Prod. Rep.* 19, 312–331.
5. Fedunova D., Huba P., Bagelova J., Antalík M. (2013): Polyanion induced circular dichroism of Thioflavin T. *Gen. Physiol. Biophys.* 32, 215–219.



Triterpenoid-based ionic liquids with enhanced antitumor potency

^aP. OSSOWICZ-RUPNIEWSKA, ^aJ. KLEBEKO, ^bI. GEORGIEVA,
^bS. APOSTOLOVA, ^bR. TZONEVA, ^cM. GUNCHEVA

^aDepartment of Chemical Organic Technology and Polymeric Materials, Faculty of Chemical Technology and Engineering, West Pomeranian University of Technology, Szczecin 71-065, Poland

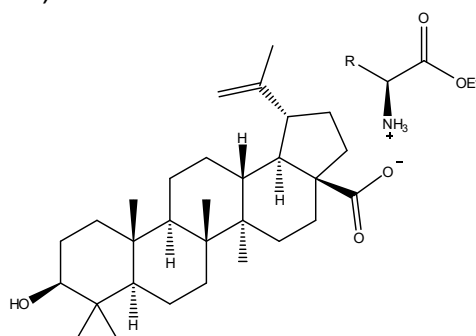
^bInstitute of Biophysics and Biomedical Engineering Bulgarian Academy of Sciences, Sofia 1113, Bulgaria

^cInstitute of Organic Chemistry with Centre of Phytochemistry, Bulgarian Academy of Sciences, Sofia 113, Bulgaria

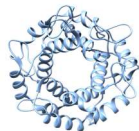
Betulinic acid (BA) is a naturally occurring pentacyclic terpene known for its inhibitory effects on various malignancies, including colon, lung, hepatic, liver, cervical, head-neck, breast, thyroid cancer leukemia, melanoma, and various blastoma [1]. The reported half-maximum inhibition constants (IC_{50}) for BA are in the micromolar range [2]. Notably, BA has been found to suppress glucose uptake and lactate production in breast cancer cells, and it exhibits anti-diabetic, anti-lipidemic, anxiolytic, anti-depressant, anti-viral, anti-bacterial, neuroprotective, and protective effects on the cardiovascular system [1].

To enhance the water solubility and potentially improve the biological activity and selectivity of BA, tailored conversion of BA into ionic derivatives has been explored. For instance, Zhao et al. reported that cholinium betulinate showed three times higher anti-HIV viral activity and 100 times higher solubility than BA [3]. Ionic liquids containing cholinium and benzalkonium cations and betulinate anion demonstrated enhanced activity against melanoma, neuroblastoma, breast adenocarcinoma, and epidermoid carcinoma, with up to 5 times lower IC_{50} compared to control experiments with BA [4]. Furthermore, trihexyltetradecylphosphonium betulinate exhibited higher selectivity against five cancer cell lines compared to other betulinic acid organic salts and BA [5].

In this study, our focus lies on the synthesis and characterization of novel betulinate amino acid ethyl esters, denoted as [BA][AAE] (1), and the evaluation of their cytotoxic effect on neoplastic (MCF-7; MDA-MB-231; HT-29 cells) and non-transformed cell lines (3T3 cells).



General structure of the target compounds



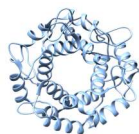
For the three cell lines, the estimated IC_{50} values vary within the range between 2.5 and 50 $\mu\text{mol/L}$. While the native BA and its AAE salts generally exhibit similar cytotoxic effects toward MDA-MB-231 and HT-29 cells, most of [BA][AAE] derivatives have shown an enhanced cytotoxic effect on MCF-7 cells compared to BA. It is noteworthy that, with the exception of the threonine-based derivative, all other novel BA salts showed lower or no toxic effect on 3T3 cells.

In summary, these findings suggest the potential utility of [BA][AAE] derivatives in the development of targeted therapies for specific cancer types with reduced toxicity to non-transformed cells.

Acknowledgment. This study has been supported by the Bulgarian National Science Fund, research grant KP-06-H69/2.

References

1. Amiri, S., Dastghai, S., Ahmadi, M., Mehrbo, P., Khadem, F. et al. (2020) Betulin and its derivatives as novel compounds with different pharmacological effects. *Biotechnol. Adv.* 38, 107409.
2. Hordyjewska, A., Ostapiuk, A., Horecka, A., Kurzepa, J. (2019) Betulin and betulinic acid: triterpenoids derivatives with a powerful biological potential. *Phytochem. Rev* 18, 929–951.
3. Zhao, H., Holmes, S., Baker, G., Challa, S., Bose, H., Song, Z. (2012) Ionic derivatives of betulinic acid as novel HIV-1 protease inhibitors. *J. Enzyme Inhib. Med. Chem.* 27(5), 715–721.
4. Challa, S., Zhao, H., Gumbs, A., Chetty, C., H. Bose, S. (2012) New ionic derivatives of betulinic acid as highly potent anticancer agents. *Bioorg. Med. Chem. Lett.* 22(4), 1734–1738.
5. Silva, A., Cerqueira, M., Prudencio, C., Fernandes, M.H., Costa-Rodrigues, J., Teixeira, C., Gomes, P., Ferraz, R. (2019) Antiproliferative organic salts derived from betulinic acid: disclosure of an ionic liquid selective against lung and liver cancer cells. *ACS Omega* 4, 5682–5689.



Adenine nanolayers on model metal oxide surfaces: XPS and NEXAFS study

^aN. POPOVYCH, ^bN. TSUD, ^bK. VELTRUSKA, ^bV. MATOLIN, ^aV. RIZAK

^a*Uzhhorod National University, Pidhirna st., 46, 88000 Uzhhorod, Ukraine*

^b*Charles University in Prague, V Holešovickách 2, 18000 Prague 8, Czech Republic*

Adenine is part of many natural bioactive compounds, important intracellular intermediates and pharmaceuticals. Elementary biomolecules (including adenine), a constituent blocks of nucleic acids, are also the building blocks of the genetic code. At the same time, TiO₂ is a biocompatible material widely used in orthopedic/dental medicine and has received extensive attention in the surface science community. By combining biotechnology and materials science, we are given tremendous opportunities to create new materials and integrated components.

To our knowledge, no detailed spectroscopic investigation is reported on adenine/TiO_x and adenine/TiO₂ (110) systems. Therefore, the aim of this work is to study the adenine interaction with the polycrystalline TiO_x and TiO₂ (110) surfaces by XPS and NEXAFS methods.

The TiO_x polycrystalline film (d=30 Å) on the titanium foil surface was obtained by thermal oxidation of the cleaned Ti foil at the T=650 K and oxygen pressure 1×10⁻⁷ torr.

The TiO₂ (110) surfaces was cleaned in UHV by using cycles of Ar⁺ sputtering and annealing at 650-700 °C. The adenine nanolayers on the titanium oxide surfaces were obtained by thermal deposition in vacuum.

Al Kα X-Ray source (1486.6 eV) was used to measure of the O 1s, C 1s, N 1s and Ti 2p_{3/2} core level spectra. NEXAFS measured with synchrotron radiation was normalized to the incident photon flux.

For study the stability of obtained structures after heating in vacuum at T=50, 75, 100, 125, 150, 200 and 250 °C the thickness of the adenine film decreases.

NEXAFS spectra (Fig. 2) were taken at the C and N K-edges using the carbon and nitrogen KVV Auger yields, at normal (NI, 90°), magic (MA, 55°) and grazing (GI, 10°) incidence of the photon beam with respect to the surface.

Accordingly, the method of obtaining titanium oxide on the polycrystalline Ti foil has been developed. Adenine thin adlayers on titanium oxide surfaces were obtained by thermal evaporation in vacuum. The mechanism of interaction of adenine molecules with the titanium oxide surfaces was established by analysis of XPS, SRPES and NEXAFS spectra.

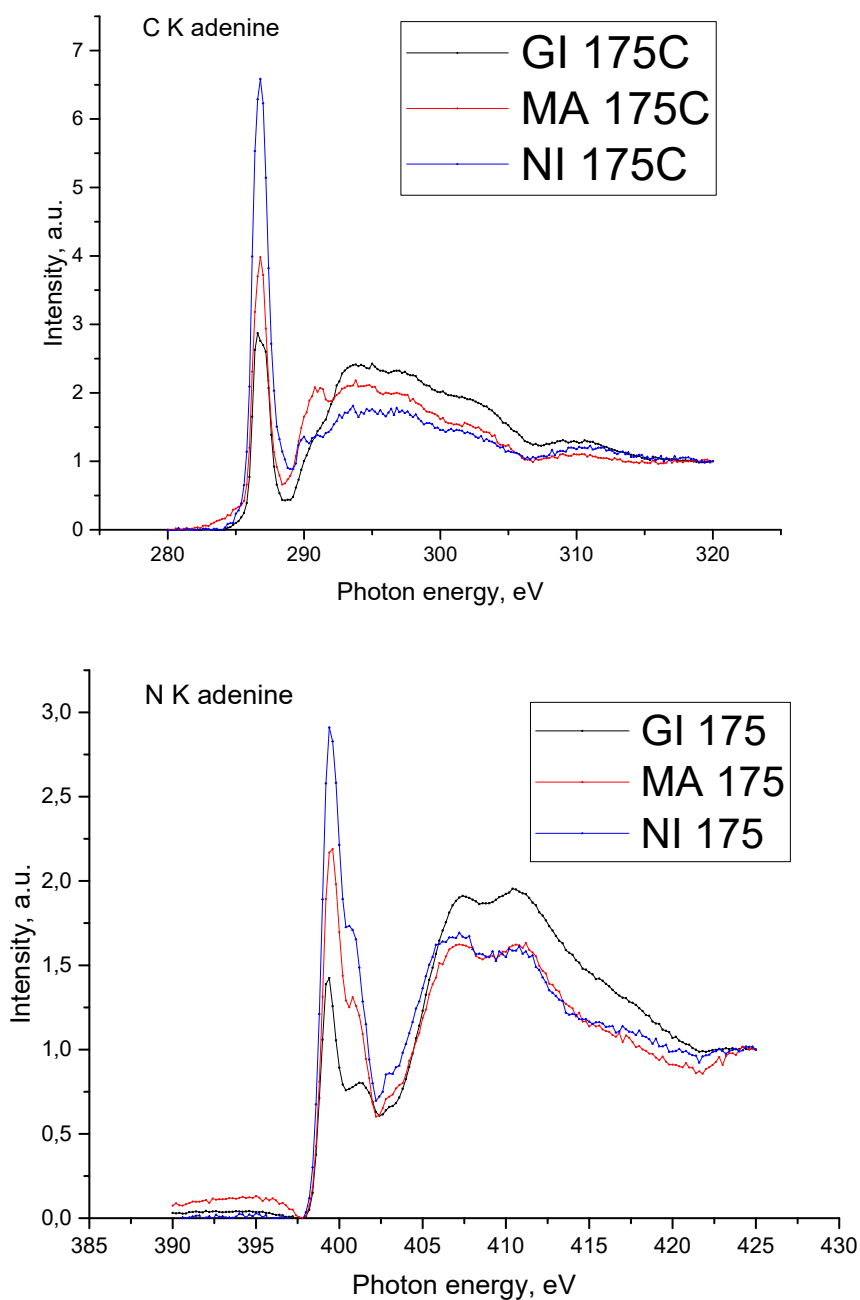
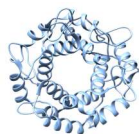
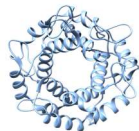


Fig.1. C K; N K-edge NEXAFS spectra (at 175C) of adenine adlayers on TiO_2 (110) surface measured in GI (black), MA (red) and NI (blue) geometry.

Acknowledgment. This work was supported by research grants from CERIC (Proposal Numbers 20157037 and 20168062). The authors gratefully acknowledge the assistance of the staff at the Nanomaterials Group (Charles University in Prague, Czech Republic) and Material Science Beamline (Elettra Sincrotrone, Trieste, Italy).



PO 20

POSTERS

Exciton transfer between LH1 antenna complex and photosynthetic reaction center dimer

^aM. PUDLÁK, ^bR. PINČÁK

^a*Department of Biophysics, Institute of Experimental Physics, SAS, Košice, Slovakia*

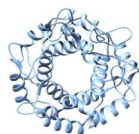
^b*Department of Theoretical Physics, Institute of Experimental Physics, SAS, Košice, Slovakia*

Purple phototropic bacteria have importance in biophysical treatment due to their ability to transform light into chemical energy in reaction centers. We deal with the exciton transfer in the antenna complex and electron transfer in the reaction center. We show that electrons are directed by the vibration modes into the needed site where they are localized [1]. We describe the exciton transport between the light-harvesting complex LH1 and the reaction center dimer. It was shown that the dimer does not act as a trap for exciton. The rate of backward exciton transfer depends on the number of chlorophyll molecules which create the LH1 antenna ring complex [2].

Acknowledgment. This work was supported by research grant VEGA 2/0076/23

References

1. Pudlák, M., Pinčák, R., & Bartoš, E. (2022). Effect of vibrational modes on electron transfer directionality: photosynthetic reaction centers. *Phys.Rev. E*, 105, 064408.
2. Pudlák, M., & Pinčák, R. (2023). Photosynthetic Complex: Exciton transfer and Electron-Hole Separation Quantum Yields. *J. Phys. Chem.A*, 127, 5795-5804.



PO 21

POSTERS

Strategies for SERS detection of selected (biomacro)molecules with key importance for human health and environmental protection: nucleic acids and glyphosate

^aF. FUENZALIDA SANDOVAL, ^aB. VARCHOLOVÁ, ^{b, c}P. MIŠKOVSKÝ,
^dS. SÁNCHEZ-CORTÉS, ^aZ. JURAŠEKOVÁ

^aDepartment of Biophysics, Faculty of Science, P. J. Šafárik University (UPJŠ), Košice, Slovakia

^bTechnology and Innovation Park, P. J. Šafárik University (TIP-UPJŠ), Košice, Slovakia

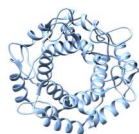
^cSAFTRA photonics, s.r.o., Košice, Slovakia

^dInstitute of the Structure of Matter, IEM-CSIC, Madrid, Spain

Long-term use of different molecules, such as pesticides, together with their subsequent accumulation in the environment as well as increasingly frequent and significant impact on humans and living organisms, has become an important issue. Therefore, it is crucial to perform both 'on-site' quick screening of these molecules and monitor them in water, soil, and in food, as well as to investigate their impact on living beings by studying, in the first plan, their interaction with biomacromolecules. Raman spectroscopy (RS), and especially surface-enhanced Raman spectroscopy (SERS), seems to be a very suitable - highly sensitive and selective - analytical technique providing 'on-site' quick and cost-effective sample screening without the need for the sample pre-treatment [1]. Besides, it can be also used to study important (biomacro)molecules and their interactions. RS as a technique of the "fingerprint" provides specific structural information at the level of molecules (i.e., information about intra- and inter-molecular vibrations) what allows us to use it to study chemical changes caused during various processes, interactions or environmental change. Due to the well-defined and low-intensity spectrum of water, RS is also a suitable technique for the study of biological samples.

The present work is devoted to SERS detection of selected (biomacro)molecules important for human health and related to environmental protection. The foremost - analytical - research line is based on the detection and analysis of very low concentration levels of a widely used, broad-spectrum herbicide glyphosate. The biophysical research line is aimed to develop an efficient methodology to study interaction profiles of the selected molecules with biomacromolecules (nucleic acids) using appropriate SERS substrates.

Glyphosate, widely known under its trade names Roundup®, is used for weed control in agricultural production fields. In the 20th century, its use increased dramatically due to the introduction of pesticide-resistant crops [2]. Toxicological studies indicate that chronic exposure to this herbicide is potentially carcinogenic and can induce different diseases [3, 4]. Glyphosate is currently approved in the EU until 15 December 2023 [5]. In this context, 'on-site' identification and quantification of chemicals such as glyphosate are essential to promote food safety, human health, national security risk assessment and disease diagnosis. Though, glyphosate SERS spectra show rather weak signals leading to not so low limit of detections by a direct



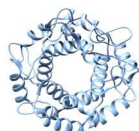
method [1, 6]. The reason is its high polarity, which seriously hinders the approach of the molecule to the surface of metallic nanostructures. Jan et al. proposed an indirect method for colorimetric determination of glyphosate [7] which inspired us to develop an innovative approach based on the SERS technique for selective and sensitive glyphosate detection.

SERS study of such immense and negatively charged molecules as nucleic acids is not a trivial task. Moreover, the use of visible and near-infrared excitations (present in the Laboratory of Raman spectroscopy at the Department of Biophysics, UPJŠ in Košice) is neither the most appropriate. However, research works can be found dealing with the possible solutions to these issues [8, 9]. Based on these works, we have prepared and tested a new class of positively-charged colloids [10] in place of the traditional negatively-charged ones in order to implement them into the SERS study of nucleic acids and their interaction with selected (pesticide) molecules.

Acknowledgment. This work was supported by research grant provided by the Slovak Research and Development Agency (APVV-19-0580). This work was also financially supported by the AEI Project number PID2020-113900RB-I00.

References

1. Duke, S.O.; Powles, S.B. (2018) Glyphosate: a once-in-a-century herbicide. *Pest Management Science* 74(5) (2018) 1027-1034.
2. Feis, A.; Gellini, C.; Ricci, M.; Tognaccini, L.; Becucci, M.; Smulevich, G. (2020) Surface-enhanced Raman scattering of glyphosate on dispersed silver nanoparticles: A reinterpretation based on model molecules. *Vibrational Spectroscopy*, 108, 103061.
3. Holanda, R.O.; da Silva, C.B.; Vasconcelos, D.L.M.; Freire, P.T.C. (2020) High pressure Raman spectra and DFT calculation of glyphosate. *Spectrochimica Acta, Part A: Molecular and Biomolecular Spectroscopy* 242, 118745.
4. Mertens, M.; Höss, S.; Neumann, G.; Afzal, J.; Reichenbecher, W. (2018) Glyphosate, a chelating agent-relevant for ecological risk assessment? *Environmental Science and Pollution Research* 25(6), 5298-5317.
5. https://food.ec.europa.eu/plants/pesticides/approval-active-substances/renewal-approval/glyphosate_en#status-of-glyphosate-in-the-eu
6. Mikac, L.; Rigó, I.; Škrabić, M.; Ivanda, M.; Veres, M. (2022) Comparison of Glyphosate Detection by Surface-Enhanced Raman Spectroscopy Using Gold and Silver Nanoparticles at Different Laser Excitations. *Molecules* 27, 5767
7. Jan, M.R.; Shah, J.; Muhammad, M.; Ara, B. (2009) Glyphosate herbicide residue determination in samples of environmental importance using spectrophotometric method. *Journal of Hazardous Materials* 169, 742–745.
8. Calderon, I.; Guerrini, L.; Alvarez-Puebla, R.A. (2021) Targets and Tools: Nucleic Acids for Surface-Enhanced Raman Spectroscopy. *Biosensors* 11, 230.
9. García-Rico, E.; Alvarez-Puebla, R.A.; Guerrini, L. (2018) Direct surface-enhanced Raman scattering (SERS) spectroscopy of nucleic acids: from fundamental studies to real-life applications. *Chemical Society Reviews* 47(13), 4909-4923.
10. van Lierop, D.; Krpetic, Z.; Guerrini, L.; Larmour, I.A.; Dougan, J.A.; Faulds, K.; Graham, D. (2012) Positively charged silver nanoparticles and their effect on surface-enhanced Raman scattering of dye-labelled oligonucleotides. *Chemical Communications*, 48, 8192–8194.



Effect of Polymyxin B on the Pulmonary Surfactant Bilayer

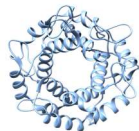
^aA. Asi SHIRAZI, ^aN. KRÁLOVIČ, ^aA. KESHAVARZI, ^aM. KLACSOVÁ, ^bJ.C. MARTÍNEZ, ^aD. UHRÍKOVÁ

^aDepartment of Physical Chemistry of Drugs, Faculty of Pharmacy, Comenius University Bratislava, Bratislava, Slovakia

^bAlba synchrotron, 08290 Cerdanyola del Vallès, Barcelona, Spain

Pulmonary surfactant (PS) is a vital lipoprotein complex that reduces the surface tension at the air-liquid interface of the alveoli, preventing them from collapsing during expiration. PS deficiency is life-threatening and is treated by administering exogenous PS preparations. Curosurf (porcine-derived exogenous PS) is the sole registered and clinically used preparation in Slovakia. To address economic and ecological concerns, synthetic PS preparations have gained interest. A previous study examined a model system (DPPC/POPC/PLPC/POPG = 50:24:16:10 wt%) that closely mimics native PS [1]. However, the SP-B protein is challenging to synthesize due to its unique 3D structure. Recent findings indicate that polymyxin B (PxB) exhibits *in vitro* surface activity indistinguishable from analogous mixtures containing the native protein SP-B of PS [2]. Polymyxin B, indicated against gram-negative bacteria, is a cyclic amphipathic decapeptide antibiotic carrying +5 charges and an acyl chain at the N-terminus.

In this study, we compared the effect of PxB on a model system of PS and Curosurf. The thermotropic phase transition was assessed using differential scanning calorimetry (DSC). We figure out that the PS model system and Curosurf undergo a gel to liquid-crystalline phase transition at a temperature of $T_m \sim 28.1$ and $T_m \sim 26.8$ °C, respectively. DSC thermograms of the PS model system in the presence of PxB indicate an increase in the main phase transition temperature (T_m) with the addition of PxB reaching its maximum at 7 wt% of PxB where $T_m \sim 32$ °C. At the higher content of PxB (up to 20 wt%), the T_m values show minimal variation, indicating that further additions of PxB have a limited impact on the thermal behavior of the complex. In contrast, PxB has no substantial effect on the T_m of Curosurf. The impact of PxB on the vesicles' surface charge was examined using electrophoretic light scattering (ELS) technique. Zeta potential measurements were conducted to assess the surface charge of the vesicles of the PS model system and Curosurf at 20 and 50 °C. The PS model system had zeta potential values of -16.8 ± 0.8 mV and -11.4 ± 3.6 mV at 20 and 50 °C, respectively. On the other hand, Curosurf had a zeta potential of -10.5 ± 1 mV at 20 and 50 °C. We observed an increase in the surface charge of the vesicles of both systems across the entire range of PxB content studied (up to 20 wt%) at both studied temperatures. The structural changes were characterized using small-angle X-ray scattering (SAXS) analysis. The SAXS patterns of the PS model system and Curosurf at 40 °C show peaks typical for a lamellar phase. Repeat distances $d = 9.42 \pm 0.19$ and $d = 8.54 \pm 0.25$ nm are distinguished for the pure PS model system and Curosurf, respectively. We observed that with the addition of PxB, the d value of both studied

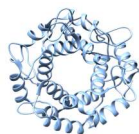


systems decreased. At the highest studied content of PxB (10 wt%), the repeat distance value of the PS model system and Curosurf reaches $d = 6.07 \pm 0.01$ and $d = 6.28 \pm 0.02$ nm, respectively. This behavior indicates that PxB interacts with the outer leaflet of the studied bilayers through electrostatic interactions between three extended positively charged diaminobutyric acid residues of PxB and negatively charged phosphate and carboxyl groups of phospholipids that result in partial incorporation of PxB into the bilayer [3]. In conclusion, the presence of PxB does not hinder the lamellar packings of the PS model system and Curosurf. Obtained results may be insightful for future studies for exogenous PS-drug combined therapy.

Acknowledgment: SAXS experiments were performed at the BL11-NCD beamline at the Alba synchrotron with the collaboration of ALBA staff. This work was funded by grants VEGA1/0223/20, APVV17-0250, and FaF/28/2023.

References

1. Calkovska A, Linderholm B, Haegerstrand-Björkman M, Pioselli B, Pelizzi N, Johansson J, Curstedt T. (2016). Phospholipid composition in synthetic surfactants is important for tidal volumes and alveolar stability in surfactant-treated preterm newborn rabbits. *Neonatology*, 109(3), 177–185.
2. Cajal Y, Rogers J, Berg OG, Jain MK. (1996). Intermembrane Molecular Contacts by Polymyxin B Mediate Exchange of Phospholipids. *Biochemistry*, 9;35(1),299–308.
3. Jiang, X., Zhang, S., Azad, M. A. K., Roberts, K. D., Wan, L., Gong, B., Yang, K., Yuan, B., Uddin, H., Li, J., Thompson, P. E., Velkov, T., Fu, J., Wang, L., Li, J. (2020). Structure-Interaction Relationship of Polymyxins with the Membrane of Human Kidney Proximal Tubular Cells. *ACS Infectious Diseases*, 6(10), 2110–2119.



New ferrocene-containing pyrazole/pyrimidine analogues of curcumin as inhibitors of amyloid- β peptide aggregation

^aK. SIPOSOVA, ^bV. KOVAC

^aDepartment of Biophysics, Institute of Experimental Physics SAS, Watsonova 47, Kosice, Slovakia

^bLaboratory of Organic Chemistry, Faculty of Food Technology and Biotechnology, University of Zagreb, Pierotti Str. 6, Zagreb, Croatia

Due to the low bioavailability of curcumin, structural modifications are an important approach to improve stability and pharmacological activity. While the presence of the methylene group and the β -diketone moiety contributes to the rapid degradation of curcumin,¹ various curcumin derivatives without the β -diketone moiety have been synthesized, most of which have maintained or improved their biological activities.² Heterocyclic derivatives and analogues of curcumin, among others, have been the subject of numerous research papers³ and show promising results in the treatment and diagnosis of Alzheimer's disease (AD)⁴. The AD is associated with slow degeneration of neurons due to the accumulation of amyloid β (A β) plaques (which is called A β peptide aggregation) and tau neurofibrillary tangles (NFTs) in the brain. Protein amyloid fibrils have great significance in biology and medicine in relation to their pathological role in numerous neurodegenerative diseases, but they also play a vital role in the function of living organisms. Even though the inhibition of amyloid fibrillation processes is of great interest, and many molecules have been investigated for their ability to interfere with amyloid aggregation of proteins, efficient low-molecular weight inhibitors of amyloid aggregation are thus far not available. Atomic force microscopy and fluorescence analysis have been utilized to investigate the amyloid aggregation of A β peptide in the presence of new pyrazole and pyrimidine analogues of curcumin (Fig.1). The experimental data have shown that they possess ability to affect A β fibrillogenesis in a dose-dependent manner. The formation of A β peptide amyloid fibrils and the disassembly of preformed fibrils is significantly affected by each of the tested compounds, however, the strongest effect is observed for pyrimidine

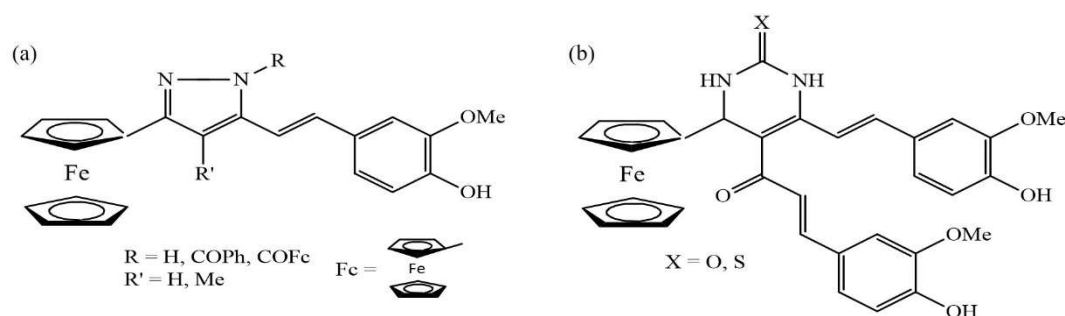
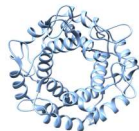


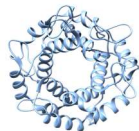
Figure 1: Chemical structures of the ferrocene-containing (a) pyrazole and (b) pyrimidine analogues of curcumin derivatives, indicating their structure-dependent anti-amyloidogenic activity. The apparent half-maximal inhibiting (IC₅₀) and half-maximal disassembly (DC₅₀) values of compounds were found to be in the micromolar concentration range.



Acknowledgment. This work has been fully supported by Croatian Science Foundation under the project IP-2020-02-9162 and by grants from MVTs SAS-MOST JRP 2021/2 (AZCAI) and Slovak Grant Agency VEGA (No. 2/0034/22).

References

1. G.Liang, S.Yang, H. Zhou, L.Shao, K. Huang, J. Xiao, Z. Huang, X. Li, Eur. J. Med. Chem. 44 (2009) 915.-919.
2. M. K. Oglah, Y. F. Mustafa, M. K. Bashir, M. H. Jasim, Sys. Rev. Pharm. 11 (2020) 472 481.
3. (a) R. M. Claramunt, C. I. Nieto, D. Sanz and J. Elguero, Afinidad LXXIV 576 (2016) 259-268.; (b) M. Ahmed, M. A. Qadir, A. Hameed, M. Imran, M. Muddassar, Chem. Biol. Drug Des. 91 (2018) 338-343.
4. (a) E. Chainoglou, D. Hadjipavlou-Litina, Int. J. Mol. Sci. 21 (2020) Article 1975.; (b) S. N. Abbas Bukhari, I. Jantan, Mini Rev. Med. Chem. 15 (2015) 1110-1121.



PO 24

POSTERS

Photopolymer microstructures for intercellular drug transport studies

^aC. SLABÝ, ^bJ. KUBACKOVÁ, ^aV. PEVNÁ, ^cV. HUNTOŠOVÁ, ^dA. STREJČKOVÁ, ^bZ. TOMORI, ^aG. BÁNO

^aDepartment of Biophysics, Faculty of Science, P. J. Šafárik University in Košice, Jesenná 5, 041 54 Košice, Slovakia

^bDepartment of Biophysics, Institute of Experimental Physics, Slovak Academy of Sciences, Watsonova 47, 040 01 Košice, Slovakia

^cCenter for Interdisciplinary Biosciences, P. J. Šafárik University, Jesenná 5, 041 54 Košice, Slovakia

^dDepartment of Chemistry, Biochemistry and Biophysics, University of Veterinary Medicine and Pharmacy in Košice, Komenského 68/73, 041 81 Košice, Slovakia

Our long-term goal is to investigate cell-cell interactions and intercellular signaling in well-defined conditions using low-number cell systems. Photopolymer microstructures prepared by two-photon polymerization direct laser writing (TPP-DLW) are well suited for the construction of small containers confining a few cells. Furthermore, TPP-DLW-prepared optically trappable microstructures can be used in conjunction with optical tweezers to transport cells into containers.

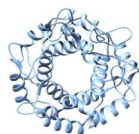
We report on the fabrication of cell micro-containers and optically trappable cell micro-manipulators prepared by TPP-DLW. The structures were made of OrmoComp®, the biocompatible [1] photoresist frequently employed in tissue engineering [2]. The manipulators were used in a bulldozer-like regime to transfer non-adherent leucemic Jurkat cells into small containers.

The new systems were utilized to study the intercellular transport of the photoactive drug Hypericin in well defined geometries. Two types of cells, with and without Hypericin, were combined in a single container at the beginning of the experiment. The evolution of Hypericin localization was followed by confocal microscopy. The results help to distinguish between different drug transport mechanisms.

Acknowledgment. This work was supported by the Slovak Research and Development Agency, grant APVV-21-0333, and by the grant agency of the Ministry of Education, Science, Research and Sports of the Slovak Republic, grant VEGA 2/0101/22. This work is the result of the implementation of the projects OPENMED (Open Scientific Community for Modern Interdisciplinary Research in Medicine) ITMS2014+: 313011V455 and BioPickmol, ITMS2014+: 313011AUW6 from the Operational Program Integrated Infrastructure funded by the ERDF.

References

1. Schizas Ch. & Karalekas D. (2011). Mechanical characteristics of an Ormocomp® biocompatible hybrid photopolymer. *Journal of the mechanical behavior of biomedical materials* 4(2011) 99-106.
2. Schlie, S., Ngezahayo, A., Ovsianikov, A., Fabian, T., Hans-Albert Kolb, Haferkamp, H., & Chichkov, B. N. (2007). Three-dimensional cell growth on structures fabricated from ORMOCER® by twophoton polymerization technique. *Journal of Biomaterials Applications*, 2007 Nov;22(3):275-87.



PO 25

POSTERS

Fatty acids in the bovine serum albumin structure influence binding parameters in its interaction with fungicide prothioconazole

a,bJ. STANIČOVÁ, aV. VEREBOVÁ

^aDepartment of Chemistry, Biochemistry & Biophysics, University of Veterinary Medicine & Pharmacy, Košice, Slovakia

^bInstitute of Biophysics & Informatics, First Faculty of Medicine, Charles University, Prague, Czech Republic

Serum albumins are the most abundant plasma proteins and contribute to a significant number of transport and regulatory processes. Bovine serum albumin (BSA) has extraordinary binding properties. It can bind under physiological conditions, not only fatty acids, peptides, and proteins but also low molecular weight endogenous and exogenous molecules [1, 2]. The presence of fatty acids that bind to multiple sites in BSA can affect the binding of many ligands, such as drugs, and toxic agents, including pesticides [3, 4].

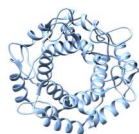
We have studied the interactions between conazole fungicides represented by prothioconazole (PTC) as the ligand and BSA on the molecular level. Our study has been concerned to its different influence on BSA containing fatty acids and the protein free of fatty acids (BSA_f), respectively.

Measurements of fluorescence spectra at different temperatures combined with theoretical binding analysis have used in our study.

Table 1. Summarization of binding and thermodynamic parameters for PTC interaction with BSA and BSA_f, respectively.

Complex	T (°C)	K _A (L/mol)	n	ΔG (kJ/mol)	ΔH (kJ/mol)	ΔS (J/mol.K)
PTC/BSA	25	1.30×10 ⁴ ± 0.01	0.99 ± 0.02	-18.97 ± 0.03	-73.03 ± 0.03	-181.40 ± 0.01
	30	1.04×10 ⁴ ± 0.01	0.97 ± 0.03	-18.07 ± 0.02		
	37	8.02×10 ³ ± 0.01	0.93 ± 0.02	-16.79 ± 0.02		
PTC/BSA _f	25	6.45×10 ⁵ ± 0.05	1.06 ± 0.01	-32.94 ± 0.002	-84.85 ± 0.02	-174.18 ± 0.07
	30	2.89×10 ⁵ ± 0.08	0.99 ± 0.01	-32.07 ± 0.003		
	37	1.66×10 ⁵ ± 0.06	0.95 ± 0.01	-30.85 ± 0.001		

From Table 1, we can see that association constants characterizing a strength of interaction have increased when the protein has not contained any fatty acids. Even the difference in their values reaches up to a multiple of one order. This fact leads to a supposition that the presence of the fatty acids within the BSA structure does not support a stronger binding of the PTC molecule within the BSA macromolecule. It looks like the fatty acids absence facilitates the incorporation of PTC inside the protein.



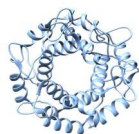
Thermodynamic parameters calculated using Van't Hoff equation (Table 1, columns 5-7) help us to determine a type of interaction. The negative values of ΔG indicate spontaneous reaction, and the negative values of ΔH and ΔS suggest that the hydrogen bonds and van der Waals forces play a major role in the incorporation [5]. Our data (Table 1) fulfill these conditions, and we can proclaim that the PTC molecule interacts with the BSA macromolecule by hydrogen bonds or van der Waals forces. Moreover, the negative values of ΔG indicate that these binding processes are spontaneous. Looking at column 5 in Table 1, we can see a significant difference in Gibbs free energy between PTC/BSA and PTC/BSA_f complexes, which shows a higher energetic release in the binding of PTC into BSA_f in comparison with PTC incorporation into BSA.

In conclusion, we can state that conazole fungicide prothioconazole interacts with bovine serum albumin, which is free of fatty acids easier than the bovine serum albumin containing the fatty acids. We suppose that the fatty acids localized in the BSA molecule probably represent some barrier for facilitated PTC molecule incorporation into the BSA macromolecule.

Acknowledgment. This work was supported by research grants from the Slovak Research Grant Agency VEGA No. 1/0242/19 and KEGA No. 012 UVLF-4/2018.

References

1. Wang, Y.Q., Tang, B.P., Zhang, H.M., Zhou, Q.H. & Zhang, G.C. (2009). Studies on the interaction between imidacloprid and human serum albumin: spectroscopic approach. *J. Photochem. Photobiol. B*, 94, 183-190.
2. Wang, Y., Wang, X., Wang, J., Zhao, Y., He, W. & Guo, Z. (2011). Noncovalent interactions between a trinuclearmonofunctional platinum complex and human serum albumin. *Inorg. Chem.*, 50, 12661-12668.
3. Buttar, D., Colclough, N., Gerhardt, S., MacFaul, P.A., Phillips, S.D., Plowright, A., Whittamore, P., Tam, K., Maskos, K., Steinbacher, S. & Steuber, H. (2010). A combined spectroscopic and crystallographic approach to probing drug–human serum albumin interactions. *Bioorganic & medicinal chemistry*, 18(21), 7486-7496.
4. Fabriciova, G., Sanchez-Cortes, S., Garcia-Ramos, J.V. & Miskovsky, P. (2004). Surface-enhanced Raman spectroscopy study of the interaction of the antitumoral drug emodin with human serum albumin. *Biopolymers: Original Research on Biomolecules*, 74(1-2), 125-130.
5. Congdon, R.W., Muth, G.W. & Splittgerber, A.G. (1993). The binding interaction of Coomassie blue with proteins. *Anal. Biochem.*, 213, 407–413.



Characterisation and purification of staphylokinase variants developed by ribosome display

^aM. ŠTULAJTEROVÁ, ^bM. TOMKOVÁ, ^{b,c}E. SEDLÁK

^a*Department of Biophysics, Faculty of Science, P.J. Šafárik University, Jesenná 5, 041 54 Košice, Slovakia*

^b*Center for Interdisciplinary Biosciences, Technology and Innovation Park, P. J. Šafárik University, Jesenná 5, 041 54 Košice, Slovakia*

^c*Department of Biochemistry, Faculty of Science, P.J. Šafárik University, Moyzesova 11, 041 54 Košice, Slovakia*

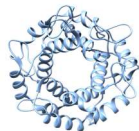
Thrombosis, which refers to the formation of blood clots in specific areas, has a considerable medical impact. The acute arterial thrombosis is the main underlying factor for the majority of myocardial infarction (heart attacks) and approximately 80% of strokes. Collectively, these conditions represent the leading cause of mortality in developed countries. (Mackman, 2008). Prompt treatment with thrombolytic drugs can restore blood flow before major brain damage has occurred and improve recovery after stroke (Wardlaw et al., 2014). An ideal thrombolytic agent is expected to prevent re-occlusions, has higher fibrin specificity, decrease bleeding complications, be retained in the blood for a longer time to minimize dosage and be less antigenic for repetitive usage. However, thrombolytic drugs have shown limited efficacy and notable hemorrhagic complication rates, offering potential for enhancement (Nikitin et al., 2021).

Bacterial staphylokinase (SAK) is a small-size plasminogen activator, which hinders the systemic degradation of fibrinogen and reduces the risk of severe hemorrhage. It has a high tendency to make fibrin-bound plasminogen turn into plasmin through formation of equimolar (1:1) complex with plasmin, which can activate inactive zymogen plasminogen to its active form, plasmin. SAK is considered to be a promising thrombolytic agent with properties of cost-effective production and negligible side effects (Nedaeinia et al., 2020).

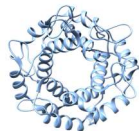
In order to enhance SAK's effectiveness and to minimize potential adverse effects, it is crucial to enhance its affinity and selectivity towards plasmin. This can be achieved through the method of directed evolution of proteins, a highly effective method for customizing protein properties to achieve new or improved functionalities. In our study, we utilized ribosome display, to evolve new SAK variants, thus modifying SAK protein characteristics. Here we provide basic characterization of the variants obtained through the aforementioned method. In addition, we outline the fundamental biophysical properties and explain the purification process of certain mutant forms.

Acknowledgment. This work was supported by the grant agency of the Ministry of Education, Science, Research, and Sport of the Slovak Republic (grant no. VEGA 1/0074/22) and by the EU H2020-WIDESPREAD-05-2020 grant No. 952333, CasProt (Fostering high scientific quality in protein science in Eastern Slovakia).

References



1. Mackman, N. (2008). Triggers, targets and treatments for thrombosis. In *Nature* (Vol. 451, Issue 7181, pp. 914–918). Nature Publishing Group. <https://doi.org/10.1038/nature06797>
2. Nedaeinia, R., Faraji, H., Javanmard, S. H., Ferns, G. A., Ghayour-Mobarhan, M., Goli, M., Mashkani, B., Nedaeinia, M., Haghghi, M. H. H., & Ranjbar, M. (2020). Bacterial staphylokinase as a promising third-generation drug in the treatment for vascular occlusion. In *Molecular Biology Reports* (Vol. 47, Issue 1, pp. 819–841). Springer. <https://doi.org/10.1007/s11033-019-05167-x>
3. Nikitin, D., Choi, S., Mican, J., Toul, M., Ryu, W. S., Damborsky, J., Mikulin, R., Kim, D. E. (2021). Development and testing of thrombolytics in stroke. *Journal of Stroke*, 23(1), 12-36. <https://doi.org/10.5853/jos.2020.03349>
4. Wardlaw, J. M., Murray, V., Berge, E., & del Zoppo, G. J. (2014). Thrombolysis for acute ischaemic stroke. In *Cochrane Database of Systematic Reviews* (Vol. 2014, Issue 7). John Wiley and Sons Ltd. <https://doi.org/10.1002/14651858.CD000213.pub3>



PO 27

POSTERS

Study of the interaction of casein micelles with curcumin by fluorescence spectroscopy and dynamic laser scattering

V. ŠUBJAKOVÁ, Z. GARAIOVÁ, T. HIANIK

*Department of Nuclear Physics and Biophysics, Faculty of Mathematics, Physics and Informatics,
Comenius University, Bratislava, Slovakia*

Curcumin is a natural bioactive substance extracted from turmeric that has many pharmaceutical activities such as anti-oxidant, anti-tumor and anti-inflammatory properties. Nevertheless, the curcumin is very poorly soluble in water resulting into limitation of its bioavailability and application in drug delivery or food industry [1]. This can be adjusted by suitable nanocarriers. The casein micelles are supramolecular structures and offer high potential as nanocarriers. They possess amphiphilic properties that make them proper for encapsulation of hydrophobic as well for hydrophilic drugs [2].

Both constituents have been studied mostly individually for their various properties and mainly for benefits in drug delivery, but the mechanism of their interaction is needed to undergo further investigation. We have focused to study the interaction between curcumin and β -casein by the fluorescence spectroscopy and dynamic light scattering methods investigating the effect of 1, 5, 10 and 50 μM curcumin concentrations on the internal casein fluorescence ($\lambda_{\text{ex}} = 290 \text{ nm}$, $\lambda_{\text{em}} = 350 \text{ nm}$) and hydrodynamic diameter together with polydispersity index (PDI), respectively.

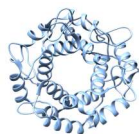
The micelles were prepared from β -casein (2 mg/ml) in Na-phosphate buffer (PB, 10 mM, pH 7) in the presence of CaCl_2 (10 mM) or without CaCl_2 under constant stirring for 1.5 h at 25 °C, followed by filtration through a 0.2 μm pore size filter.

The hydrodynamic diameter of casein micelles was $27.32 \pm 1.07 \text{ nm}$ (PDI = 0.44) and increased to $63.95 \pm 0.54 \text{ nm}$, (PDI=0.08) in the presence of CaCl_2 . The observed increase in the size and reduced PDI indicates more homogenous distribution that confirm stabilizing effect of CaCl_2 on casein nanostructures. The addition of curcumin did not affect significantly the size of casein micelles either without or with CaCl_2 . Zeta potential was also examined. The presence of all investigated concentrations of curcumin decreased the tryptophan fluorescence intensity from casein micelles.

Acknowledgment. This work was supported by VEGA grant 1/0554/23.

References

- [1] Esmaili, M., Ghaffari, S. M., Moosavi-Movahedi, Z., Atri, M. S., Sharifzadeh, A., Farhadi, M., Yousefi, R., Chobert, J.-M., Haertlé, T., & Moosavi-Movahedi, A. A. (2011). Beta casein-micelle as a nano vehicle for solubility enhancement of curcumin; food industry application. *LWT - Food Science and Technology*, 44(10), 2166–2172.
- [2] Sadiq, U., Gill, H., & Chandrapala, J. (2021). Casein micelles as an emerging delivery system for bioactive food components. *Foods*, 10(8).



PO 28

POSTERS

Thermodynamic properties of the F type ferryl intermediate of the cytochrome c oxidase

^aA. TOMKOVÁ, ^aT. SZTACHOVÁ, ^bM. FABIÁN, ^aD. JANCURA

^aDepartment of Biophysics, Faculty of Science, P.J. Šafárik University, Jesenná 5, 041 54 Kosice, Slovakia.

^bCenter for Interdisciplinary Biosciences, Technology and Innovation Park, P. J. Šafárik University, Jesenná 5, 041 54 Košice, Slovakia

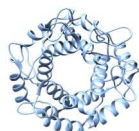
Membrane-bound respiratory cytochrome *c* oxidases (CcO) catalyze oxygen reduction by ferrocyanochrome *c* (c^{2+}). Four cofactors facilitate electron transfer in CcO: Cu_A , the iron of heme *a* (Fe_a), the iron of heme a_3 (Fe_{a3}), and Cu_B . Cu_A is the first electron acceptor from c^{2+} . These electrons are rapidly redistributed between Cu_A and Fe_a and then electron flow continues from Fe_a to the catalytic Fe_{a3} - Cu_B center, where O_2 is reduced to water. The energy released during ET from c^{2+} to O_2 in CcO drives the formation of an electrochemical proton gradient on the inner mitochondrial membrane in eukaryotes. Proton gradient is built by two different mechanisms and one of them is a proton pumping [1]. In spite a large progress in understanding of the pumping by respiratory oxidases its mechanism has not been elucidated yet. The reduction of O_2 to H_2O at the catalytic binuclear center (BNC) occurs through a sequence of several oxy-intermediates. It is quite certain that from these intermediates, two ferryl states, **P** and **F**, are involved in the H^+ pumping [2]. The reduction of **F** by one electron transfer to BNC leads to the formation of the oxidized CcO (**O**). The energy released by this reaction should be sufficient to pump at least one H^+ through the membrane and transfer one proton into BNC. However, the amount of energy liberated at this stage was estimated only indirectly [2].

In this work, we determined the amount of released energy, the enthalpy change (ΔH), associated with the transition of **F**-to-**O**. The transition of **F**-to-**O** was monitored by UV-Vis spectrometry and in parallel measurement, the ΔH of this reaction was registered by isothermal titration calorimetry. The results showed the reduction of **F** by c^{2+} is linked with the change of enthalpy -10.3 kcal/mol (0.44 eV) (pH 8.0, 5 °C) that is sufficient for a transfer of 2 positive charges through the membrane during the mitochondrial respiration.

Acknowledgment. This work was supported by the project "Open scientific community for modern interdisciplinary research in medicine (OPENMED)-ITMS2014+: 313011V455" from the Operational Program Integrated Infrastructure funded by the ERDF and by the Slovak Grant Agency (VEGA 1/ 0028/22).

References

1. Wikstrom, M. (1977) Proton pump coupled to cytochrome c oxidase in mitochondria, *Nature* 266, 271 - 273.
2. Wikstrom, M., Krab, K., and Sharma, V. (2018) Oxygen Activation and Energy Conservation by Cytochrome c Oxidase, *Chem Rev* 118, 2469-2490.



PO 29

POSTERS

Conformation changes of bovine serum albumin caused by binding of fungicide prothioconazole with regard to the presence of fatty acids in the protein molecule

^aV. VEREBOVÁ, ^{a,b}J. STANIČOVÁ

^aDepartment of Chemistry, Biochemistry & Biophysics, University of Veterinary Medicine & Pharmacy, Košice, Slovakia

^bInstitute of Biophysics & Informatics, First Faculty of Medicine, Charles University, Prague, Czech Republic

Bovine serum albumin (BSA) is an unglycated globular protein found in blood plasma. Many endogenous and exogenous compounds (drugs, hormones, xenobiotics, and fatty acids) that enter the bloodstream are transported and eliminated as a result of forming a complex with serum albumins. BSA contributes to the osmotic pressure and maintenance of blood pH, increases the solubility of hydrophobic drugs in plasma, and affects blood circulation, metabolism, and efficacy of drugs [1].

Crystallographic studies have shown that the structure of BSA consists predominantly of α - helices and no β - folded sheet [2]. The presence of fatty acids that bind to multiple sites in BSA can affect its conformation after the binding of many ligands, such as drugs, and toxic agents, including pesticides [3].

In this contribution, the conformation changes of BSA containing fatty acids and BSA fatty acids free (BSA_f) due to the binding of conazole fungicides represented by prothioconazole (PTC) have been studied.

Biophysical methods of optical spectroscopy (absorption spectroscopy, 3D fluorescence spectroscopy, optical dichroism spectroscopy) were used in the study.

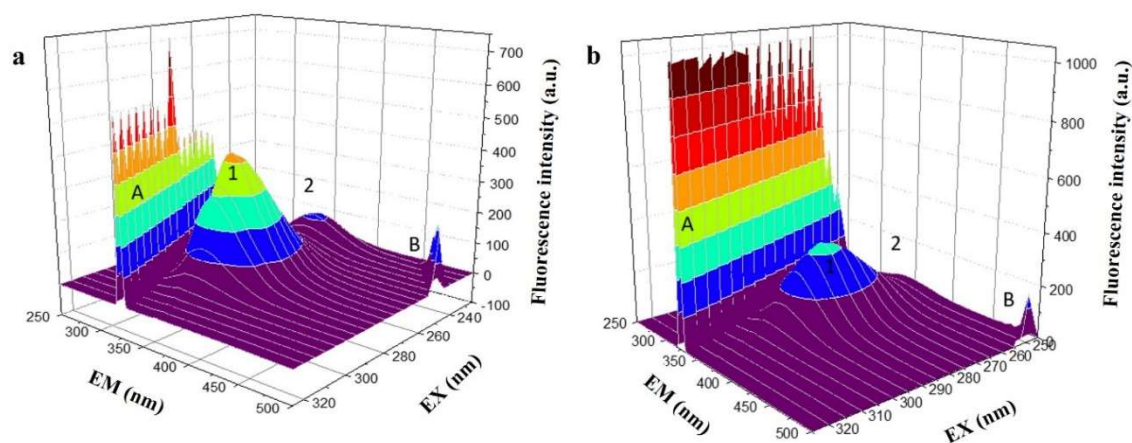
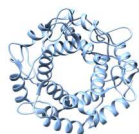


Fig. 1 3D fluorescence spectra of BSA without (a) and in the presence of PTC in the concentration ratio 1:16 (b)

In Fig. 1, we can see the decreasing tendency of peak 1 after adding PTC to BSA solutions. This decrease suggests the binding of PTC near Tyr or Trp of individual proteins, which is consistent with fluorescence measurements (not shown). We can also observe the reduction of peak 2, which indicates changes in the peptide structure



(Fig. 1). Its decreasing tendency after PTC binding indicates that there is a slight destabilization of individual proteins and a slight unfolding of the polypeptide chain leading to conformational changes [4]. A significant difference in the intensities of peaks 1 and 2 between PTC/BSA and PTC/BSA_f complexes has been recorded (not shown). This result correlates with CD spectroscopy measurements (Table 1).

Table 1. α – helix content in BSA and BSA_f, respectively, after PTC incorporation into the protein as obtained by CD spectroscopy.

Complex	α – helix content
BSA	56.16 %
BSA/PTC 1/5	55.50 %
BSA/PTC 1/9	53.20 %
BSA _f	47.57 %
BSA _f /PTC 1/5	38.90 %
BSA _f /PTC 1/9	36.99 %

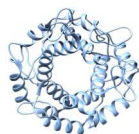
CD results suggest that PTC may interact with amino acid residues of the BSA polypeptide chain, resulting in slight protein destabilization and a more open conformation [5]. After the binding of PTC to the proteins, there is a considerable difference in an α – helix content between BSA and BSA_f (Table 1).

In conclusion, we can state that conazole fungicide prothioconazole affects the conformation of bovine serum albumin, which is free of fatty acids more significantly than the bovine serum albumin containing fatty acids. We suppose that the BSA is more vulnerable when fatty acids are not localized in the protein molecule.

Acknowledgment. This work was supported by research grants from the Slovak Research Grant Agency VEGA No. 1/0242/19 and KEGA No. 012 UVLF-4/2018.

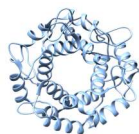
References

1. Peters jr., T. (1995). All about albumin: biochemistry, genetics, and medical applications. Academic press.
2. Carter, D. C., Ho, J. X. (1994). Structure of serum albumin. In: *Advances in protein chemistry*. Academic Press, 153-203.
3. Buttar, D., Colclough, N., Gerhardt, S., MacFaul, P.A., Phillips, S.D., Plowright, A., Whittamore, P., Tam, K., Maskos, K., Steinbacher, S. & Steuber, H. (2010). A combined spectroscopic and crystallographic approach to probing drug–human serum albumin interactions. *Bioorganic & medicinal chemistry*, 18(21), 7486-7496.
4. Tian, F.F., Jiang, F.L., Han, X.L., Xiang, C., Ge, Y.S., Li, J.H., Zhang, Y., Li, R., Ding, X.L. & Liu, Y. (2010). Synthesis of a novel hydrazone derivative and biophysical studies of its interactions with bovine serum albumin by spectroscopic, electrochemical, and molecular docking methods. *The Journal of Physical Chemistry B*, 114(46), 14842-14853.
5. Ding, F., Diao, J.X., Sun, Y., Sun, Y. (2012). Bioevaluation of human serum albumin–hesperidin bioconjugate: insight into protein vector function and conformation. *Journal of agricultural and food chemistry*, 60(29), 7218-7228.

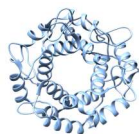


LIST OF PARTICIPANTS

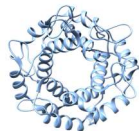
1	AHMAD NABEEL	ALL INDIA INSTITUTE OF MEDICAL SCIENCES NEW DELHI ANSARI NAGAR, NEW DELHI, INDIA
2	ANCHAL	DEPARTMENT OF BIOPHYSICS, UNIVERSITY OF DELHI, SOUTH CAMPUS NEW DELHI, DELHI. INDIA
3	ANTOŠOVÁ ANDREA	DEPARTMENT OF BIOPHYSICS, INSTITUTE OF EXPERIMENTAL PHYSICS, SLOVAK ACADEMY OF SCIENCES, KOŠICE, SLOVAKIA
4	ARGÜELLO DIANA GABRIELA	LABORATORIO DE INTEGRACIÓN DE SEÑALES CELULARES, IHEM (CONICET-UNCUYO), MENDOZA, ARGENTINA
5	BÁNO GREGOR	DEPARTMENT OF BIOPHYSICS, PAVOL JOZEF ŠAFÁRIK UNIVERSITY IN KOŠICE, SLOVAKIA
6	BAUEROVA VLADENA	INSTITUTE OF MOLECULAR BIOLOGY, SLOVAK ACADEMY OF SCIENCES, BRATISLAVA, SLOVAKIA
7	BEDLOVIČOVÁ ZDENKA	DEPARTMENT OF CHEMISTRY, BIOCHEMISTRY AND BIOPHYSICS, UNIVERSITY OF VETERINARY MEDICINE AND PHARMACY, KOŠICE, SLOVAKIA
8	BEDNÁRIKOVÁ ZUZANA	DEPARTMENT OF BIOPHYSICS, INSTITUTE OF EXPERIMENTAL PHYSICS, SLOVAK ACADEMY OF SCIENCES, KOŠICE, SLOVAKIA
9	CEHLÁR ONDREJ	INSTITUTE OF NEUROIMMUNOLOGY, SLOVAK ACADEMY OF SCIENCES, BRATISLAVA, SLOVAKIA
10	CHANG CHIA-YOU	DEPARTMENT OF CHEMICAL ENGINEERING, NATIONAL TAIWAN UNIVERSITY, TAIPEI, TAIWAN
11	ČELKOVÁ ADRIÁNA	DEPARTMENT OF PHYSICAL CHEMISTRY OF DRUGS, FACULTY OF PHARMACY, COMENIUS UNIVERSITY, BRATISLAVA, SLOVAKIA
12	DEMČÁKOVÁ VERONIKA	DEPARTMENT OF BIOPHYSICS, PAVOL JOZEF ŠAFÁRIK UNIVERSITY IN KOŠICE, SLOVAKIA
13	DŽUPPONOVÁ VERONIKA	DEPARTMENT OF BIOPHYSICS, PAVOL JOZEF ŠAFÁRIK UNIVERSITY IN KOŠICE, SLOVAKIA CENTER FOR INTERDISCIPLINARY BIOSCIENCES, TECHNOLOGY AND INNOVATION PARK, PAVOL JOZEF ŠAFÁRIK UNIVERSITY IN KOŠICE, SLOVAKIA
14	FEDOROVÁ VIKTÓRIA	DEPARTMENT OF BIOPHYSICS, INSTITUTE OF EXPERIMENTAL PHYSICS, SLOVAK ACADEMY OF SCIENCES, KOŠICE, SLOVAKIA
15	FEDUNOVÁ DIANA	DEPARTMENT OF BIOPHYSICS, INSTITUTE OF EXPERIMENTAL PHYSICS, SLOVAK ACADEMY OF SCIENCES, KOŠICE, SLOVAKIA
16	FONTANA LORENA INES	LABORATORIO DE INTEGRACIÓN DE SEÑALES CELULARES, IHEM (CONICET-UNCUYO), MENDOZA, ARGENTINA
17	GALA MICHAL	DEPARTMENT OF BIOPHYSICS, PAVOL JOZEF ŠAFÁRIK UNIVERSITY IN KOŠICE, SLOVAKIA CENTER FOR INTERDISCIPLINARY BIOSCIENCES, TECHNOLOGY AND INNOVATION PARK, PAVOL JOZEF ŠAFÁRIK UNIVERSITY IN KOŠICE, SLOVAKIA
18	GARAGUSO IGNAZIO	BECKMAN COULTER, EUROPARK FICHTENHAIN, KREFELD, GERMANY



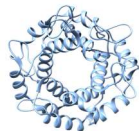
19	GARAIOVÁ ZUZANA	DEPARTMENT OF NUCLEAR PHYSICS AND BIOPHYSICS, FACULTY OF MATHEMATICS, PHYSICS AND INFORMATICS, COMENIUS UNIVERSITY, BRATISLAVA, SLOVAKIA
20	GAŽOVÁ ZUZANA	DEPARTMENT OF BIOPHYSICS, INSTITUTE OF EXPERIMENTAL PHYSICS, SLOVAK ACADEMY OF SCIENCES, KOŠICE, SLOVAKIA
21	GUCKÝ ADRIÁN	DEPARTMENT OF BIOCHEMISTRY, INSTITUTE OF CHEMISTRY, FACULTY OF SCIENCE, PAVOL JOZEF ŠAFÁRIK UNIVERSITY IN KOŠICE, SLOVAKIA
22	GUNCHEVA MAYA	INSTITUTE OF ORGANIC CHEMISTRY WITH CENTRE OF PHYTOCHEMISTRY, BULGARIAN ACADEMY OF SCIENCES, SOFIA, BULGARIA
23	HOVAN ANDREJ	DEPARTMENT OF BIOPHYSICS, PAVOL JOZEF ŠAFÁRIK UNIVERSITY IN KOŠICE, SLOVAKIA
24	HOW SU-CHUN	DEPARTMENT OF CHEMICAL ENGINEERING AND BIOTECHNOLOGY, TATUNG UNIVERSITY, TAIPEI, TAIWAN
25	JANCURA DANIEL	DEPARTMENT OF BIOPHYSICS, PAVOL JOZEF ŠAFÁRIK UNIVERSITY IN KOŠICE, SLOVAKIA
26	JURAŠEKOVÁ ZUZANA	DEPARTMENT OF BIOPHYSICS, PAVOL JOZEF ŠAFÁRIK UNIVERSITY IN KOŠICE, SLOVAKIA
27	KADEŘÁVEK PAVEL	MASARYK UNIVERSITY, BRNO, CZECH REPUBLIC
28	KERTI LUKÁŠ	DEPARTMENT OF PHYSICAL CHEMISTRY OF DRUGS, FACULTY OF PHARMACY, COMENIUS UNIVERSITY, BRATISLAVA, SLOVAKIA
29	KESHAVARZI ATOOSA	DEPARTMENT OF PHYSICAL CHEMISTRY OF DRUGS, FACULTY OF PHARMACY, COMENIUS UNIVERSITY, BRATISLAVA, SLOVAKIA
30	KHAJEHPOUR MAZDAK	DEPARTMENT OF CHEMISTRY, UNIVERSITY OF MANITOBA, WINNIPEG, MANITOBA, CANADA
31	KLACSOVÁ MÁRIA	DEPARTMENT OF PHYSICAL CHEMISTRY OF DRUGS, FACULTY OF PHARMACY, COMENIUS UNIVERSITY, BRATISLAVA, SLOVAKIA
32	KUBACKOVÁ JANA	DEPARTMENT OF BIOPHYSICS, INSTITUTE OF EXPERIMENTAL PHYSICS, SLOVAK ACADEMY OF SCIENCES, KOŠICE, SLOVAKIA
33	LAI YU-REN	DEPARTMENT OF CHEMICAL ENGINEERING, NATIONAL TAIWAN UNIVERSITY, TAIPEI, TAIWAN
34	LI MAI SUAN	INSTITUTE OF PHYSICS, POLISH ACADEMY OF SCIENCE, WARSAW, POLAND
35	MÁŠA MARTIN	BECKMAN COULTER, PRAHA, CZECH REPUBLIC
36	MÜLLER SERGIO	LABORATORIO DE INTEGRACIÓN DE SEÑALES CELULARES, IHEM (CONICET-UNCUYO), MENDOZA, ARGENTINA
37	NEMERGUT MICHAL	CENTER FOR INTERDISCIPLINARY BIOSCIENCES, TECHNOLOGY AND INNOVATION PARK, PAVOL JOZEF ŠAFÁRIK UNIVERSITY IN KOŠICE, SLOVAKIA LOSCHMIDT LABORATORIES, DEPARTMENT OF EXPERIMENTAL BIOLOGY, FACULTY OF SCIENCE, MASARYK UNIVERSITY, BRNO, CZECH REPUBLIC
38	NIEDZIALEK DOROTA	LABORATORY OF MOLECULAR BASIS OF BIOLOGICAL ACTIVITY, INSTITUTE OF BIOCHEMISTRY AND BIOPHYSICS, POLISH ACADEMY OF SCIENCES, WARSAW, POLAND



39	OLAJOŠ JAKUB	DEPARTMENT OF BIOCHEMISTRY, INSTITUTE OF CHEMISTRY, FACULTY OF SCIENCE, PAVOL JOZEF ŠAFÁRIK UNIVERSITY IN KOŠICE, SLOVAKIA
40	PINTO LAURA SOLEDAD	LABORATORIO DE INTEGRACIÓN DE SEÑALES CELULARES, IHEM (CONICET-UNCUYO), MENDOZA, ARGENTINA
41	POLÁK ADAM	BIOMEDICAL RESEARCH CENTER, INSTITUTE OF VIROLOGY, SLOVAK ACADEMY OF SCIENCES, BRATISLAVA, SLOVAKIA DEPARTMENT OF MOLECULAR BIOLOGY, FACULTY OF NATURAL SCIENCES, COMENIUS UNIVERSITY, BRATISLAVA, SLOVAKIA INSTITUTE OF NEUROIMMUNOLOGY, LABORATORY OF STRUCTURAL BIOLOGY OF NEURODEGENERATION, SLOVAK ACADEMY OF SCIENCES, BRATISLAVA, SLOVAKIA
42	POPOVYCH NATALIA	UZHGOROD NATIONAL UNIVERSITY, UZHGOROD, UKRAINE
43	RIVERA LAUTARO	LABORATORIO DE INTEGRACIÓN DE SEÑALES CELULARES, IHEM (CONICET-UNCUYO), MENDOZA, ARGENTINA
44	SHIRAZI ASI ALI	DEPARTMENT OF PHYSICAL CHEMISTRY OF DRUGS, FACULTY OF PHARMACY, COMENIUS UNIVERSITY, BRATISLAVA, SLOVAKIA
45	SLABÝ CYRIL	DEPARTMENT OF BIOPHYSICS, PAVOL JOZEF ŠAFÁRIK UNIVERSITY IN KOŠICE, SLOVAKIA
46	STANIČOVÁ JANA	DEPARTMENT OF CHEMISTRY, BIOCHEMISTRY AND BIOPHYSICS, UNIVERSITY OF VETERINARY MEDICINE AND PHARMACY, KOŠICE, SLOVAKIA INSTITUTE OF BIOPHYSICS AND INFORMATICS, FIRST FACULTY OF MEDICINE, CHARLES UNIVERSITY, PRAGUE, CZECH REPUBLIC
47	STEFÁN GÁBOR	ABL&JASCO HUNGARY, LTD., BUDAPEST, HUNGARY
48	ŠIPOŠOVÁ KATARÍNA	DEPARTMENT OF BIOPHYSICS, INSTITUTE OF EXPERIMENTAL PHYSICS, SLOVAK ACADEMY OF SCIENCES, KOŠICE, SLOVAKIA
49	ŠKRABANA ROSTISLAV	INSTITUTE OF NEUROIMMUNOLOGY, LABORATORY OF STRUCTURAL BIOLOGY OF NEURODEGENERATION, SLOVAK ACADEMY OF SCIENCES, BRATISLAVA, SLOVAKIA
50	ŠTROFFEKOVÁ KATARÍNA	DEPARTMENT OF BIOPHYSICS, PAVOL JOZEF ŠAFÁRIK UNIVERSITY IN KOŠICE, SLOVAKIA
51	ŠTULAJTEROVÁ MONIKA	DEPARTMENT OF BIOPHYSICS, PAVOL JOZEF ŠAFÁRIK UNIVERSITY IN KOŠICE, SLOVAKIA
52	ŠUBJAKOVÁ VERONIKA	DEPARTMENT OF NUCLEAR PHYSICS AND BIOPHYSICS, FACULTY OF MATHEMATICS, PHYSICS AND INFORMATICS, COMENIUS UNIVERSITY, BRATISLAVA, SLOVAKIA
53	TOMKOVÁ ADRIÁNA	DEPARTMENT OF BIOPHYSICS, PAVOL JOZEF ŠAFÁRIK UNIVERSITY IN KOŠICE, SLOVAKIA
54	VEREBOVÁ VALÉRIA	DEPARTMENT OF CHEMISTRY, BIOCHEMISTRY AND BIOPHYSICS, UNIVERSITY OF VETERINARY MEDICINE AND PHARMACY, KOŠICE, SLOVAKIA
55	VÍGLASKÝ VIKTOR	DEPARTMENT OF BIOCHEMISTRY, INSTITUTE OF CHEMISTRY, FACULTY OF SCIENCE, PAVOL JOZEF ŠAFÁRIK UNIVERSITY IN KOŠICE, SLOVAKIA



56	WIECZOREK GRZEGORZ	MOLECURE S.A. WARSAW, POLAND
57	ZÁHRADNÍKOVÁ ALEXANDRA	DEPARTMENT OF CELLULAR CARDIOLOGY, INSTITUTE OF EXPERIMENTAL ENDOCRINOLOGY, BIOMEDICAL RESEARCH CENTER, SLOVAK ACADEMY OF SCIENCES, BRATISLAVA, SLOVAKIA
58	ŽOLDÁK GABRIEL	CENTER FOR INTERDISCIPLINARY BIOSCIENCES, TECHNOLOGY AND INNOVATION PARK, PAVOL JOZEF ŠAFÁRIK UNIVERSITY, KOŠICE, SLOVAKIA CENTER FOR INTERDISCIPLINARY BIOSCIENCES, CASSOVIA NEW INDUSTRY CLUSTER, CNIC, KOŠICE, SLOVAKIA



INDEX OF AUTHORS

A

AHMAD, N. **PO 1**
ANTALIK, M. **PO 17**
ANTOŠOVÁ, A. **PO 2, PO 8**
APOSTOLOVA, S. **PO 18**
ASAKEREH, I. **PL 11**

B

BÁNO, G. **SC 4, PO 25**
BARRERA, E. **SC 7, PO 16**
BAUER, J.A. **PL 13**
BAUEROVÁ-HLINKOVÁ, V. **PL 13**
BEDLOVIČOVÁ, Z. **PO 3**
BEDNÁRIKOVÁ, Z. **PL 5, SC 8, PO 4, PO 5, PO 8**
BENDO VÁ, K. **PL 8**
BENKO, M. **SC 3**
BERKA, V. **PO 12**
BHATTACHARYA, A. **SC 5**
BIRO, T. **SC 9**
BITALA, A. **SC 3**
BITTNER FIALOVA, S. **SC 8**
BLACKLEDGE, M. **PL 8**
BOROVSKÁ, B. **PO 5**
BUCSI, A. **PO 6**
BUSTOS, D.M. **SC 7, PO 16**

C

CEHLÁR, O. **PL 5, PL 9**
CHANG, C.Y. **SC 12**
CRHA, R. **PL 5**
ČELKOVÁ, A. **PO 6**

D

DEMČÁKOVÁ, V. **PO 7**
DOKOUPILOVÁ, S. **SC 8**
DŽUPPONOVÁ, V. **SC 2**

E

EHRARDT, L. **SC 5**

F

FABIAN, M. **PO 12, PO 28**
FEDOROVÁ, V. **SC 9**
FEDUNOVÁ, D. **PO 8**
FERRAGE, F. **PL 8**

FIALOVÁ, L. **PL 5**
FRECER, V. **PO 13**

G

GALA, M. **SC 1**
GANČÁR, M. **SC 8, PO 2, PO 8**
GARAGUSO, I. **SC 5**
GARAIOVÁ, Z. **PO 9, PO 27**
GAŽOVÁ, Z. **SC 8, PO 2, PO 4, PO 5, PO 8**
GEORGIEVA, I. **PO 18**
GOEL, A.M. **PO 10**
GUCKÝ, A. **PO 11**
GUNCHEVA, M. **PO 8, PO 18**

H

HIANIK, T. **PO 9, PO 27**
HORVAT, L. **PO 15**
HOVAN, A. **SC 4**
HOW, S.C. **SC 10**
HRICOVINI, MICHAL **PL 9**
HRITCOVINI MILOS **PL 9**
HRITZ, J. **PL 5, PO 4**
HROMADKOVA, T. **PL 13**
HUMENIK, M. **SC 9**
HUNTOŠOVÁ, V. **SC 4, PO 24**

I

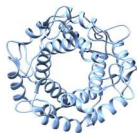
IVOŠEVIĆ DENARDIZ, N. **PO 15**

J

JANCURA, D. **PO 12, PO 28**
JASEŇÁKOVÁ, Z. **PL 8**
JURAŠEKOVÁ, Z. **PO 21**

K

KADEŘÁVEK, P. **PL 5, PL 8, PL 9**
KESHAVARZI, A. **PO 14, PO 22**
KERTI, L. **PO 13**
KHAJEHPOUR, M. **PL 11**
KLACSOVÁ, M. **PO 6, PO 14, PO 15, PO 22**
KLEBEKO, J. **PO 18**
KOLKOVÁ, K. **SC 6**
KORABECNY, J. **PO 11**
KOVAČ, V. **PO 23**
KOVACECH, B. **PL 5**



KOZELEKOVÁ, A. **PO 4**
KOŽURKOVÁ, M. **PO 11**
KRÁLOVÁ, I. **PO 9**
KRALOVIC, N. **PO 22**
KRÁSNY, L. **PL 8**
KUBACKOVÁ, J. **PO 24**
KURIN, E. **SC 8**
KUTEJOVÁ, E. **PL 13**

L

LAI, Y.R. **SC 10, SC 11**
LI, M.S. **PL 1**

M

MAĎAR, M. **PO 3**
MAREK, J. **SC 8, PO 2, PO 8**
MARQUUARDSEN, T. **PL 8**
MARTINEZ, J.C. **PO 6, PO 14, PO 22**
MARTONOVÁ, K. **PL 9**
MATULIN, V. **PO 19**
MESKOVA, K. **PL 9**
MIŠIĆ RADIĆ, T. **PO 15**
MIŠKOVSKÝ, P. **SC 4, PO 21**
MUČAJI, P. **SC 8**
MÜLLER, S. **SC 7, PO 16**

N

NAGY, M. **SC 8**
NARASIMHAN, S. **PL 8**
NEMČOVIČ, M. **SC 3**
NEMČOVIČOVÁ, I. **SC 3**
NEMERGUT, M. **PL 6**
NIEDZIALEK, D. **PL 2, PL 3**
NJEMOGA, S. **PL 5, PL 9**

O

OLAJOŠ, J. **PO 17**
OSSOWICZ-RUPNIEWSKA, P. **PO 18**
OZHELEVSKA, O. **PO 11**

P

PADRTA, P. **PL 8**
PAVELKOVA, J. **PL 12**
PEVNÁ, V. **SC 4, PO 24**
PIESTANSKY, J. **PL 5**
PINČÁK, R. **PO 20**
POLÁK, A. **SC 3**
POPOVYCH, N. **PO 19**

PUDLÁK, M. **PO 20**

R

RABATINOVÁ, A. **PL 8**
REZASOLTANI, H. **PL 11**
RIVERA, L. **SC 7, PO 16**
RIZAK, V. **PO 19**

S

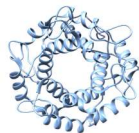
SALVI, N. **PL 8**
SANCHEZ-CORTES, S. **PO 21**
SANDOVAL, F.F. **PO 21**
SEDLÁK, E. **PO 26**
SHARAKI, B.T. **PL 11**
SHARMA, P. **PO 1**
SHARMA, S. **PO 1**
SHIRAZI, A.A. **PO 14, PO 22**
SINGH, T.P. **PO 1**
SKRABANA, R. **PL 5, PL 9**
SLABY, C. **PO 24**
STANIČOVÁ, J. **PO 25, PO 29**
STREJČKOVÁ, A. **PO 24**
SZTACHOVA, T. **PO 12, PO 28**
ŠANDEROVÁ, H. **PL 8**
ŠIPOŠOVÁ, K. **SC 9, PO 23**
ŠTROFFEKOVÁ, K. **PL 10**
ŠTULAJTEROVÁ, M. **PO 26**
STYKOVÁ, E. **PO 3**
ŠUBJAKOVÁ, V. **PO 27**
ŠURIN-HUDÁKOVÁ, N. **PO 3**

T

TOMKOVÁ, A. **PO 12, PO 28**
TOMKOVÁ, K. **PL 9**
TOMKOVÁ, M. **PO 26**
TOMKOVÁ, S. **PL 10**
TOMORI, Z. **PO 24**
TRIZNA, L. **PL 7**
TSUD, N. **PO 19**
TUŽIČIN, D. **PL 8**
TVRDOŇOVÁ, M. **PO 5**
TYBURN, J.-M. **PL 8**
TZONEVA, R. **PO 18**

U

UHART, E. **SC 7, PO 16**
UHRÍKOVÁ, D. **PO 6, PO 14, PO 15, PO 22**



V

VANIK, V. **PO 8**
VARCHOLOVA, B. **PO 21**
VARHAČ, R. **PO 17**
VELÍSKOVÁ, M. **PO 9**
VELTRUSKÁ, K. **PO 19**
VEREBOVÁ, S. **PO 25, PO 29**
VÍGLASKÝ, V. **PL 7**

W

WANG, S.S.S. **SC 10, SC 11, SC 12**
WETTER, E. **PL 10**
WIECZOREK, G. **PL 2, PL 3**

Y

YANG, Y.Y. **SC 10**

Z

ZACHRDLA, M. **PL 8**
ZAHRADNÍK, I. **PL 12**
ZAHRADNÍKOVÁ, A. **PL 12**
ZAPLETAL, V. **PL 8**
ŽÍDEK, L. **PL 8**
ŽOLDÁK, G. **PL 4, SC 2, PO 7**
ZVARIK, M. **PO 9**



Váš špecialista pre laboratórium!

Od roku 1995 sme partnerom pre Vašu laboratórnu prax. Dodávame výrobky overených renomovaných značiek pokrývajúce celé spektrum práce v biologickom alebo biochemickom laboratóriu.

Ponúkame Vám:

❖ **kompletné služby v odbore našej pôsobnosti**

- Molekulárna biológia
- Chemikálie a biochemikálie
- Plastový materiál
- Médiá a séra
- Syntéza olíg
- Imunológia
- Proteomika
- Genomika
- Široké spektrum sekvenačných služieb

❖ **individuálny prístup pri riešení Vašich požiadaviek**

- Certifikovaní partneri
- Komplexné odborné poradenstvo, design a konzultácie
- Odborný servis pre všetky produkty
- Všetko potrebné pre presné, reprodukovateľné a konzistentné výsledky vo výskume a diagnostike

"Od maličkostí závisia veľké veci"

Ponúkame Vám kvalitné služby za rozumné ceny. Naši odborne vyškolení spolupracovníci sú pripravení Vám poradiť.

Viac informácií o našej spoločnosti nájdete na: www.ktrade.sk



bioTech
innovative

Široká ponuka malých laboratórnych prístrojov



Innovative technologies for your laboratory



SUPR-DSF for full fluorescence spectra of proteins run in 384-well microplate.

DIFFERENTIAL SCANNING FLUORIMETRY



MMS for analysis of 2° structure of biomolecules in 96-well microplate.

MICROFLUIDIC MODULATION SPECTROSCOPY (MMS)

SpeciOn

Efficient and Thorough Biomolecules analysis

From Stability to Structure: Scaling Up, Small Molecules to Complexes

For additional information don't hesitate to contact.

+420 605 505 639

www.specion.cz

kolkova@specion.cz

Discover more on our website via the QR code.



MASS PHOTOMETRY

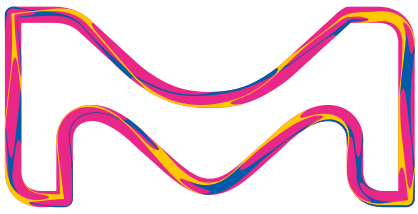
TwoMP measures the mass distribution of biomolecules without labels.



CIRCULAR DICHROISM

The high-performance Circular Dichroism instrument for analysis of 2° structure.





MERCK

streamline

laboratory labeling

New: MilliSentials™ Lab Labeling System

Are you using yesterday's tools for
tomorrow's research?

The MilliSentials Lab Labeling System provides a complete laboratory labeling solution with laboratory grade labels, a compact WIFI capable printer, and custom-designed laboratory labeling software. The MilliSentials Lab Labeling System offers a complete labeling system specifically designed for the laboratory.



SigmaAldrich.com/MilliSentials

© 2022 Merck KGaA, Darmstadt, Germany and/or its affiliates. All Rights Reserved. Merck, the vibrant M and Millipore are trademarks of Merck KGaA, Darmstadt, Germany or its affiliates. All other trademarks are the property of their respective owners. Detailed information on trademarks is available via publicly accessible resources.

The life science business
of Merck operates as
MilliporeSigma in the
U.S. and Canada.

Millipore®

Preparation, Separation,
Filtration & Monitoring Products



**Váš partner v oblasti medicíny,
vedy a výskumu.**

www.sarstedt.com

info.sk@sarstedt.com

Tel: 02/321 84 930

Ponúkame riešenia šité na mieru pre najrozmanitejšie oblasti použitia vrátane molekulárnej biológie, biochémie a bunkovej biológie. Kvalita produktu je prispôbená aplikácii, čo umožňuje čo najvyššiu úroveň reprodukovateľnosti v analytike.

Čisté podmienky v priestoroch a automatizované výrobné procesy sú požiadavky na certifikované štandardy kvality Sarstedt "PCR Performance Tested", "Biosphere® plus", "TC-Test" a "Cryo Performance Tested". Týmto spôsobom môžeme spoľahlivo zabrániť aj najnižším stupňom kontaminácie. S cieľom poskytnúť potrebné záruky sa certifikácie neustále prispôbujú stavu výskumu.

Reagenčné a centrifugačné skúmavky



Mikroskúmavky a reagenčné mikroskúmavky



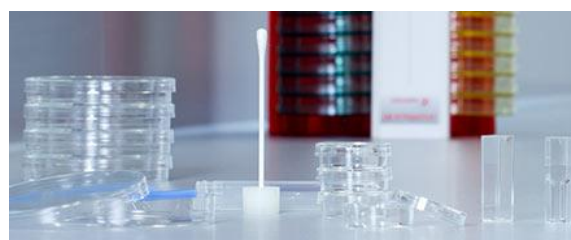
PCR a molekulárna biológia



Manipulácia s kvapalinami



Mikrobiológia



Kultivácia buniek a tkanív



Forezná medicína



Sarpette® M - Nový rad vysoko kvalitných pipiet



Váš spoľahlivý partner už od roku 1990!

REVOLÚCIA V MERANÍ pH ! Merajte pH bezdrôtovo cez Bluetooth

Výhody BT pH metra :

- ✓ Sú nerozbitné - neobsahujú žiadne sklo!
- ✓ Skladujú sa suché
- ✓ Bezproblémové meranie kašovitých / gélových médií
- ✓ Bezkáblový systém
- ✓ Umožňujú merať pH v objeme 1 kvapky

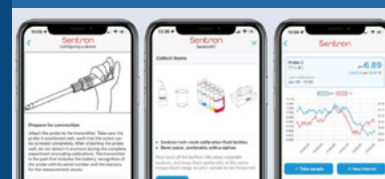
[PODROBNOSTI](#)

[BROŽÚRA](#)

Rôzne typy sônd



Postačí Vám Váš SMARTfón alebo tablet a aplikácia firmy SENTRON.
Už žiadne papiere!



CHRÁŇTE SI VAŠE ZDRAVIE KVALITNÝMI RUKAVICAMI

NOVINKA!



PLNE CERTIFIKOVANÉ, CENOVO ZAUJÍMAVÉ A KVALITNÉ RUKAVICE MAXTER

[PODROBNOSTI](#)



Dvojvrstvové rukavice. Najvyšší laboratórny štandard

Pre zvýšené chemické a biologické riziko máme v ponuke najvyšší štandard laboratórnych rukavíc firmy SHIELD Scientific. Rukavice sú vyrobené z 2 vrstiev (technológia twinSHIELD), a preto dokážu zadržať aj veľmi problematické látky kde Vám štandardné rukavice nepomôžu!



[BROŽÚRA](#)

[KOMPLEXNÁ CHEMICKÁ
ODOLNOSŤ](#)

JEDINÉ RUKAVICE NA TRHU S AQL 0,25!